UNIVERSIDAD COMPLUTENSE DE MADRID
FACULTAD DE CIENCIAS BIOLÓGICAS
Departamento de Bioquímica y Biología Molecular

TESIS DOCTORAL

Pulmonary surfactant& drug delivery

Surfactante pulmonar y vehiculización de fármacos

MEMORIA PARA OPTAR AL GRADO DE DOCTOR

PRESENTADA POR

Alberto Hidalgo Román

Directores

Antonio Cruz Rodríguez
Jesús Pérez Gil

Madrid
Ed. electrónica 2019

UNIVERSIDAD COMPLUTENSE DE MADRID

FACULTAD DE CIENCIAS BIOLÓGICAS

Departamento de Bioquímica y Biología Molecular

PULMONARY SURFACTANT & DRUG DELIVERY

SURFACTANTE PULMONAR Y VEHICULIZACIÓN DE FÁRMACOS

PhD Thesis

ALBERTO HIDALGO ROMÁN

PhD Supervisors

ANTONIO CRUZ RODRÍGUEZ
JESÚS PÉREZ GIL

Madrid, Spain 2018

The research included in this PhD Thesis has been conducted in the Department of Biochemistry and Molecular Biology of Universidad Complutense de Madrid (Spain) under the supervision of Prof. Antonio Cruz and Prof. Jesús Pérez Gil Rodríguez. Part of the experimental work was performed in collaboration with Prof. Jahar Bhattacharya, from Columbia University Medical Center (NY, USA).

The financial support to complete this Thesis was provided by the Spanish Ministry of Economy and Competitiveness (BIO2012-30733 and BIO2015-67930-R) and Programa de I+D en Tecnologías de la Comunidad de Madrid (P2013/MIT-2807). Some experiments and materials have been developed with partial support of the company Chiesi Farmaceitici S.p.A. (Parma, Italy).

TABLE OF CONTENTS

TABLE OF CONTENTS

SUMMARY

The advances in nanotechnology and medicine are opening doors to new diagnostic and therapeutic possibilities, which are not accessible with the current approaches. However, the discovery of new therapeutic agents also requires the development of innovative drug delivery strategies. In this context, the pulmonary route is proposed as a powerful entrance for innovative treatments. The respiratory system offers very favourable deatures that improve the delivery and pharmacokinetics of drugs intended for both local and systemic therapies. Apart from being a non-invasive route, the alveolar clearance of drugs and nanoparticles is considerably slower than in other parts of the body due to low enzymatic activity. Additionally, a very large respiratory surface (<140 m^2 approximately) and a thin alveolar epithelium, with high permeability and considerable vascularisation, are key factors to facilitate adsorption and targeting of drugs. However, during its evolution, the lung has developed several barriers to prevent the access of undesirable entities. Therefore, it is essential to investigate how to overcome them and evaluate the paradoxical possibility of using them for drug entry. In this sense, pulmonary surfactant, which has been poorly considered in pulmonary drug delivery research, is named to become a powerful tool to vehiculize novel therapeutics agents.

Pulmonary surfactant is an essential membrane-based lipid-protein material synthetized and secreted to the alveolar region by type-II pneumocytes in the form of multilamellar structures. It coats the respiratory surface and is in charge of preventing alveolar collapse while minimizing the necessary work during breathing. Throughout respiration, the alveoli are continuously dilating and contracting, forcing pulmonary surfactant to adapt to such highly dynamic environment. Its sophisticated composition, including 90% lipids and 10% hydrophilic (SP-A and -D) and highly-hydrophobic (SP-B and -C) proteins, allows pulmonary surfactant for efficiently adsorbing and travelling over the respiratory air-liquid interface. Once there, the compression that occurs upon exhalation forces the interfacial films to fold, forming a three-dimensional network of interconnected membranes with unique mechanical properties, and excluding certain lipids, lipid/protein complexes and any other non-compressible molecules from the interface. As a consequence, during the expansion (upon inhalation) free-surfactant regions could be generated, favouring the spreading of pulmonary surfactant towards the alveoli following the Marangoni Effect, and also the adsorption of new pulmonary surfactant coming from type-II pneumocytes. Therefore, these phenomena could facilitate not only the interfacial trip of pulmonary surfactant and the transport of therapeutics over the respiratory surface, but also their release in the perialveolar region during the process of breathing.

Levering the exceptional interfacial properties of pulmonary surfactant, the main objective of this Thesis is to explore the potential of this surface-active system to vehiculize different drugs through the airways and set the basis of a novel and less-invasive strategy, the interfacial therapy. In order to accomplish this objective the following specific aims are proposed:

1. Stablish and optimize different strategies to combine several molecules of medical interest with clinical and synthetic pulmonary surfactants.
2. Evaluate the possible detrimental effects of the vehiculized molecules on the interfacial behaviour of pulmonary surfactant.
3. Verify the vehiculizing potential of different surfactant formulations through *in vitro* air-liquid interfaces.
4. Determine the implications of compression-expansion breathing dynamics on this novel drug delivery strategy.
5. Confirm the feasibility of the interfacial therapy *in vivo*, determining the main factors implicated and testing its potential synergistic therapeutic effects.

The present Thesis has explored the vehiculizing capabilities of pulmonary surfactant *in vitro* and *in vivo*. Combining different biophysical techniques with fluorescence spectroscopy or fluorescence and atomic force microscopy (AFM), the feasibility of this new drug delivery strategy has been firstly evaluated *in vitro.* The Captive Bubble Surfactometer, which emulates the interfacial mechanics of the alveolus, has been used to evaluate the functionality of surfactant/drug mixtures. Langmuir-Blodgett techniques permits the structural characterisation of surfactant and surfactant/drug films. With interfacially-connected Whilhelmy and Langmuir-Blodgett troughs, an *in vitro* model of the respiratory air-liquid interface has been designed and optimised to perform different vehiculization assays. It has been evaluated how pulmonary surfactant behaves and travels along the interface, what happens if it shares the trip with different drugs, and whether the vehiculized entities are excluded from the interfase under compression-expansion cycling. The results demonstrated that different drugs (corticosteroids and tacrolimus) can be incorporated without affecting the functionality of pulmonary surfactant, while it is capable of vehiculizing them along the air-liquid interface. Additionally, breathing-like compression-expansion cycling favours the interfacial trip of surfactant-containing drugs, enhances adsorption of new material and facilitates drug release processes.

Although the biophysical models provide a robust understanding of elementary processes involved in the interfacial pulmonary drug delivery, to transfer properly the generated knowledge

to clinics further experiments are required to take into account the native context that the desired therapy will encounter in the lungs. Therefore, this Thesis has also addressed the pulmonary surfactant-promoted drug delivery approached directly on real lungs using *in vivo* model systems. The distribution, synergistic anti-inflammatory effects and the cells that internalised the drug tacrolimus have been evaluated in LPS-induced murine models of Acute Lung Injury (ALI). The experiments confirmed that the combined therapy with tacrolimus and porcine-derived exogenous surfactant had considerably better anti-inflammatory effects, preventing the pulmonary oedema and reducing the infiltration of inflammatory cells into the alveolar spaces. Additionally, the presence of pulmonary surfactant enhanced the internalization of tacrolimus into macrophages at the alveolar spaces.

Hence, this Thesis has established for the first time the basis of a new and non-invasive strategy targeting the lungs and likely peripheral locations. Clinical and synthetic surfactants could be the basis of ideal materials to vehiculize different therapeutics (i.e. anti-inflammatory or antibiotic drugs, antibodies, etc.) over the respiratory surface and help them to reach deeper regions in the lung, including the alveoli, where playing a better and more efficient therapeutic activity.

RESUMEN

Uno de los retos de los últimos años ha sido diseñar y desarrollar nuevas estrategias para el transporte de fármacos, particularmente estrategias menos invasivas y dirigidas a dianas específicas del organismo. En este sentido, los nuevos avances en nanotecnología y biomedicina están abriendo nuevas posibilidades terapéuticas y de diagnóstico. Una de las vías con mayor potencial para la administración de fármacos, tanto para tratamientos locales como periféricos, es a través de las vías aéreas, especialmente para compuestos con baja solubilidad en medios acuosos y con escasa biodisponibilidad cuando se administran por vías convencionales (oral o tópica). Las ventajas más evidentes que presenta el sistema respiratorio frente a otras vías de administración son su gran superficie (100 m^2 aprox.), el fino epitelio alveolar que lo recubre, la permeabilidad de sus membranas y su alta vascularización (5 L/min aprox.), que permiten una elevada y rápida absorción de moléculas. Además, la degradación de fármacos en los pulmones es lenta, debido a la baja actividad enzimática intra y extracelular. Sin embargo, durante su evolución el sistema respiratorio ha desarrollado diversas barreras para evitar el acceso de sustancias y microorganismos nocivos. Por tanto, resulta esencial investigar cómo sobrepasarlas y evaluar la posibilidad paradójica de usarlas para transportar fármacos. En esta línea, el surfactante pulmonar, que no ha sido tenido en cuenta en la mayoría de los estudios de transporte de fármacos, se propone como una herramienta eficaz para vehiculizar una nueva generación de agentes terapéuticos.

El surfactante pulmonar es un material formado por membranas de lípidos y proteínas sintetizado y secretado al espacio alveolar por los neumocitos tipo II en forma de estructuras multilamelares. Cubre toda la superficie respiratoria y está encargado de prevenir el colapso alveolar minimizando el trabajo necesario durante el proceso de respiración. Durante este proceso, los alveolos está continuamente dilatándose y contrayéndose, forzando al surfactante pulmonar a adaptarse a estas condiciones tan dinámicas. Su sofisticada composición, 90% lípidos y 10% proteínas hidrofílicas (SP-A y SP-D) e hidrofóbicas (SP-B y SP-C), permite al surfactante adsorberse eficientemente la interfase que se forma entre la fina capa de agua que recubre toda la superficie respiratoria y el aire que respiramos, y viajar rápidamente a lo largo de ella. Una vez en la interfase, la compresión originada durante la exhalación fuerza a la película interfacial de surfactante a plegarse, formando una red de estructuras tridimensionales interconectadas con propiedades biofísicas únicas. Estas estructuras están enriquecidas en todos aquellos componentes del surfactante que, incapaces de soportar elevadas presiones superficiales, favorecen la exclusión de complejos lípido-proteicos y de cualquier otro compuesto poco compresible. Como consecuencia, durante la expansión de la interfase (inhalación) se podrían

generar espacios libres de surfactante, que favorecen la difusión interfacial hacia los alveolos, atendiendo al efecto Marangoni, y la adsorción de nuevo surfactante proveniente de los neumocitos tipo II. Esto podría facilitar no solo el viaje interfacial del surfactante pulmonar y el transporte de fármacos a lo largo de la superficie respiratoria, sino también la liberación de fármaco durante el proceso de reparación.

Aprovechando las características únicas del surfactante pulmonar, el objetivo principal de esta Tesis es explorar el potencial de este sistema para vehiculizar diferentes agentes terapéuticos a través de las vías aéreas y establecer las bases de una nueva estrategia terapéutica menos invasiva, la terapia interfacial. Para ello se plantean los siguientes objetivos específicos:

1. Establecer y optimizar diferentes estrategias para combinar diferentes moléculas de interés médico con surfactantes clínicos y sintéticos.
2. Evaluar los posibles efectos deletéreos de las moléculas vehiculizadas en el comportamiento interfacial de surfactante pulmonar.
3. Verificar el potencial vehiculizador de diferentes formulaciones de surfactante a través de modelos de interfases aire-líquido *in vitro*.
4. Determinar las implicaciones de la dinámica respiratoria en esta nueva estrategia terapéutica.
5. Confirmar la viabilidad de la terapia interfacial en modelos *in vivo*, determinando los principales factores implicados y analizando su potencial efecto sinérgico.

En la presente Tesis Doctoral se han explorado las capacidades vehiculizadoras del surfactante pulmonar *in vitro* e *in vivo.* Combinando diferentes técnicas biofísicas con espectroscopía de fluorescencia o microscopía de fluorescencia o de fuerzas atómicas (AFM), se ha evaluado por primera vez *in vitro* la viabilidad de esta nueva estrategia de vehiculización. El Surfactómetro de Burbuja Cautiva (CBS), que emula la mecánica de compresión-expansión alveolar, se utilizó para evaluar la funcionalidad interfacial de las mezclas surfactante/fármaco. Las técnicas de Langmuir-Blodgett se usaron para la caracterización estructural de las películas de surfactante y el efecto que los fármacos podrían tener sobre ellas. Con balanzas de Wilhelmy y Langmuir-Blodgett conectadas entre sí por puentes interfaciales se ha recreado una superficie respiratoria *in vitro* para realizar diferentes experimentos de vehiculización. Con estos nuevos modelos biofísicos, se ha podido evaluar cómo se comporta y cómo viaja el surfactante pulmonar a lo largo de la interfase aire-líquido, qué pasa si comparte el viaje interfacial con otros pasajeros y si éstos son excluidos de la interfase durante los ciclos de compresión y expansión. Los

resultados obtenidos demostraron que diferentes fármacos (corticosteroides y tacrolimus) pueden ser incorporados y transportados en los complejos del surfactante sin alterar sus propiedades interfaciales. Además, los ciclos de compresión y expansión favorecen el viaje interfacial y la vehiculización, promueven la adsorción de nuevo material y facilitan la liberación del fármaco de la interfase.

Aunque los modelos biofísicos aportan un conocimiento amplio de los procesos elementales implicados en el transporte interfacial de fármacos, para poder transferir adecuadamente este conocimiento a la clínica, es necesario realizar experimentos adicionales teniendo en cuanta el contexto nativo que las moléculas de interés encontrarán en los pulmones. Por tanto, en esta Tesis también se han llevado a cabo experimentos en sistemas *in vivo*. Utilizando modelos de ALI (del inglés, Acute Lung Injury) inducido por LPS, se ha evaluado la distribución y efectos antinflamatorios sinérgicos, así como el tipo de células que son capaces de internalizar el tacrolimus. Los experimentos confirmaron que la terapia combinada de surfactante con tacrolimus mejoraba enormemente los efectos antinflamatorios del fármaco, previniendo el edema pulmonar y reduciendo la infiltración de células proinflamatorias en los espacios alveolares. Además, la presencia de surfactante pulmonar promovía la internalización de tacrolimus por macrófagos en el espacio alveolar.

En resumen, en esta Tesis Doctoral se han establecido por primera vez las bases de una estrategia de vehiculización de fármacos nueva y menos invasiva cuya diana puede ser no solo el sistema respiratorio, sino a través de éste, el resto del organismo. Los surfactantes clínicos actuales u otros sintetizados *ad hoc* podrían ser la base de nuevos adyuvantes ideales para vehiculizar diferentes agentes terapéuticos (por ejemplo fármacos antiinflamatorios, antibióticos, anticuerpos, etc.) a lo largo de la superficie respiratoria y ayudarlos a alcanzar regiones más profundas y distales del pulmón, incluyendo los alveolos, donde puedan ejercer una mejor y más eficiente actividad terapéutica.

This introduction is based on two review articles:

- ***Hidalgo, A.***; Cruz, A.; Perez-Gil, J. Barrier or carrier? Pulmonary surfactant and drug delivery. *Eur J Pharm Biopharm* **2015**, *95* (Pt A), 117-27.
- ***Hidalgo, A.***; Cruz, A.; Perez-Gil, J. Pulmonary surfactant and nanocarriers: Toxicity versus combined nanomedical applications. *Biochimica et biophysica acta* **2017**, *1859* (9 Pt B), 1740-1748.

INTRODUCTION

The applications of nanotechnology are diverse. Particularly, in biomedicine and healthcare, nanotechnology has the potential to advance from current general treatments to safer, more personalised, precise, and patient-friendly therapies. Nanotechnology is creating great expectations in diagnosis, drug delivery and targeted actions. Since Richard Feynman, Physics Nobel Prize awardee in 1965, seeded the first concepts of nanotechnology in his talk "There's Plenty of Room at the Bottom" at the California Institute of Technology in 1959 [1], many researchers have focused on this promising nanoscale technology. As a consequence public and private global investment has increased not only to pursue the generation of knowledge but also its transference to society[2]. It is estimated that global nanomedicine market moved $134.4 billion in 2016 and $151.9 billion in 2017, and the total market for nanomedicine products is projected to grow and reach $293.1 billion by 2022[3].

It is obvious that nanotechnology can contribute to develop new therapeutic strategies and improve the diagnosis and treatment of different diseases considerably. In particular, nanomedicines may reach the place of action with extreme precision, while triggering careful drug release. Furthermore, more than 90% of new drugs are classified as class II or IV, according to the Biopharmaceutical Classification System (BCS), meaning that they have low solubility in water[4, 5]. This creates the need to design new tools and strategies associated with development of novel therapies.

In this context, the pulmonary route is called to become a powerful way of entry for innovative treatments. The respiratory system presents unique features that may facilitate the delivery and pharmacokinetics of drugs intended for both local and systemic therapies. Sophisticated devices for delivering inhaled drugs have been made available in recent times, but this route of drug administration has been known thousands of years ago as the basis of ancestral techniques, such as burning and inhaling aromatic and medicinal plants[6, 7]. It is a non-invasive route, with a slow clearance of drugs and nanoparticles due to low enzymatic activity. Thus, the pulmonary route often allows a reduction of drug dosage while still reaching a high local concentration[8]. Additionally, a very large respiratory surface (more than 140 m^2 approximately), and a thin alveolar epithelium, with high permeability and considerable vascularisation are key factors to facilitate adsorption, targeting and rapid onset of action. As a result, dose and dosing frequency could be reduced, ultimately constituting an easier and more patient-friendly delivery route, especially the chronic lung diseases. However, during evolution, the respiratory system has developed several barriers to prevent the access of pathogens and undesirable and harmful compounds. These barriers pose a serious handicap for drug administration. Therefore, it is crucial

to investigate how to overcome these barriers and evaluate the paradoxical possibility of using them to design novel tools for drug entry.

Historically considered a barrier against pathogens and harmful particles and essential for the process of breathing, pulmonary surfactant (PS) offers great opportunities to solve the solubility problem of hydrophobic drugs while reaching deep regions in the lungs. This PhD Thesis explores the potential use of pulmonary surfactant as a vehicle for delivering drugs stabilising vasic concepts to develop a new and non-invasive drug delivery strategy: the interfacial therapy. In this introduction, based on two already published review articles[4, 9], the importance of vehiculizing therapies will be firstly explained, as well as the anatomy of the respiratory system and its relevant properties for drug entry. Then, it will describe what pulmonary surfactant is, how it works and the main actors during its synthesis and recycling. Finally, surfactant-related pathologies, current therapeutic surfactants and key aspects that should be considered when using pulmonary surfactant as a carrier will be deeply discussed.

Why should we vectorize drugs?

When drugs enter the body, they must overcome different barriers until reaching the target location. Therefore, diverse strategies need to be developed to facilitate the entrance of therapeutic agents, while extending their retention time and optimizing the release of the drug. Novel formulations have been developed through the generation of insoluble complexes that cluster the drug in nanometer-size defined particles. This approach has been explored to administer corticosteroids, sex hormones, insulin, siRNA, anti-bodies or even stem cells. Many other structures and sophisticated micro- and nano-vehicles have been studied for more than 30 years to address a so-called 'smart' vehiculization. Drug vehiculization, vectorization or encapsulation principally look for: (i) protecting drugs from degradation, (ii) increasing adsorption and cellular penetration rates, (iii) controlling drug distribution to increase efficacy and decrease side-effects, and (iv) improving diagnostic imaging techniques. Furthermore, vehicles could be functionalised to: (a) increase their biological half-life (e.g. coating with PEG), (b) target defined locations in the body with specific ligands, (c) allow drug release under particular physiological or pathological conditions (in response to changes in pH, temperature, etc.), (d) avoid or make use of lysosomal degradation once the carrier enters into the cell, and/or (e) engineer multifunctional nanosystems[10]. In general, every nanocarrier that enters in the body should be biocompatible, biodegradable and possess high drug uploading capacity[11].

Several approaches developed according to those principles are currently at preclinical and clinical trials, such as polymeric carriers, lipid nanosystems or dendrimers. Nevertheless, as important as the vehicles are the 'motorways'. One of the challenges in the last years has been to develop non-invasive and patient-friendly drug delivery strategies which could allow reducing dosages and secondary effects while targeting specific locations in the body. In this sense, the respiratory system is proposed as a perfect way of entry and has been increasingly considered in the design and development of new drug delivery strategies. The particular features of the respiratory surface and the presence of pulmonary surfactant, together with lung physiology, make the respiratory system a good choice when looking for a powerful and non-invasive way of delivering for different therapies.

Dissecting the anatomy and physiology to understand pulmonary drug delivery

The respiratory system is specialized in capturing O_2 from the environment and clearing CO_2 produced by cellular metabolism. In terrestrial animals, adult amphibians and lungfishes, this phenomenon is carried out by very complex structures adapted to take oxygen from air, the lungs. In addition to the breathing process, the lung establishes a first barrier protecting the respiratory system from the entrance of external noxious agents such as particles and different potentially pathogenic microorganisms. It is therefore necessary to properly understand the functions, anatomy and physiology of the respiratory system when considering pulmonary drug delivery.

In mammals, the lung is a branching organ composed by tubes that progressively subdivide from conducting to respiratory regions, reaching a total surface of more than 140m^2 (see **Figure *1***) The former includes the nasal cavity, nasopharynx, trachea, bronchi and terminal bronchioles, whose main function is to move air into and out of the lung. The respiratory area, on the other hand, includes respiratory bronchioles and air sacs or alveoli, which are involved in gas exchange between the atmosphere and the bloodstream. In humans, air flows efficiently along their 23 tubular bifurcations from the trachea to alveoli, decreasing in diameter (up to 200 µm approx.) and wall thickness (until 0.1-0.4 µm approx. in alveoli)[12]. Continuously exposed to the environment and, therefore, to potentially harmful compounds and microorganisms, the respiratory system has developed a very sophisticated multi-layered barrier consisting of several structured levels and innate defensive agents.

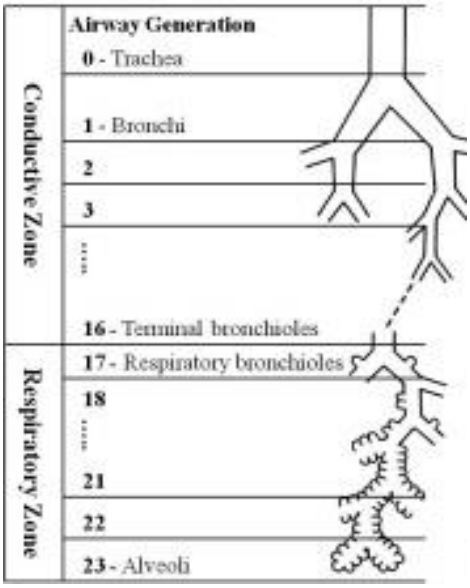

Figure 1: Diagram of pulmonary airways. *Representation of the 23 bifurcations that occurs from trachea to alveoli. Notice that the conductive zone contains 16 bifurcations, while the respiratory area 5 (from the 17th to 23rd) [12].*

When exogenous entities enter the respiratory system, the first layer that they encounter is the mucus and an aqueous hypophase in the conductive regions, lining ciliated and club cells[13]. This first layer mostly traps and clears foreign bodies to prevent their progression to the respiratory region, the alveolar spaces. If avoiding the first line of defence, the respiratory area contains additional layers to restrain them. It is limited by a very thin cell monolayer of type I and II pneumocytes[14]. The former transports ions and proteins, and is in charge of the gas exchange, while the latter synthesises the pulmonary surfactant (PS) complex. This cell monolayer is covered by a thin aqueous film where alveolar macrophages (AM**φ**) can be found. On top of this aqueous layer is where pulmonary surfactant carries out its physiological function[15]. The whole defence system at the respiratory spaces therefore includes mucus and the mucociliary escalator at the upper airways, and PS with its integrated defence collectin proteins and macrophages (M**φ**) at the distal alveolar spaces. Other defensins and antibiotic molecules are secreted into the aqueous layer coating the whole lung to aid maintaining sterility[16, 17]. Under the epithelium, there is an interstitial layer with endothelial cells forming the blood and lymphatic capillaries. The tight junctions sealing the layers of pulmonary cells and endothelium complete the defence system of the respiratory surface.

In addition to these barriers, which also oppose to the entrance of therapeutic agents, there is also a steric hindrance as a consequence of lung geometry. Progressive slimming of wall thickness facilitates gas exchange, the local action of drugs and their potential entrance into the

bloodstream, but unfortunately leaves the body exposed to potentially deleterious agents. However, the gradual reduction of the diameter of pulmonary ducts contributes to prevent their entrance to deep lung regions. The delivery of drugs and nanocarriers targeted to the deepest regions also have to deal with this limitation. Therefore, understanding the processes by which different bodies are retained and deposited into different regions of the lungs could help to optimise drug delivery approaches.

An ancient entrance for novel therapeutic strategies

The respiratory system has been considered as an accessible drug delivery route for thousands of years, when our ancestors burned and inhaled aromatic and medicinal plants to treat problems in the body, relieve the pain caused by injuries, or stimulate the nervous system. The lung provides a non-invasive route and it possesses large surface area, thin alveolar epithelium, high permeability and considerable vascularisation. Nowadays, the inhalation pathway is being considered by an increasing number of therapeutic approaches, both for local and systemic targets[18]. For example, delivering peptidic drugs has been systematically explored using inhalable formulations as an alternative to the non-feasible oral administration[19]. Administration of inhaled insulin, for instance, has been object of intense research and investment with still non-acceptable results, a probable consequence of inefficient strategies to overcome pulmonary barriers in a predictable and quantitative way.

There are many variables that condition the fate of any particle or microorganism entering the airways. As mentioned above, the anatomy of the lung plays an important role. But there are other factors that also affect deposition in lungs, such us the ventilation parameters (breath pattern, flow rates and tidal volume), the place where particles are initially deposited, as well as the physiological or pathological scenarios. In addition to the intrinsic factors of the respiratory context, the particle properties (shape, size, density and surface) are also fundamental[4, 20, 21]. In order to properly classify nanoparticles, in drug delivery the aerodynamic rather than the geometric diameter is extensively used. The former considers size, density and shape of particles as a body, instead of only size, as the latter (e.g. a large porous sphere may have a small aerodynamic diameter but a large geometric diameter)[4].

More than 80% of submicron-size particles are exhaled or expectorated together with the mucus. The rest can be deposited following three main phenomena: inertial impaction, gravitational sedimentation and diffusion[4, 22, 23, 24]. Particles as of 5µm, such us pollen, fungal

spores or fog, settle in the upper airways by inertial impaction. Bodies between 0.4µm and 5µm, like bacteria, the biggest automobile-emitted particles and smog, are usually deposited on the respiratory surface by sedimentation. In the case of viruses, tobacco smoke, smaller automobile-emitted particles or nanoparticles smaller than 0.5µm, they normally reach the alveolar region by diffusion, a Brownian-motion-based phenomenon[22, 25]. The shape, size, density and surface of vehicles should therefore be optimized to efficiently reach the desirable location, to get either local or peripheral action. When the effect is intended to be local, the target will depend on the place where the pain, pathogen or injury are located. However, if the treatment is targeted beyond the lung to other organs, it should reach a region where the surface area, permeability and vascularization is high enough. The upper airways only constitute 5% of the respiratory surface, vascularity is low and clearance by mucus and ciliated cells is highly active[26]. However, the alveolar region possesses 95% of the area, there are plenty of lymphatic and blood capillaries and the trans-epithelial transport is favoured by its thin membranes. A proper combination of drugs and properly designed nanocarriers with pulmonary surfactant could enhance vehiculation over the respiratory surface to alveoli, not only with the purpose of optimizing distribution but also to prevent clearance, which could reduce dosage, side effects and considerably improve efficacy.

Pulmonary surfactant: A promising approach for transporting drugs

Since Kurt von Neergaard suggested in 1929 the existence of a surface active material in the lungs, several studies have been carried out in order to describe its composition, structure and function, as well as the disorders related with its dysfunction or deficiency [27]. However, it was not until 25 years later when the Briton Richard Pattle and the American John Clemens concurrently confirmed the existence of the pulmonary surfactant system [27]. The main function of this material is to reduce surface tension at the air-liquid respiratory interface down to values below 2mN/m, preventing pulmonary collapse during expiration and minimizing the work required to open the lungs during inspiration [28]. Additionally, this material also plays a role in defence, acting as a barrier against pathogens and undesirable elements, serves to maintain the fluid balance across the alveolar-capillary barrier and transports mucus and inhaled particles hindering their adhesion within the upper airways[29].

The absence or disruption of this material impedes the normal breathing cycle. At the first contact of the lungs with the breathing air, alveoli would collapse leading unavoidably to death. Consequently, different surfactants formulations, typically obtained from animal sources, have been developed to take care of preterm neonates, where this essential system has not properly

matured yet. Apart from surfactant replacement therapies (SRTs), new surfactant-based therapeutic advances are currently under study, such as new procedures of PS administration (e.g. aerosolization or nebulisation) or its use as a drug delivery system[29, 30].

Due to its unique biophysical properties, which will be further explained below, pulmonary surfactant has the capability to adsorb very rapidly (within seconds) into the lung air-liquid interface and, once there, to spread efficiently over it. Since it is mainly composed by lipids, it offers a perfect hydrophobic environment to solubilise different poorly water-soluble molecules. Conversely, PS is not an effective agent to retain hydrophilic substances because of intrinsically dynamic and permeable character[30, 31, 32, 33]. Consequently, it is important to combine PS with carriers that could retain not only hydrophobic, but also hydrophilic molecules, whilst they interact and travel associated to PS. In order to better understand the therapeutic possibilities of PS *per se* and as a drug delivery system, it is necessary to firstly revise what pulmonary surfactant is and how it works in the lungs.

A general view of pulmonary surfactant composition, structure and function

Pulmonary surfactant is a lipid-protein surface-active material that coats the whole respiratory surface in mammals. It is synthetized by type II pneumocytes and secreted in the form of multilamellar structures into the alveolar spaces[28]. It is composed of approximately 90% lipids and 10% proteins[34, 35] (see). Although the lipid composition varies between different species[36, 37, 38] and according to environmental[39], physiological[40] or pathological[41] conditions, it is mainly made up of phospholipids, with the saturated species dipalmitoylphosphatidylcoline (DPPC) representing around 40% by mass[30]. Due to its saturated acyl chains, DPPC can reach a highly lateral packed state during compression of alveolar interface, which makes it the key responsible for the surface tension reduction capabilities of surfactant. Apart from DPPC, PS contains other unsaturated phosphatidylcholines (25%) and the anionic phosphatidylglycerol (8%). Additional lipids are phosphatidylethanolamine (5%), phosphatidylinositol (3%), phosphatidylserine and

sphingomyelin, as well as neutral lipids, being cholesterol the most abundant (8-10%)[34, 42].

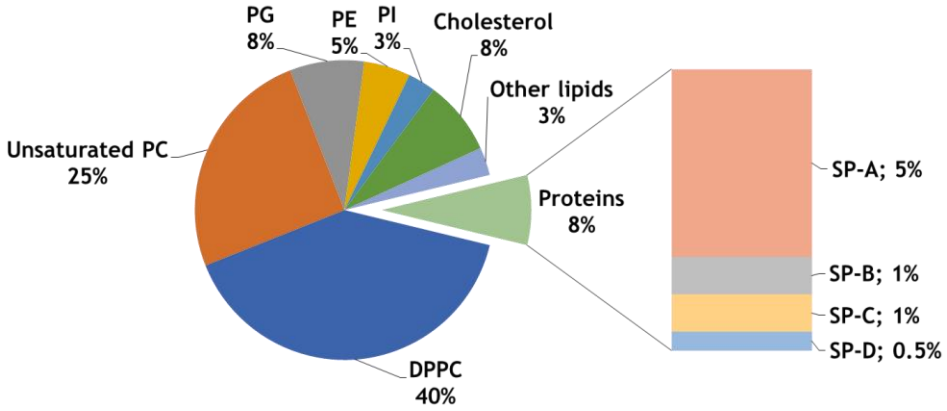

Figure 2: ***Pulmonary surfactant composition.*** DPPC: dipalmitoylphosphatidylcholine; PC: phosphatidylcholine; PG: phosphatidylglycerol; PE: phosphatidylethanolamine; PI: phosphatidylinositol; SP: surfactant protein (elaborated with data from [30]).

Although proteins constitute the smallest percentage by mass in PS, they are crucial for its function. There are four specific surfactant proteins known so far, which can be classified into two different groups: the hydrophobic proteins SP-B and SP-C[34], and the hydrophilic proteins SP-A and SP-D. The formers contribute to mechanical stability of the interfacial films and are directly involved in interfacial adsorption of surface active molecules into the air-liquid interface. It has been demonstrated that deficiencies or lack of surfactant proteins produce severe dysfunctions in the respiratory process. Of particular importance is the lack of total SP-B, which leads to death shortly after birth[30]. The hydrophilic proteins, on the other hand, belong to the C-type lectin superfamily of collectins, whose main functions are related to surfactant homeostasis and the innate host defence, facilitating the recognition, binding, and clearance of pathogens from the lung[43]. SP-A and SP-D also exhibits anti-inflammatory effects, through inhibition of the activation of the complement system, and blocking of the binding of Toll-like receptor (TLR) ligands to TLR2, TLR4 and TLR co-receptors MD2 and CD14 in alveolar macrophages[43, 44, 45, 46].

The different components of pulmonary surfactant are assembled and stored as tightly packed membranes in lamellar bodies (LB) in type-II pneumocytes. These structures have a spherical shape with 1-3μm size and contain multiple concentrically organized membranes[47, 48]. SP-B and the ATP-binding cassette transporter A3 (ABCA3) seem to play an essential role for their biogenesis[28]; ABCA3 would translocate phospholipids at the inner membrane, while SP-B oligomers could form allowing PLs distribution. After contacting and fusing with the plasma membrane, LBs are secreted into the water-lining alveolar subphase. Subsequently, different structures are generated as a consequence of changes in pH, hydration and calcium concentration, finally creating a surface membrane network[28, 47, 49]. Particularly remarkable is the reorganization

of a fair portion of these membranous structures into the so-called tubular myelin (TM), directly formed from LBs and containing numerous square-shaped tubular membrane arrays organised in a net-like structure apparently stabilised by SP-A[47, 50, 51] (see **Figure *3***). This structure has not shown a clear implication in reducing surface tension[52], and it has been speculated that could possesses an antimicrobial role[53, 54], acting as a sticky three-dimensional net trapping microbes and undesirable matter.

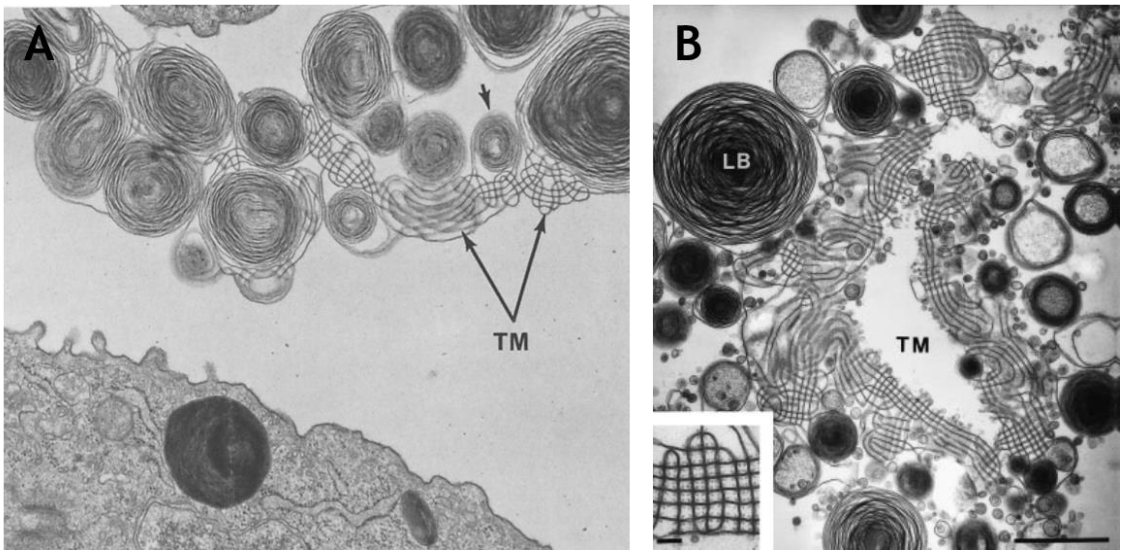

Figure 3: Electron micrograph section of rat lung showing lamellar bodies (LB) and tubular myelin (TM). ***A****: At the bottom of the micrograph a type II pneumocyte with a LB can be appreciated. Also secreted LB (small arrow) and TM (large arrows) are shown [55].* ***B****: LB and TM secreted into the subphase (bar = 1µm). At lower left it is detailed the TM structure (bar = 0.1µm) [35].*

Regarding SP-B and SP-C, both enable the adsorption of new surface active molecules from this network into the air-liquid interface. Once there, PS components form very rapidly a layer that diffuses laterally through the interface[28]. This membrane network of interconnected membranes seems to facilitate the incorporation of new material[28] and O_2 diffusion from the alveolar air spaces into the inner alveolar layers[56]. In an analogous fashion, surfactant could also facilitate the spreading of therapeutic molecules over the respiratory surface to reach the alveolar region.

How pulmonary surfactant works at the respiratory air-liquid interface

Water molecules in the bulk phase attract and interact one to another in all directions, mainly through hydrogen bonds and dipole-dipole interactions. When molecules of water are exposed to air, the attractive interactions unbalance and water tends to minimize the surface area in contact with the airspace, maintaining a constant volume. The force that withstand surface expansion is known as surface tension, which, in the case of water at 37°C is around 70mN/m[54]. At the respiratory surface, lined by a layer of water, a hydrophobic-hydrophilic interface is generated. The

resulting surface tension would hinder the process of breathing, maximising the effort required to expand the alveoli (at inspiration). This is prevented by the presence of a surface active material into this interface, the pulmonary surfactant. Phospholipids, which are the main component of pulmonary surfactant, are amphipathic molecules able to interact with water and, at the same time, orientate their hydrophobic acyl chains to air. As a consequence, they replace interfacial water molecules in contact with air and reduce surface tension to very low values, depending on their interfacial density(see **Figure *4***).

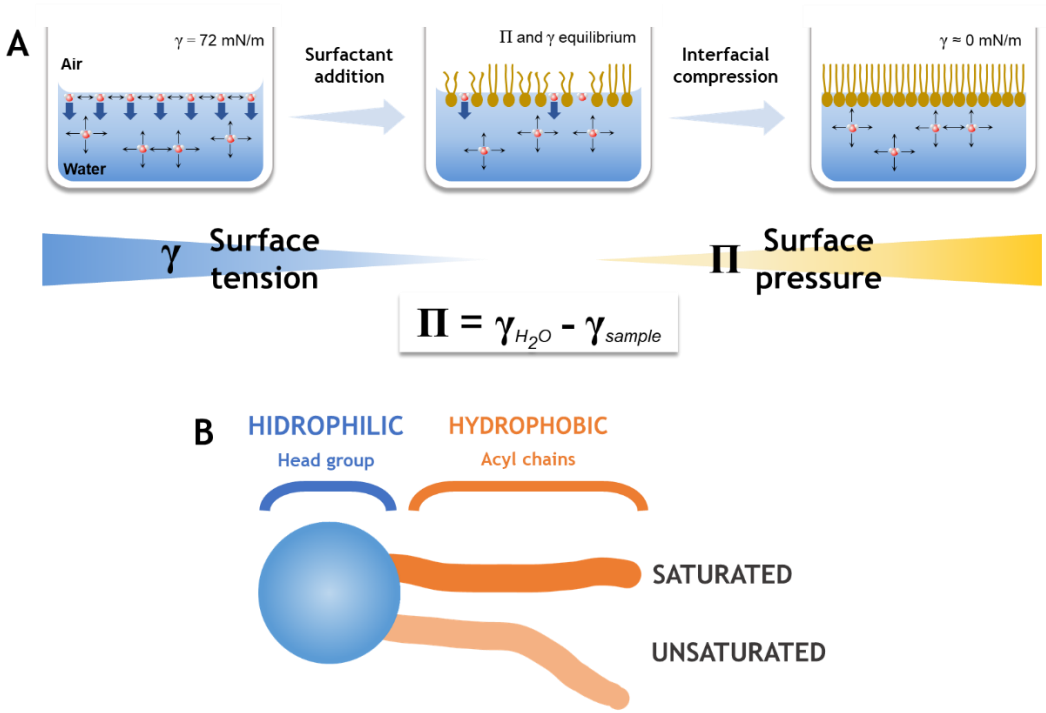

Figure 4: Role of phospholipids in the air-liquid interface. A: Schematic representation of the interfacial behaviour of phospholipids and reduction of surface tension (increase of surface pressure). **B:** *Structure of a phospholipid.*

The alveoli, where pulmonary surfactant is most abundant, are continuously compressing and expanding, forcing the pulmonary surfactant film to adapt to such highly dynamic environment. Thus, surfactant must simultaneously exhibit three essential properties to work efficiently at the interface: (i) very rapid interfacial adsorption to replace used surfactant, (ii) proper compressibility to reach very low (<2 mN/m) surface tension at the endo of expiration and (iii) efficient re-spreading capabilities when alveoli re-expand during inspiration[57]. The high lateral pressures (low tensions) reached during expiration, when the interfacial surfactant film is subjected to compression, produces the exclusion from the interface of those molecules that do not support extreme packing through a process known as squeeze-out (see ***Figure 5***). Once surfactant surface film reaches tensions lower than 25mN/m (surface pressures higher than 45mN/m) during

compression, it folds through three-dimensional transitions, creating a multilamellar reservoir excluded from the interface. Folded layers maintain association with the interfacial films and contribute to its mechanical stabilisation at the minimal tensions (or maximal pressures). At this stage, protein SP-C seems to facilitate the folding of interfacial films, as it appears to induce membrane curvature[58], the exclusion of certain lipids and lipid/protein complexes from the interface[47], and the formation of three-dimensional phases . SP-B, on the other hand, stabilises the interfacial film by endorsing formation of membrane-membrane contacts[59, 60, 61], providing mechanical stability to compressed multi-layered films.

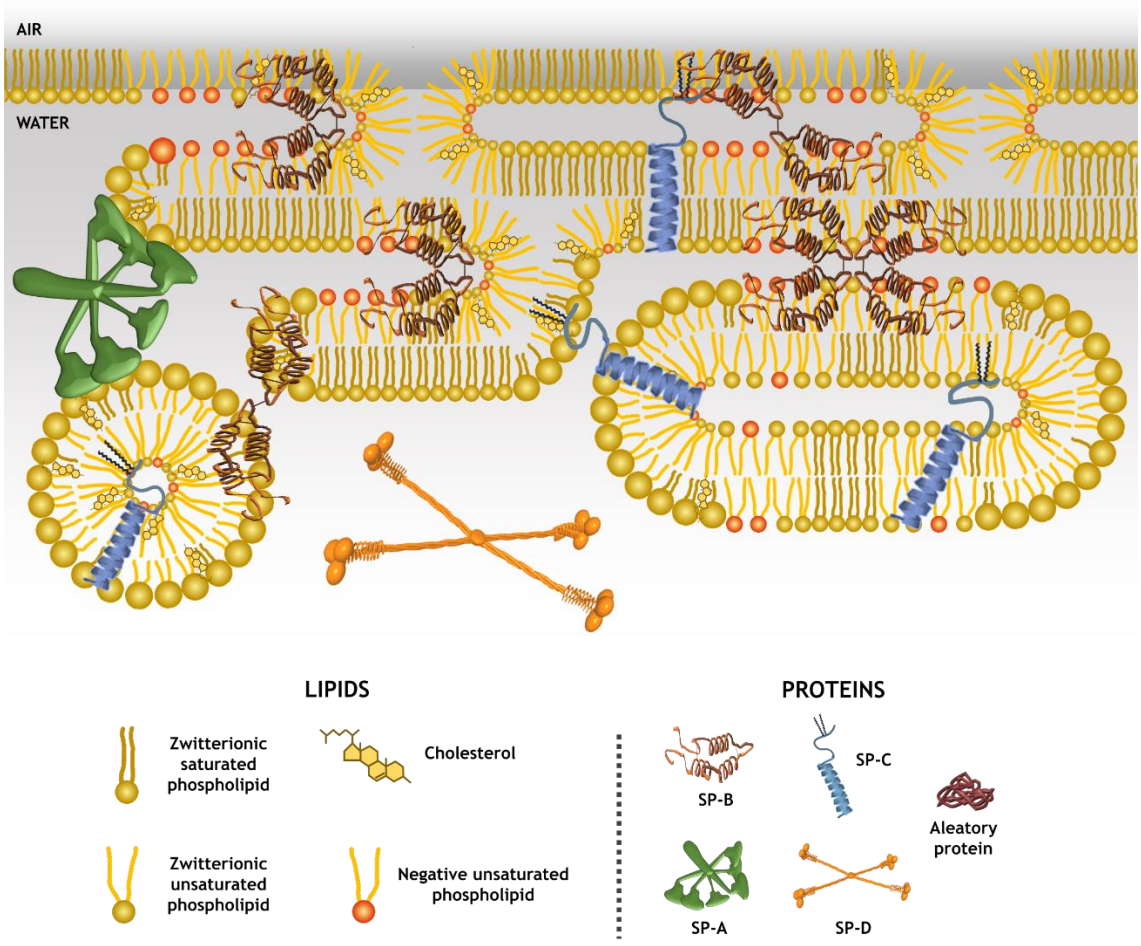

Figure 5: **Interfacial behaviour of pulmonary surfactant.** Scheme representing the complex structure of the interfacial multi-layered membrane-based film established by pulmonary surfactant at the respiratory surface. The main lipid and protein components are represented as they would be assembled in surfactant structures according to current models.

Upon expansion, SP-B and SP-C are thought to promote insertion of new-coming surfactant and re-spreading of phospholipids from the reservoirs back into the interface[28, 30, 61]. Over the continuous compression-expansion cycles at the highly oxidative environment of the respiratory spaces, surfactant components are progressively altered and reorganised loosing activity. This

used and spent material needs to be removed from the alveolar spaces and replaced by new material continuously secreted by type II pneumocytes[62].

Sustainable Cleaning: recycling, clearing and degrading surfactant

As essential as the presence of pulmonary surfactant lining the respiratory surface is to regulate its amount and quality throughout life. The balance between how much surfactant is produced and replenished is critical for the correct homeostasis of respiratory surface. When surfactant is freshly secreted by Type-II pneumocytes, it constitutes large aggregates that rapidly adsorb into the air-liquid interface. Upon compression-expansion cycles and as a consequence of the continuous contact with highly oxidative environment, this interfase-associated material suffers a compositional and structural transformation that ends in its conversion into lighter fractions or small aggregates[63, 64]. These fractions, mainly constituted by small vesicles enriched in low compressible surfactant compounds [65], have been considered as 'used' surfactant and need to be removed from the alveolar lining fluid[65]. To efficiently accomplish this process, which it is estimated to be rapid (10% per hour, approx.[66]), several mechanisms are involved. About 65% of the 'spent' surfactant is uptaken by Type-II pneumocytes and recycled[67], around 20% is cleared by AMφ[15, 67, 68] while the rest 15% is lost through the upper airways via mucociliary escalator[69].

Recycling by type-II pneumocytes

In an attempt to optimize the energy invested during surfactant synthesis, several mechanisms reuptake and reutilize the 'spent' surfactant components, which can be reincorporated into lamellar bodies in Type-II pneumocytes. The predominant recycling pathway proceeds via SP-A-dependant endocytosis, though SP-D[70, 71] and SP-C[58] seem to play additional roles promoting interconversions of the ultrastructure of surfactant. It has been reported that SP-A, by binding to the membrane receptor P63/CKAP4, mediates internalization of phospholipids via clathrin-coated vesicles[72]. Once into the Type-II pneumocytes, phospholipids are arranged in early endosomes and subsequently transferred to lamellar bodies in a calmodulin-dependant manner[73], while SP-A is rapidly re-secreted. In addition to this clathrin-mediated pathway, a nonclathrin actin-dependent endocytosis also happens independently to SP-A, yet it only represents the 3.5% of uptake[74]. Surfactant SP-D is able to interact with lipids through its CRD globular domain [75, 76], and break liposomes *in vitro*. It is hypothesized that SP-D could bind to surfactant membranes and promote their conversion, into small vesicles that could be easily internalised by type II pneumocytes but not macrophages[70, 71]. As a matter of fact, SP-D can interact with the membrane receptor Ig-Hepta/GPR116 expressed in type II cells. The presence

of SP-D in the alveolar lining fluid can be detected by this receptor, which seems to stimulate the recycling pathway but blocks synthesis[77]. Apart from recycling, which is the main pathway, these epithelial cells also export phosphatidylcoline (PC) through the lipid transporter ABCA1 and catabolise surfactant, mainly by the action of phospholipase A2 (PLA2), to maintain proper homeostasis[62].

Clearance by alveolar macrophages

Macrophages are usually in charge of maintaining a low inflammatory context, ensuring the correct function of the tissue, performing non-immune, tissue-specific and homeostatic functions[78]. The microenvironment that macrophages encounter in the lungs is markedly fluctuant and peculiar. The continuous exposure to environmental antigens, hypoxia, oxidation, microflora, airway mucus, surfactant and epithelial cells that constantly change this microenvironment[44], forces pulmonary macrophages (PM**φ**) to adapt to such variable framework. Under homeostatic situations, PM**φ** can be found in several locations where they play location-specific roles: bronchiolar submucosa, alveolar interstitium, vascular adventitia and luminal side of alveoli[79]. Particularly the latter harbours the so-called alveolar macrophages (AM**φ**), while the other PM**φ** are considered as a larger and more heterogenous group, the interstitial macrophages (IM**φ**). Although the ontogeny of M**φ** is still unclear, the development of sophisticated tools to trace haematopoiesis in unperturbed organisms is helping to achieve unprecedented understanding of M**φ** biology. As in other tissue-resident macrophages, steady-state AM**φ** are widely thought, at least in mice, to derive from foetal progenitors rather than by haematopoiesis from adult hematopoietic stem cells (HSCs)[80, 81]. However, it is known that during inflammation and stress situations IM**φ** and adult monocytes-derived M**φ** migrate to alveoli and contribute to alveolar homeostasis[44, 78]. During embryogenesis, several waves of pre-macrophages seed the lungs under the expression of L-plastin, which promotes trans-epithelial migration and colonization of the alveolar space[82]. But it is not until the first contact with air at birth when the actual alveolar niche is generated. Then, circulating foetal monocytes[83, 84] and already-there M**φ**[85] start to acquire the AM**φ**-specific characteristics and markers (i.e. CD11c or SiglecF). Production and secretion of granulocyte-macrophage colony-stimulating factor (GM-CSF) by type-II pneumocytes triggers the expression of peroxisome proliferator-activated receptor gamma (PPAR**γ**), necessary for developing the alveolar M**φ**-specific transcriptomic profile, adapting the cells to the lung environment and acquiring a high lipid load function[84, 86, 87]. However, the Immunological Genome Project has shown that GM-CSF/ PPAR**γ** pathway is present in other tissue-resident M**φ**. Thus

other signals such us the already-known Bach2[88], C/EBPβ[89] and TGFβ[90] must be present for the differentiation and function of AMφ.

Apart from being the guardians of the alveolar surface in continuous communication with the rest of the alveolar-resident and non-resident cells in order to maintain an adequate inflammatory/anti-inflammatory balance[91, 92, 93, 94, 95], AMφ are the cells in charge of pulmonary surfactant clearance[15, 28, 62]. Although a small part of the 'used' surfactant can be also degraded by type-II pneumocytes, AMφ are the main actors. Orchestrated primarily by GM-CSFR/PPARγ signalling pathway, AMφ have developed a sophisticated machinery to uptake, sort and metabolise surfactant lipids and proteins. Examples of proteins that are known to be part of this complex machinery, directly- or indirectly-controlled by GM-CSFR/PPARγ pathway, include: ABC transporters (ABCA1 and G1, implicated in cholesterol efflux), scavenger receptors class II such as SR-BI (involved in the metabolism of cholesterol) or CD36 (associated with cell adhesion, phagocytosis of apoptotic cells and metabolism of long-chain fatty acids), and lysosomal enzymes. Any disruption of these machineries could lead to an impairment of alveolar homeostasis causing pathologies such as pulmonary alveolar proteinosis (PAP) or pulmonary fibrosis.

Surfctant-related pathologies

As described above, the pulmonary surfactant system and a collection of cellular and molecular mechanisms work together to ensure the correct functioning and homeostasis of the lungs. Any inherited or acquired abnormality affecting this complex and perfectly coordinated system lead to both acute and chronic respiratory pathologies. Some of these anomalies, depending on the pathogenic context and age, ultimately end in different clinical syndromes such as neonatal respiratory distress syndrome (NRDS), acute respiratory distress syndrome (ARDS), interstitial lung diseases (IDL), surfactant metabolism dysfunctions (SMD), or combinations of them.

NRDS, also known as respiratory distress syndrome (RDS), is related to the absent of surfactant at the moment of birth. In preterm new-borns this lack of surfactant derives from immature lungs, as pulmonary surfactant is secreted during the last weeks of gestation. This can be easily prevented or reverted nowadays by intratracheal administration of an exogenous surfactant (surfactant replacement therapy; SRT), Exogenous surfactant not only restores the deficiency but contributes to stimulate the production and secretion of endogenous surfactant. surfactant by pneumocytes. In parallel, mothers at risk of premature delivery are usually treated with corticoids to trigger surfactant production in the baby. Completely different is ARDS, which is

associated to lung injury and inflammation and characterised, in children and adults, by interstitial and bloodstream fluid leakage into the into the alveolar spaces, complicating or preventing respiration. Some of the blood components and inflammatory mediators inactivate surfactant by mechanisms that are only partly known, contributing to the pathology. However, surfactant dysfunction is only part of the alterations in ARDS lungs. In enfants, ARDS can also be triggered by meconium or milk aspiration, or as a consequence of severe pneumonia[96]. Interstitial lung diseases, on the other hand, can be originated by several causes such as genetic mutations (i.e. SP-A genes: SFTPA1 and SFTPA2; or essential components of telomerases such as telomerase reverse transcriptase (TERT) or the telomerase RNA component (TERC)) [97], exposure to harmful agents (i.e. silica, asbestos, tobacco smoke or some medications) or autoimmunity. These pathologies ultimately end in scarring (fibrosis) and, consequently, stiffness of the lungs, hindering the process of breathing and finally producing respiratory failure.

When the GM-CSFR/PPAR**γ** pathway is altered in AM**φ**, either by mutations or auto-antibodies[97], the metabolism of pulmonary surfactant fails and it is accumulated into the alveolar spaces. This aberrant accumulation of surfactant, which cannot properly accomplish the biophysical functions, is known as pulmonary alveolar proteinosis (PAP)[98]. Apart from being unfunctional, such amounts of lipids and surfactant proteins obstruct alveolar airspaces impeding gas exchange and triggering the inflammation process. Nowadays, the treatment consists in carrying out bronchoalveolar lavages to remove all surfactant debris. However, this therapy is highly invasive and unpleasant for the patient. Hence, other alternatives such as AM**φ** transplantation are being investigated in mice models with promising results[99, 100].

Mutations in the SP-B gene usually result fatal as, this protein is essential for surfactant synthesis, packing in LB, ultrastructure and interfacial activity, apart from contributing to proSP-C maturation. Mutations in the ABCA3 gene are lethal as well, as this transporter is equally required for LB biogenesis. Deficiencies and abnormalities in ABCA2 have been related to severe diseases in the lungs associated with surfactant homeostasis such as anomalous LBs, dysfunctional pulmonary surfactant or congenital PAP . Finally, although mutations in SP-C gene are not lethal at first instance, they produce several pathologic phenotypes such as fibrosis, inflammation, higher susceptibility to infection and in the worst cases, interstitial diseases ending in respiratory failure at variable ages.

Therapeutic surfactants

Since Mary Ellen Avery and Jere Mead realized that the hyaline membrane disease (current RDS) was due to a deficiency in pulmonary surfactant[101], the idea of a surfactant replacement therapy (SRT) emerged. The first approach was developed using a synthetic surfactant made of only lipids, but resulted to be noneffective as a consequence of the lack of pulmonary surfactant proteins. Without these proteins, surface active lipid films are simply not formed and SRT has no effect[102]. In the 1970s, natural surfactants obtained from animal sources, principally bovine and porcine, started to be studied showing clear clinical improvements in rabbits[103, 104] and lambs[105]. Consequently, in the 1980s several clinical trials were performed in neonates and soon after natural surfactants were established as an efficient treatment for NRDS[106, 107].

Nowadays there are numerous clinical surfactants obtained from porcine and bovine sources by mincing lungs (Curosurf® from Chiesi Farmaceutici; Survanta® from Abbot Laboratories) or by performing saline bronchoalveolar lavages (Surfacen® from CENSA; Infasurf® from Forest Laboratory; Alveofact® from Boehringer Ingelheim; Bles® from BLES Biochemicals). Although they present differences related with composition and functional, morphological, interfacial and biochemical features [42], all of them are approved for treating Respiratory Distress Syndrome by SRT.

Nonetheless, these animal-derived surfactant preparations are relatively susceptible to inactivation, may present substantial batch-to-batch variations, are expensive to produce and supplies are limited. An additional major problem is the non-null possibility of animal-to-human transmission of potential pathogenic agents. Hence, other non-animal preparations that could allow producing surfactant in large quantities at reasonable cost while controlling composition and reducing inactivation/susceptibility are preferred. In this sense, entirely synthetic surfactants are currently proposed as a potential choice, but some considerations are critical regarding alveolar stability and appropriate performance *in vivo*. As mentioned, not only lipids, specially DPPC, but also the hydrophobic proteins SP-B and SP-C, or at least analogues of these proteins, are essential to sustain proper surfactant dynamics [102]. This was the reason why Exosurf®, the first synthetic surfactant formulation designed by GlaxoWellcome to contain only lipids, was not as effective as animal-derived surfactants [108]. The complex lipid composition of pulmonary surfactant and the troubles derived from production of effective SP-B and SP-C analogues make the production of synthetic surfactants with clinical application still challenging and not resolved issue.

In spite of the difficulties, there are some advances. Different SP-B and SP-C analogues have been synthetized emulating some structural motifs and biophysical properties of the native

proteins, exhibiting a reasonably good behavior [109]. Thus, new surfactant formulations are emerging in the recent years. The KL_4-based surfactant [110], Surfaxin®, is the unique entirely synthetic surfactant that has reached the market and is indicated for the prevention of RDS in preterm infants. Venticute®, a surfactant containing recombinant SP-C [111], has been studied in the VALID trial, a multi-national clinical phase III investigation, but has not been approved yet as no benefits were observed in mortality rate or blood oxygenation, probably because of the absence of SP-B [108]. Another synthetic surfactant that shows promising effects is CHF 5633, which is composed by two phospholipids (DPPC and POPG (1-palmitoyl-2-oleoyl-sn-glycero-3-phosphoglycerol)) and both SP-B and SP-C analogues. In comparison with an animal derived surfactant (Curosurf®), CHF 5633 seems to produce significant benefits in premature lambs whose endogenous surfactant is inactivated [112].

Pulmonary surfactant as a shuttle for drug delivery

The exceptional properties of pulmonary surfactant were early suggesting the idea of using it to transport therapeutic agents deep into the distal airways. The hydrophobic components of PS provide a perfect environment to host poorly soluble drugs and nanocarriers, and bring about the opportunity to accomplish novel and creative approaches for treating not only respiratory pathologies, but also others alongside the body [4]. Furthermore, the ability of PS to spread along the air-liquid interface could help to deliver drugs directly into the alveolar region, something difficult to achieve using current strategies. The combination of drugs or nanocarriers with PS can hide and protect them from clearance in the lung. As a consequence, it could facilitate reduction of doses, secondary effects and costs, as well as producing synergistic effects while increasing local effectiveness. On the other hand, in a similar manner to the exclusion of pulmonary surfactant components from the interfase upon compression-expansion cycling during breathing, the additional passengers that may share the interfacial trip could be progressively released once at the alveolar spaces. Altogether PS-based drug delivery could open new avenues to more personalised, precise and efficient therapies in respiratory medicine.

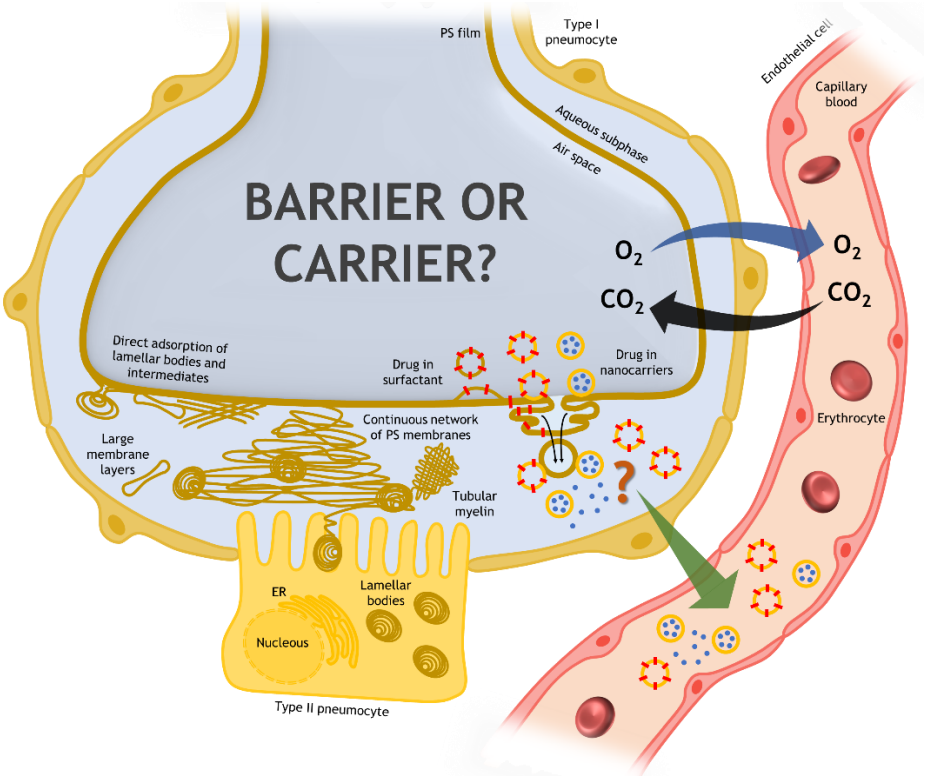

Figure 6: Schematic representation of an alveolus and associated blood capillary showing the vehiculizing strategy concept.

The feasibility of using pulmonary surfactant as a carrier was demonstrated during the 1990s. In 1999, Herting *et al.* demonstrated that administering a specific IgG combined with Curosurf® to newborn babies suffering from group B streptococcal (GBS) pneumonia, improved lung function and decreased bacterial growth, with no negative effects in PS nor IgG actions [113]. Since then, extensive work with antibiotics[114, 115, 116], antimicrobial peptides[117], recombinant adenoviral vectors[118], antioxidant enzymes[119], corticosteroids[120, 121, 122] or nanocarriers[123, 124, 125, 126, 127, 128] combined with surfactant, have demonstrated synergistic effects and promising perspectives not only *in vitro* and *in silico*, but also *in vivo*, evidencing the unlimited possibilities of pulmonary surfactant as a drug delivery system.

Key aspects in surfactant-assisted drug delivery

The use of pulmonary surfactant as a drug delivery system calls requires keeping in mind several important aspects concerning the way it is administered and how the lung environment and the expected target will condition the strategy to follow.

i) Friendly administration:

The current method of clinical PS administration is based on intratracheal instillation. Such methodology requires hospitalization and intubation, something that could produce acute airway

obstruction, hypoxia and bradycardia[129], is unpleasant for the patient, takes a lot of time and is expensive. The possibility of using non-invasive and patient-friendly formulations is strongly preferred and is now an intensive matter of research. Administering synthetic PS as a dry powder was briefly studied during the 1980s [130, 131]. Judging by the latest advances in dry powder inhalers (DPIs) for drug delivery [132], this method could be a promising strategy, but no recent studies have evaluated the possibility to deliver dry preparations of synthetic or natural PS. Nebulized formulations were tested with no satisfactory results in the 90's [133], but the recent advances in nebulizing technology have considerably improved surfactant nebulization. Furthermore, recent *in vivo* studies have shown promising results during continuous positive pressure ventilation (CPAP) in spontaneous breathing rabbits (synthetic surfactant)[134] and preterm lambs (Curosurf®, a porcine-derived surfactant)[135, 136], where surfactant was better distributed into the whole lung and some physiological parameters (oxygenation and lung function) were also improved with respect to intratracheal instillation[136].

ii) Endogenous surfactant status

When the pathological condition requiring intervention includes an impairment of the endogenous surfactant function, the exogenous surfactant must work properly and possess intrinsic prophylactic and therapeutic effects by itself, regardless the addition of drugs or combined nanosystems. It is widely accepted that surfactant replacement therapy is effective in preventing different lung diseases such as NRDS[96] or bronchopulmonary dysplasia (BPD)[137], and can ameliorate certain cases of acute lung injury (ALI)[138] and even asthma attacks[139]. Simultaneously, different anti-inflammatory and antibiotic drugs are being used to treat these diseases or to alleviate inflammation derived from the respiratory support techniques used for SRT[120, 121, 122, 140]. Therefore, a combination of both is starting to be used with promising results. It is important to take into account that the pathogenic surfactant-inactivating context may also affect the therapeutic surfactant or surfactant/drug preparation. Thus development of inactivation-resistant surfactants may potentiate therapeutic strategies in these cases.

On the other hand, when the endogenous surfactant works properly, a dose of exogenous surfactant can be used as a mere excipient to vehiculize the therapeutic agent, with interfacial adsorption and spreading properties being the most important properties that the surfactant vehicle should maintain. In this sense, the optimization of synthetic surfactants gains prominence, where PS composition and properties should favour an efficient drug delivery, and not necessarily that much the intrinsic surface-stabilization properties. Nevertheless, surfactant overdose may

impair the phagocytic activity of lung macrophages [141] and result in acute airway obstruction or problems with fluid and electrolyte balance. Thus, the surfactant dose here is crucial and need to be optimised to maintain the vehiculizing properties while reducing the potential toxicity.

iii) Nature of the treatment

Although pulmonary surfactant constitutes a highly favourable environment for transporting hydrophobic agents directly dispersed into it, it is not a proper container for hydrophilic compounds due to its intrinsic dynamism and the high porosity of its membranes [32, 33]. New advances in nanotechnology could allow the generation of optimized nanocarriers that could encapsulate hydrophilic and hydrophobic drugs while properly interacting and travelling associated within pulmonary surfactant.

iv) Mutual surfactant/drug/nanocarrier effects

The biophysical effects of antituberculotic drugs on PS surface performance have been studied using DPPC monolayers as a model. The research performed by Chimote and Banerjee in 2004 combined DPPC with either isoniazid (INH) or a triple drug mixture (INH/rifampicin/ethambutol) and observed that both combinations achieved superior surface properties than DPPC alone [142]. More recently, another study evaluated the impact of rifampicin (Rif) on the biophysical activity of Curosurf® and Survanta®. These experiments, performed in a pulsating bubble surfactometer, showed that Curosurf® was able to incorporate higher amounts of Rif and that the antibiotic interfered with both therapeutic surfactants in a concentration-dependent manner [143]. Additionally, other antibiotics (amikacin, cefepime and colistimethate sodium) have also been studied, revealing the impact of the drugs in PS and vice versa. Amikacin and cefepime did not affect PS while colistimethate did. When the impact of PS on antibiotics were evaluated, amikacin was the only antibiotic that was no affected [144].

Understanding the effects that nanocarriers have on PS is essential to optimize the design and production of improved drug delivery systems through the airways, not only to avoid deleterious effects but also to optimise synergistic effects from their combination. Drugs and nanocarriers can directly or indirectly affect the functional properties of surfactant. They could induce pulmonary inflammation[145, 146], oxidative stress and lipid peroxidation[147, 148], indirectly leading to PS impairment[149, 150]. The transference of surfactant components, especially the hydrophobic and positively charged proteins SP-B and SP-C, to nanocarriers during the so-called corona formation (adsorption of a layer of molecules at the surface of the nanostructures) is in

essence the factor determining the direct detrimental effects of nanocarriers on surfactant[124, 151, 152, 153, 154]. It is known that the hydrophobicity, size and surface charge of nanocarriers determine the formation of the surfactant corona[155]. Furthermore, the adverse effects of certain nanocarriers also depend on the administered dose; at low doses the initial interfacial adsorption and dynamic surface tension were not negatively affected, while at higher loads they were [152].

v) Local or peripheral target

The target is another important aspect to consider, which defines the development of novel drug delivery approaches. For instant, if the target is to treat tuberculosis, drug vehiculization should pursue reaching the alveolar region and then internalization by AM**φ**, where *Mycobacterium tuberculosis* completes its life cycle. On the other hand, if the target is a different location over the body, drug delivery needs to go through several barriers including type I pneumocytes, the capillary endothelium and the immune system. Therefore, it is crucial to understand pathophysiology and homeostasis in the lung to design, optimize and evaluate novel drug delivery strategies.

OBJECTIVES

Levering the exceptional interfacial properties of the pulmonary surfactant system, the main objective of this Thesis is to explore the potential of pulmonary surfactant to vehiculize different therapeutic agents through the airways using the air-liquid interface, setting the basis of a novel and less-invasive strategy, the interfacial therapy. In order to accomplish this objective the following specific aims are proposed:

1. Stablish and optimize different strategies to combine several molecules of medical interest with clinical and synthetic pulmonary surfactants.
2. Evaluate the possible detrimental effects of the vehiculized molecules on the interfacial behaviour of pulmonary surfactant.
3. Verify the vehiculizing potential of different surfactant formulations through *in vitro* air-liquid interfaces.
4. Determine the implications of compression-expansion breathing dynamics on the interfacial vehiculization of drugs by pulmonary surfactant.
5. Confirm the feasibility of surfactant-assisted interfacial vehiculization *in vivo*, determining the main factors implicated and testing its potential synergistic surfactant/drug therapeutic effects.

MATERIALS AND METHODS

In this section, only the most general materials and methods are described. The specific techniques, procedures and materials used to perform the experiments on each chapter are conveniently explained on the corresponding chapter. Unless otherwise stated, all chemicals were purchased from commercial suppliers (Sigma-Aldrich®, Merck KGaA or Macron Fine Chemicals™) and used without further purification. Water was from a Merck-Millipore Direct-Q3 purification system.

PULMONARY SURFACTANT SYSTEMS: THE VEHICLES

Native pulmonary surfactant

The isolation of native surfactant was carried out from bronchoalveolar lavages (BAL) obtained from porcine lungs, following a protocol optimized at the laboratory [149, 156, 157]. Concisely, BALs were performed by introducing a buffer solution (5mM Tris, 150mM NaCl, pH 7.4) through the trachea, while massaging vigorously the lungs. Each lavage was filtered to remove the tissue debris and centrifuged at 1000g, 4 °C during 5 minutes to eliminate cells and debris. Then, it was ultra-centrifuged in an angular rotor at 100,000g during 1 hour at 4 °C. The pellet was resuspended and ultra-centrifuged in a discontinuous NaBr density gradient during 2 hours at 120,000g in a swinging-bucket rotor. Finally, the purified PS complexes, located between the 0% and 13% NaBr layers of the gradient, were obtained and homogenised in NaCl 0.9%, storing them as small aliquots at -80 °C until used (see **Figure *7***).

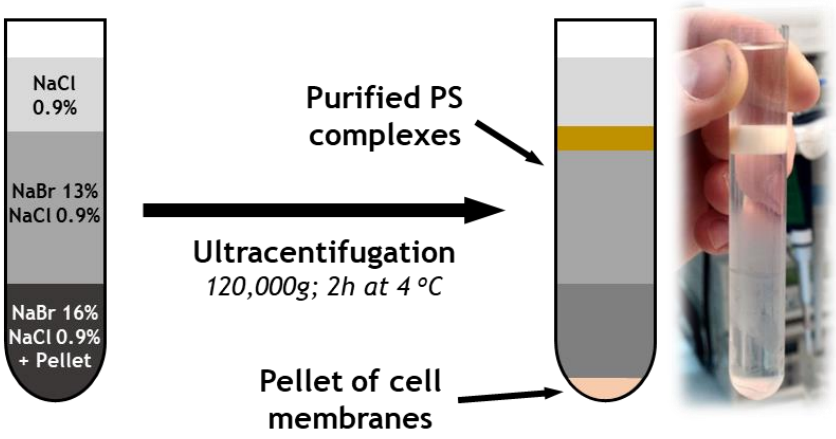

Figure 7: ***Density gradient used to purified pulmonary surfactant.*** *It allows for separating the surfactant complexes from the rest of material with a higher density, mainly rests of erythrocytes and white blood cells.*

Poractant Alpha (Curosurf®)

Poractant Alpha (Curosurf® or Csf) is a modified natural surfactant produced by reconstitution of a hydrophobic lipid/protein fraction obtained from minced porcine lungs. It is

commercialised by Chiesi Farmaceutici (Parma, Italy) for clinical use. It contains polar lipids and the hydrophobic surfactant proteins (SP-B and SP-C), with no cholesterol, and is served at a phospholipid concentration of 80 mg/mL. When needed, it was diluted with a buffer solution (5mM Tris, 150mM NaCl, pH 7.4).

CHF5633

CHF5633 is a fully synthetic surfactant containing equimolar proportions of dipalmitoylphosphatidylcholine (DPPC) and 1-palmitoyl-2-oleoyl-*sn*-glycero-3-phosphoglycerol (POPG) and peptide analogues of the hydrophobic surfactant proteins SP-B (CWLCRALIKRIQALIPKGGRLLPQLVCRLVLRCS) and SP-C (IPSSPVHLKRLKLLLLLLLLILLLILGALLLGL) [112]. It was also provided by Chiesi, at a concentration of 80 mg/mL. When needed, it was diluted with a buffer solution (5mM Tris, 150mM NaCl, pH 7.4).

Organic extracts

Organic extracts (OE) from NS, Poractant alfa or CHF5633 were obtained as described by Bligh and Dyer [158]. Firstly, proteins were flocculated by incubating 30 minutes at 37 °C in the presence of chloroform and methanol mixed at the proportions chloroform/methanol/water 1:2:1 (v/v/v). To allow the formation of two phases, a new volume of chloroform and water were added to the mixture and then centrifuged at 3000g and 4 °C during 5 minutes. In order to rescue the maximum amount of PS components, successive lavages with chloroform and methanol were performed. After each lavage, the hydrophobic components of NS were collected from the organic phase at the bottom and storage at -20 °C until used.

MEMBRANE-BASED VEHICLES

Multilamellar vesicles and organic extract reconstitution

To prepare multilamellar vesicle (MLV) suspensions, an appropriate volume of a chloroform/methanol (2:1 v/v) solution of the DPPC/POPG (7:3 w/w) mixture (lipids obtained from Avanti Polar Lipids Inc.), or of the organic extracted materials, was dried under a nitrogen stream and then under vacuum for two hours to remove organic solvent traces. The dried films were then hydrated with a buffered solution (5 mM Tris, 150 mM NaCl, pH 7.4) at 45 °C, a temperature above the melting temperature of all the lipids in the mixtures (T_m = 41°C for DPPC). The hydration was accomplished in one hour with vigorous shaking every 10 min.

Large unilamellar vesicles

Large unilamellar vesicles (LUVs) of DPPC/POPG (7:3 w/w) were prepared by extruding MLV suspensions several times through polycarbonate membranes of 100 nm pore size (Whatman® Nuclepore Track-Etched Membranes, 19mm diameter, 0.1µm pore) in a mini-extruder (Avanti Polar Lipids Inc.), to obtain a relatively homogeneous suspension of unilamellar vesicles of ca. 100nm diameter. The extrusion was also carried out at 45°C.

PASSENGERS

Corticosteroids

Beclomethasone dipropionate (BDP), in the form of powder, or taking part of the aqueous suspension Clenil®, was provided by Chiesi Farmaceutici (Parma, Italy). Budenoside (BUD) powder was also obtained from Chiesi, and its solubilised formulation (Pulmicort®) was purchased from Astra Zeneca (Södertälje, Sweden). To determine the amount of the steroid incorporated into the surfactant membranes, an aliquot of 10 µL of BDP-containing surfactant was diluted in 1 mL of methanol and the absorbance of the solution was measured at 235nm (ε_{235}= 0.0704 $M^{-1}cm^{-1}$). The fluorescent derivative of BDP (BANB) was synthetized and provided by Prof. Guillermo Orellana's laboratory (Department of Organic Chemistry, Faculty of Chemistry, Complutense University, Madrid, Spain). The synthesis is briefly summarised in the *Vehiculization troughs* section of the *Chapter I* (for additional details, see supplementary in [159]).

Tacrolimus

Tacrolimus (TAC or FK506, +98%) was provided by Sinoway Ind. Co. (China) in the form of powder. The fluorescent derivative (TAC·NileBlue) was synthetized by Prof. Guillermo Orellana's laboratory following an analogous method described by Glahn-Martínez *et al.* [160] and provided in the form of powder.

INCORPORATION OF THE PASSENGERS INTO SURFACTANT MEMBRANES

In order to incorporate the corticosteroids into the surfactant preparations, three different protocols have been followed. In a first type of experiments, the proper amount of corticosteroid, diluted in methanol, was dried on the wall of plastic tubes under a nitrogen flow. Then a volume of 50 µL of different surfactant or lipid suspensions were added into the tubes and incubated for 30 min at 37°C, with stirring every 10 min. Alternatively, BDP or BUD were directly incorporated into organic extracts from NS or Poractant alfa and the mixture was then dried and resuspended in saline following the same protocol than used for the formation of membranes (1h, 45 °C,

vigorous shaking every 10 min, see section *Multilamellar vesicles and organic extract reconstitution*). In a third alternative, BDP or BUD were incorporated into clinical surfactants Poractant alfa or CHF5633 upon incubation with clinical formulations of the corticosteroids such as Clenil® or Pulmicort®. For some experiments, Clenil-like corticosteroid emulsions were previously prepared by combining the excipients of Clenil to solubilize the proper amount of BDP, the mixture BDP/BANB (see below), or BUD.

In the case of TAC, it was previously diluted in methanol and then directly incorporated into the DPPC solution in chloroform/methanol (2:1 v/v) or the organic extract obtained from NS, as convenience. When needed, the mixtures were conveniently reconstituted in a buffered solution as described above in the section *Multilamellar vesicles and organic extract reconstitution*.

PHOSPHOLIPID QUANTIFICATION ASSAY

The concentration of phospholipid was evaluated following a protocol established by Rouser *et al.* in 1966 [161]. It is a colorimetric methodology based on the quantification of the phosphorous present in phospholipids after conversion to inorganic phosphate using perchloric acid at 260 °C. The colorimetric reaction took place at 100 °C for 7 minutes after addition of water, ammonium heptamolybdate 2.5% (w/v) and ascorbic acid 10% (w/v). Finally, the absorbance at 820 nm of each sample was determined in a UV/Visible spectrometer (Beckman DU840) and interpolated in a standard curve made with inorganic phosphate (KH_2PO_4). Due to the heterogenic composition of pulmonary surfactant, the molecular weight of DPPC (734.04 g/mol) was considered to calculate its mass as it is the most abundant phospholipid in the pulmonary surfactant system.

SURFACE TROUGHS

In the present Thesis the traditional Langmuir-Blodgett and Wilhelmy troughs have been used to design and optimize two novel *in vitro* models of the respiratory air-liquid interface, one static and the other dynamic. The idea is to study the potential use of pulmonary surfactant as a drug delivery system and the implications of compression-expansion breathing-like cycles on this novel strategy. **Figure *8*** shows a schematic representation of a basic surface trough and the elementary components. The surface pressure sensors having a Wilhelmy plate were purchased from NIMA technologies (Coventry, UK). The Wilhelmy plate (21 mm perimeter; 24 mm x 10 mm x 0.5 mm) was made with a grade 41 Ashless Filter Paper (Whatman®, GE Healthcare Life Sciences). The Langmuir-Blodgett trough was also purchased from NIMA technologies. The Wilhelmy trough was designed in collaboration with the UCM Research Support Centre (CAI).

Both the static and dynamic setups will be further explained in the *Key techniques* section of Chapter I and Chapter II, respectively.

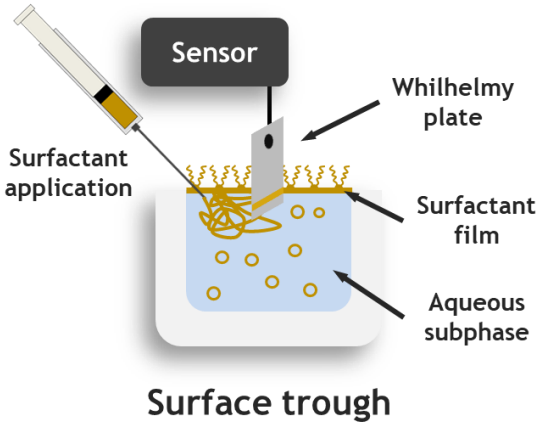

Figure 8: ***Schematic representation of a surface trough.***

FLUORESCENCE SPECTROSCOPY

In order to investigate the vehiculizing potential of pulmonary surfactant, the molecules transported by pulmonary surfactant were measured in both donor and recipient troughs using an Aminco Bowman Series 2 spectrofluorometer. The two fluorescent drug derivatives evaluated in this thesis were labelled with an analogous of NileBlue, a far red fluorescent dye ($\lambda_{excitation}$ = 590 nm; $\lambda_{emission}$ = 650 nm). The emission spectra were taken at 25 °C and the sensitivity was set differently for the samples from the donor and recipient troughs as considerably more amount of fluorescent molecules were in the donor. Every sample were stored at 4 °C in dark conditions until measured to avoid the photobleaching of the sample.

FLUORESCENCE MICROSCOPY

To analyse the structure of DPPC monolayers and surfactant films, images were taken from films doped with 1% (molar ratio) NBD-PC (Molecular Probes®, Thermo Fisher Scientific), transferred as Langmuir-Blodget films onto glass coverslips in continuous compression conditions (barrier speed: 25 cm^2/min; deeper speed: 5 mm/min). Images were acquired with an ORCA R2 10600 (Hamamatsu Photonics K.K.) camera coupled to the epifluorescence microscope Leica DM 4000B (Leica Microsystems). The fluorescence microscope is an optical microscope that uses fluorescence to observe the sample of interest with the light source coming from the top (epifluorescence) and falling upon the upper side of the sample. In some experiments, the fluorescent derivative of tacrolimus was added conveniently as a trace (1% by mass with respect to lipids); when the amount of drug was higher than 1% by mass, the rest was completed with non-modified drug.

For the experiments performed *in vivo* to determine which type of cells internalised tacrolimus, the images were taken under the Olympus IX-81 inverted fluorescence microscope at the laboratory of Prof. Jahar Bhattacharya in Columbia University in New York City. In this case, the fluorescent derivative of tacrolimus was used to track the drug over the lungs (1.5% by mass with respect to lipids).

ATOMIC FORCE MICROSCOPY

This technique scans the surface of a sample measuring its topographical profile. A tip connected to a flexible structure (cantilever) interacts with the sample and oscillates upon the differences in height. The oscillation is detected by the reflexion of a LASER focused on the top of the tip (Figure *9*). This technique allows analysing the lateral organization of phospholipid films and the three-dimensional structures formed associated to pulmonary surfactant. The preparations were made following the same method as used for epifluorescence microscopy but transferring the films to mica plates, instead. Mica is a multi-layered structure whose layers are atomically flat and very easy to exfoliate, offering a perfect background for topographical profiling. The measurements of DPPC monolayers were taken by using an AFM MultiMode SPM (Digital Instruments, Inc./Veeco Metrology Group) at the UCM Research Support Centre (CAI) for Microscopy in Madrid (Spain). In the case of the experiments performed with surfactant films, the measurements were taken using a NanoWizard II AFM (JPK Instruments, Berlin) at the Unidad de Biofisika (CSIC, UPV/EHU) in Bilbao (Spain) in contact mode, using silicon nitride tips and cantilevers E and D. The data were processed using the JPK Data Processing software.

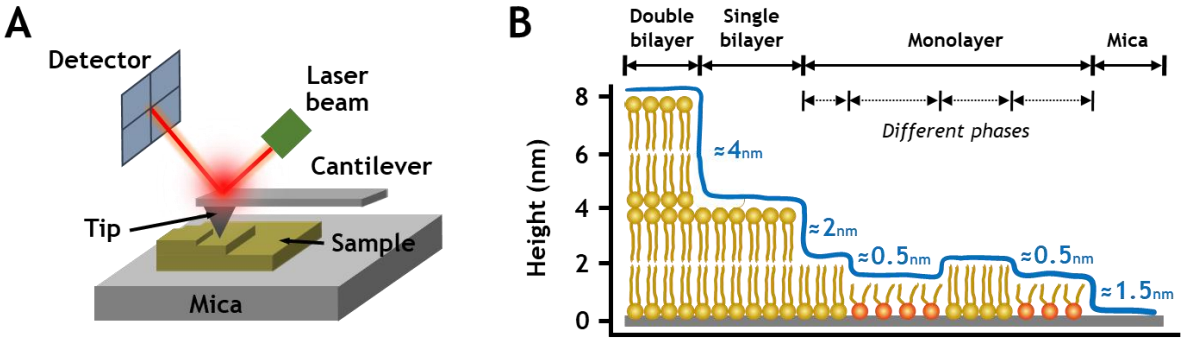

Figure 9: Schematic representation of an AFM. ***A)*** *Representation of the main components of an AFM. The AFM scans the surface of a sample and determine the topographical profile. This is detected by means of the reflexion of a LASER that is focused on the top of a tip placed at the end of a flexible structure (cantilever). The surface-promoted movements of the cantilever change the reflexion angle of the LASER and it is translated into differences in height, obtaining a topographical profile.* ***B)*** *Correspondence of the topographical profile with the structures observed in phospholipid samples.*

The results included in the present chapter were published in the article:

- Hidalgo, A., F.; Fresno, N.; Orellana, G.; Cruz, A.; Perez-Gil, Jesús. Efficient interfacially-driven vehiculization of corticosteroids by pulmonary surfactant. *Langmuir* **2017,** *33* (32), 7929-7939.

CHAPTER I:

The proof of concept

INTRODUCTION

The development of innovative drug delivery strategies is essential to increase the efficiency and efficacy of therapies, while targeting drugs to precise locations avoiding systemic side effects. As aforementioned, more than 90% of new drugs are poorly soluble in water. Therefore, the investigation of new strategies to facilitate solubilization of new generation drugs and to establish novel sites for drug entry is acquiring high importance nowadays. This chapter presents a proof of concept of the vehiculizing capacity of pulmonary surfactant to establish the basis of a protocol to optimise the combination of PS and drug passengers. Regardless of the drug, nanocarrier or whatever passenger to be vehiculized by surfactant, this work proposes that the optimization of the vehiculization process requires the systematic characterization of three essential issues *in vitro* prior to evaluate vehiculization *in vivo*: (a) how the therapeutic agent can be incorporated into natural or synthetic surfactants, (b) whether the presence of the drug affect surfactant function, and (c) whether the combination with surfactant enables the distribution of the drug over the air-liquid interface.

In this study, two hydrophobic drugs, the corticosteroids beclomethasone dipropionate (BDP) and Budesonide (BUD), were selected as an example to show the vehiculizing potential of pulmonary surfactant through the respiratory air-liquid interface and to design the general protocol to optimize it. These compounds are anti-inflammatory drugs widely used to treat different respiratory diseases, such as asthma or bronchopulmonary dysplasia (BPD)[162, 163, 164]. In particular, the combination of BDP and PS has shown synergistic effects to reduce certain markers of inflammation[122], improving respiratory function in preclinical models [121]. Moreover, clinical pilot studies utilized intra-tracheal instillation of BUD suspended in pulmonary surfactant to improve its delivery to the lung periphery for the prevention of BPD. They reported a substantially reduced incidence of BPD with no observed immediate or long-term adverse effects [165]. For local action in the lungs, BDP or BUD are currently delivered in the form of aerosol, but new systems are needed to reduce systemic exposure, lung clearance and the total dosage, as well as to reach other target locations such as distal airways more efficiently. Nowadays several clinical surfactants obtained from bovine or porcine sources are being used to treat preterm new-borns[4, 42], and new synthetic preparations are under development[112, 166]. Therefore, it is crucial to investigate and compare the abilities of clinical surfactants of different nature to transport different passengers as these corticosteroids.

In the current work, a surfactant preparation produced from minced porcine lung tissue (Curosurf®), and, CHF5633, a fully synthetic surfactant containing surrogates of hydrophobic

proteins SP-B and SP-C, have been selected and compared with whole native surfactant purified from porcine lung, with respect to their capabilities to incorporate and vehiculize BDP or BUD over the air-liquid interface. The interaction of BDP with PS membranes was first studied to optimize incorporation of corticosteroids into surfactant complexes. Then, the effect of BDP or BUD on the PS behaviour was analysed using a Captive Bubble Surfactometer. Finally, the spreading properties and corticosteroid transporting potential of PS was evaluated with selected drug/PS combinations applied in a novel setup that couples two traditional Wilhelmy troughs connected by an interfacial bridge.

KEY TECHNIQUES

Captive Bubble Surfactometer

In 1989, Schurch *et al.* published a method that somehow reproduced the interfacial dynamics of an alveolus *in vitro*, the captive bubble surfactometer (CBS). It allows to evaluate surfactant activity at the surface of a millimetre-sized air bubble confined into an aqueous solution. The bubble is subjected to several compression-expansion cycles, mimicking breathing dynamics at physiological conditions of temperature, humidity and pH[167]. As explained above, pulmonary surfactant prevents pulmonary collapse during the expansion of alveoli and needs to withstand continuous compression and expansion dynamics *in vivo*. In order to ensure that any extra compound combined with surfactant does not alter its functionality, every surfactant/drug combination needs to be tested under physiologically-relevant conditions in the CBS.

This unique device allows to perform four different sequential experiments to (i) evaluate the initial adsorption to the air-liquid interface (initial adsorption), (ii) test the post-expansion adsorption and re-spreading once the bubble is subjected to a first expansion (post-expansion adsorption), (iii) analyse the behaviour of interfacial films during 4 slow compression-expansion cycles, where the bubble is reduced or enlarged in discrete steps (quasi-static cycles), and (iv) study the behaviour of the films during 20 cycles of continuous compression and expansion preformed during 1 minute, a rate similar to the normal breathing rate in humans (dynamic cycles).

To start the assay, 200 nL of the sample to be tested at a lipid concentration of 25mg/mL, is injected into a buffered subphase containing sucrose to increase density (150 mM NaCl, 10% sucrose (p/v), 5 mM Tris, pH 7.4) inside a cylindrical sealed thermostatised chamber. The injection liberates the surfactant close to the interface of a small air bubble (around 4-5 mm diameter), previously formed and settled on the base of an agarose cap that acts as a hydrated

support. The bubble can then be compressed and expanded by mean of a piston driven by a computer-controlled engine (see Figure 10). Volume, surface area and surface tension can be calculated and monitored along the whole experiment by measuring the height and the diameter of the bubble. The experiment is recorded by a video camera and then analysed by a specific software[168, 169].

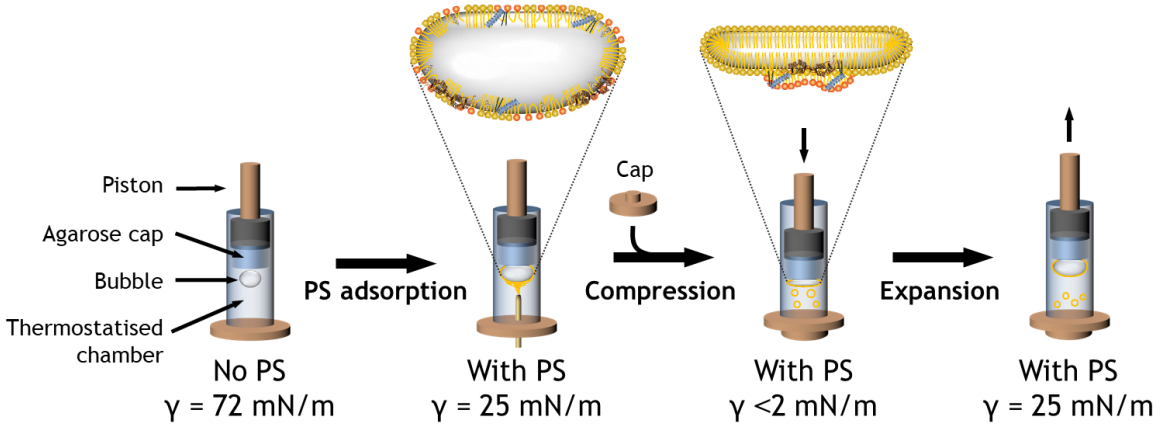

Figure 10: ***Operational scheme of captive bubble surfactometer (CBS) experiments.*** CBS experiments start with the injection of a small volume (typically 200 nL) of concentrated surfactant (25 mg/mL phospholipid) near the surface of a millimetre-sized air bubble formed in a thermostated chamber containing a buffered dense saline solution. After 5 min to allow surfactant for adsorption and further 5 min after expansion of the bubble to facilitate surfactant spreading to form a surface active film, the chamber is closed and subjected to compression-expansion cycles mimicking breathing dynamics.

Vehiculization troughs

In order to evaluate the ability of pulmonary surfactant preparations to efficiently travel and vehiculize drugs along the air-liquid interface, a novel setup was designed in the laboratory based on the original Yu and Possmayer's design[170]. This novel device, named double or vehiculization trough, mimics somehow a respiratory surface *in vitro* and consists of two surface troughs connected by an interfacial bridge (a hydrated No. 1 Whatman filter paper). A small volume of any surfactant sample, with or without the drug, can be deposited by injection into the aqueous subphase, or spreading or nebulizing directly onto the interface of one of the troughs (donor), which is assumed to mimic the upper airways. Once adsorbed into the donor interface, surfactant is expected to diffuse through the interfacial bridge (conductive airways) and reach the recipient trough (distal airways). This interfacial trip is continuously monitored by following the changes in surface pressure (or surface tension) in both donor and recipient troughs (see Figure 11). To control the experimental temperature, the set-up is confined in an isolated container and continuously thermostated. Subphase in both troughs usually consists in buffer (5 mM Tris, 150 mM NaCl, pH 7.4) to maintain pH under control.

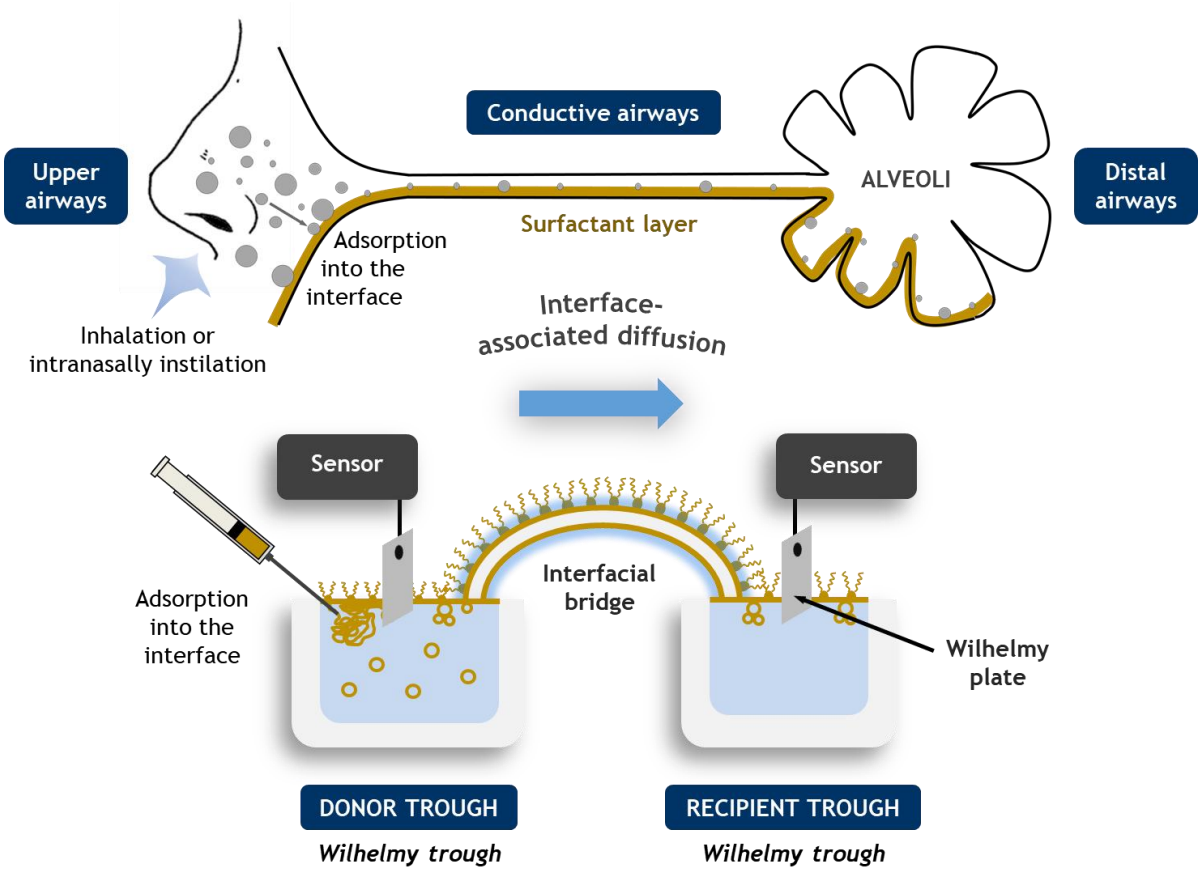

Figure 11: ***Concept of the vehiculization trough.*** Consisting of two different Wilhelmy troughs connected by an interfacial bridge, the vehiculization trough reproduces a respiratory surface in vitro. Pulmonary surfactant is deposited into the donor trough (upper airways) and is expected to travel interfacially through the interfacial bridge (conductive airways) to finally reach the recipient trough (distal airways). The process is continuously monitored by measuring the surface pressure in both donor and recipient troughs.

Following this concept, several variants can be designed to approach specific situations. Although this device is highly versatile, there are three critical parameters that need to be considered when designing the experiments and analysing their results: surfactant concentration, surface area of the troughs and size of the interfacial bridge. Previous work in our laboratory showed that, under limiting conditions of surfactant concentration (<10 mg/mL), differences in spreading velocity were observed depending on the size of the interfacial bridge (data not shown). However, at the concentration used to perform the experiments in this Thesis (50 mg/mL), those differences are negligible. In this case, the recipient surface area is determinant and it is necessary to contemplate it when comparing experiments. The larger the recipient area, the longer time is needed for the surface pressure to start rising and reach the equilibrium surface pressure, as more material is required to cover the whole interfase. Concretely in this chapter, the donor surface area was 315 mm^2; the recipient 106 cm^2).

To evaluate if surfactant can transport any kind of passenger, it has to be detected it in the recipient trough. The election of the detection method not only depends on the passenger (fluorescence, HPLC, mass spectrometry, electrophoresis, microscopy, etc.), but also on the available amount at the recipient trough. As the trip depends on the concreted moment of molecular layers over the, the total amount of vehiculized molecules is limited by the recipient surface area. The larger the surface area, the higher the amount of molecules available for detection. Therefore, a method sensitive enough is required to detect the vehiculized entities in small quantities, otherwise there is a risk to incur false negatives. An additional possibility is to increase the amount of molecules collected from the interfase.

In this Thesis, the most frequent method to detect the vehiculized drug was fluorescence, in many cases upon repeated collection of the material at the recipient interface. In this chapter, in order to follow the diffusion of corticosteroids between donor and recipient troughs, a fluorescent-labelled derivative of beclomethasone dipropionate (BANB, Figure 12) was prepared. The synthesis of BANB involves saponification of beclomethasone dipropionate (BDP) into beclomethasone, followed by oxidation of the latter with periodic acid to a carboxylic acid derivative (BC, Figure 12). Finally, conjugation of BC to an amine derivative of the strongly fluorescent dye NileBlue (ANB) is carried out by amidation, after activating the BC with a mixture of 1-ethyl-3-(3-dimethylaminopropyl)carbodiimide and 1-hydroxybenzotriazole to provide the beclomethasone-Nile Blue conjugate (BANB, Figure 12). BANB was purified by column chromatography on silicagel upon eluting the raw product with a chloroform/methanol/NH_4OH (6:1:0.1 v/v/v) mixture. The fluorescence (λ_{ex} = 590 nm; λ_{em} = 650 nm) was measured in samples taken from both donor and recipient troughs using an Aminco Bowman Series 2 spectrofluorometer.

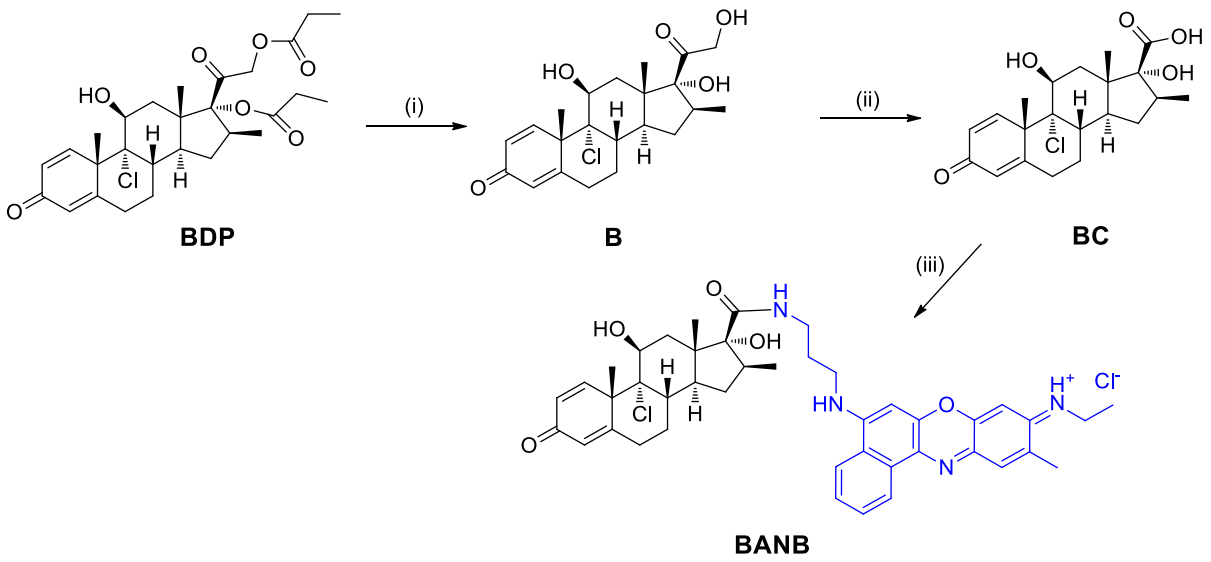

Figure 12: ***Synthesis of the far-red fluorescent derivative of beclomethasone tagged with pseudo NileBlue (BANB).*** Reagents and conditions: (i) $KHCO_3$, MeOH, 72 h, r.t.; (ii) H_5IO_6, dioxane/H_2O, r.t., 48 h; (iii) 1-ethyl-3-(3-dimethylaminopropyl)carbodiimide hydrochloride (EDC · HCl), amino pseudo Nile Blue (ANB) derivative, 1-hydroxybenzotriazole (HOBT), Et_3N, CH_2Cl_2, r.t., 24 h.

RESULTS

Incorporation of corticosteroids into surfactant membranes

In order to evaluate the amount of drug that the different lipids systems were able to incorporate, an identical amount of BDP (100µg) was dried on plastic tubes and exposed to increasing total amounts of different lipid and lipid-protein suspensions, including NS and its organic extract, and MLVs and LUVs made of DPPC/POPG (7:3, w/w). After incubation at 37 °C during 30 min shaking every 10 min, each mixture was separated into two fractions: (a) the membrane suspension bearing the solubilised drug and (b) the remaining drug on the tube walls. The amount of BDP was then evaluated by absorption measurements, where an aliquot of 10µL of BDP- or BUD-containing surfactant was diluted in 1mL of methanol and the absorbance measured at 235 nm (ε_{235}= 0.0704 M-1cm-1). **Figure 13** represents the percentage of BDP that was found associated to the membrane lipids as a function of the amount of lipid. The fraction of drug associated with lipid membranes rose following a linear trend, while the drug that remained on the tube decreased with a similar slope.

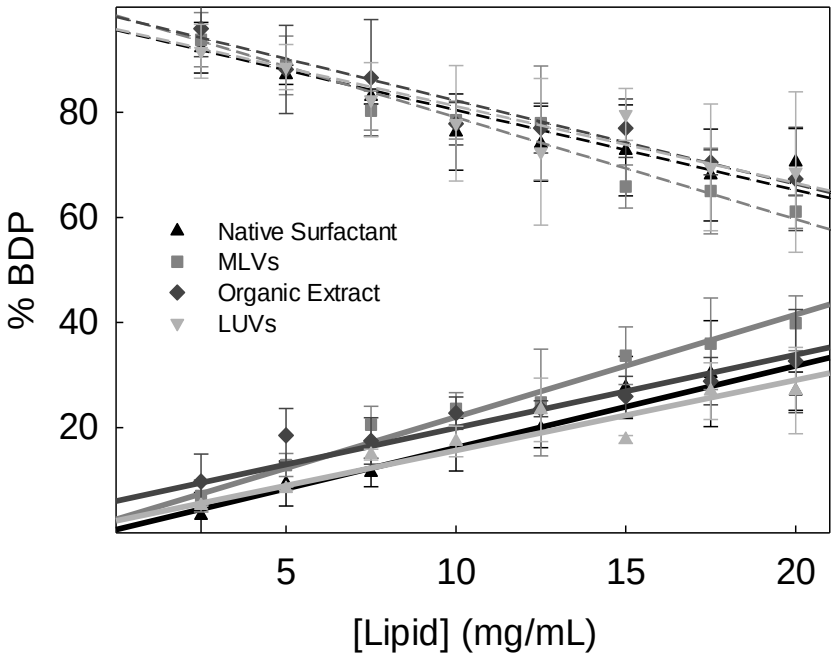

Figure 13: ***Incorporation of BDP into surfactant lipid and lipid/protein suspensions.*** The proportion of corticosteroid (100 μg) incorporated (solid lines) and non-incorporated (dashed lines) from dried films into suspensions of NS, its organic extract, or MLV or LUV suspensions made of DPPC/POPG (7:3, w/w), has been plotted as a function of the concentration of phospholipid. Lines represent the linear plots that better fit the experimental data.

To confirm whether the different lipid suspensions follow a similar saturation tendency as an evidence of the drug incorporation into the membranes, different amounts of BDP were exposed to identical lipid concentration (20mg/mL) of the different surfactant materials. **Figure 14**A shows how each sample incorporates the drug following an apparent hyperbolic saturation curve. At lower drug/lipid ratios, LUVs of DPPC/POPG apparently captured more drug compared with the other samples. Suspensions of NS or of its OE followed very simillar trends, but capturing slightly less drug than pure lipid unilamellar suspensions. MLVs, on the other hand, were the samples capturing less drug at low drug/lipid ratios, likely because only the outer layers are effectively exposed to the drug. However, at higher drug/lipid ratios, MLVs tend to exhibit similar drug loading capacities than the other analysed preparations. In **Figure 14**B, the saturation curves of BDP incorporated into the clinical surfactants Poractant alfa and CHF5633, can also be compared. Interestingly, they exhibit similar ability to solubilize BDP than native surfactant or its organic extract, in both qualitative and quantitative terms. At lower drug/lipid ratios Curosurf® seems to incorporate more amount of BDP than CHF5633, in a similar manner to LUVs (see Figure 14). However, it saturates at lower amounts of BDP than any other assessed preparation.

Regarding CHF5633, it follows a similar tendency to native surfactant or its organic extract (see Fig. 6), being able to incorporate more amount of BDP than Curosurf®.

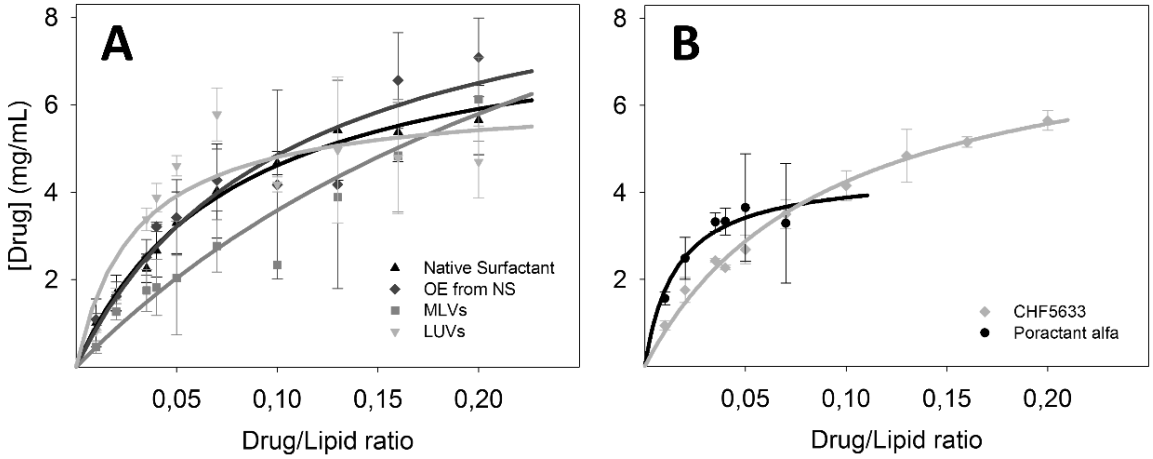

Figure 14: ***Saturation curves of different pulmonary surfactant materials by BDP.*** The capacity of different pulmonary surfactant lipid or lipid/protein suspensions to incorporate the corticosteroid has been assessed by plotting the amount of incorporated drug vs. the total amount of drug (drug/lipid weight ratio) at which the suspensions have been exposed. A) Saturation curves for NS, its organic extract and MLV and LUV pure lipid suspensions (DPPC/POPG, 7:3 w/w). B) Saturation curves for clinical surfactants Poractant alfa and CHF5633. Lines represent the best fit of experimental data to a hyperbolic saturation curve.

Impact of corticosteroids on surfactant functional properties

Once established that the drug interacts and is incorporated into surfactant complexes, the impact of the drug on the biophysical properties of surfactant to form and sustain surface active films under physiological constrains was analysed using the CBS. At 10% BDP/lipid ratio, most surfactant preparations were above its 80% saturation limit and, therefore, this amount of corticosteroid was selected to analyse the effects of the presence of the drug on the interfacial behaviour of the different surfactants. In **Figure 15** the activity of NS and its reconstituted OE is analysed and compared in the absence and in the presence of 10% BDP.

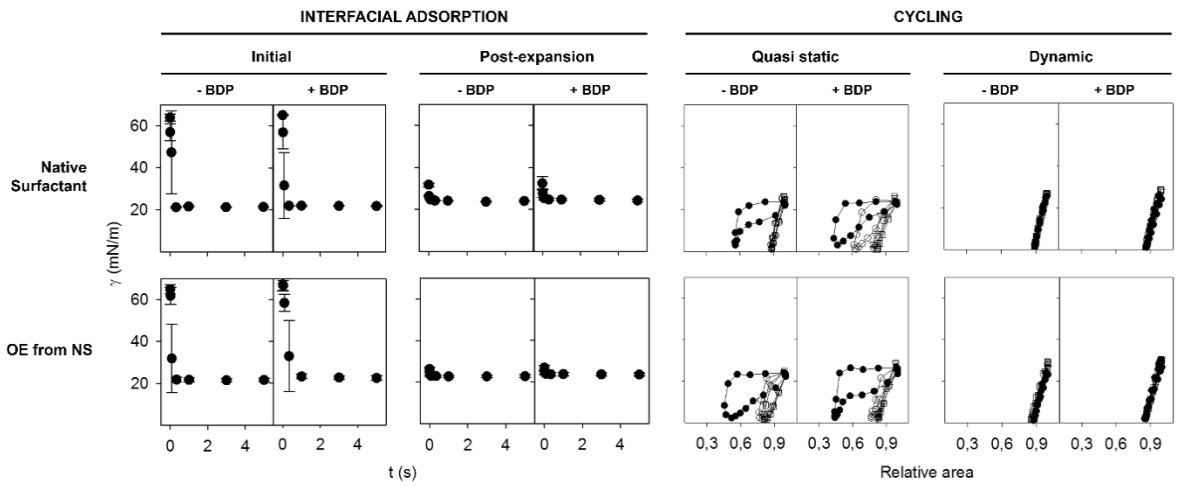

Figure 15: ***Effect of BDP on the functional behaviour of NS and its organic extract, as assessed in the CBS.*** Π-t interfacial adsorption kinetics are compared in the absence or presence of BDP, for suspensions of NS (above) and of its organic extract (below), during either initial (left) or post-expansion (center left) adsorption. Data are average and error bars the standard deviation upon averaging the results of three different experiments. Representative Π-A compression-expansion isotherms, obtained during slow quasi-static (center right) or rapid breathing-like dynamic (right) compression-expansion cycling are also compared in the presence or absence of the drug. In the graphs the four quasi-static (1^{st} to 4^{th} from left to right) and 1^{st}, 10^{th}, and 20^{th} dynamic cycles are compared.

Both, native surfactant and its organic extract showed very good initial and post-expansion interfacial adsorption that was not substantially affected by the presence of drug. This means that the presence of the corticosteroid into the surfactant complexes does not alter their ability to rapidly associate to the air-liquid interface, to transfer lipid surface active species to form an orientated surface film that reduces surface tension to equilibrium values around 22-24 mN/m (seen in initial adsorption kinetics), and to spread and replenish the interface from associated structures once it is expanded (assessed in post-expansion adsorption). The main differences introduced by the presence of BDP are observed at the quasi-static compression-expansion isotherms. In these experiments, compression-expansion cycles are applied to the bubble in discrete slow steps, intercalated by lapse periods of time during which the film can relax. The analysis of these isotherms allows getting information about the compressibility properties and the stability of the films, which can reorganize or experiment three-dimensional transitions usually detected by the presence of plateaus at the isotherms. These reorganizations or plateaus, typically observed in the first cycles, would be only partially detected under the kinetically limited conditions imposed by rapid compression-expansion cycles mimicking breathing dynamics. Q-static isotherms displayed in **Figure 15** show how the presence of the corticosteroid induces the manifestation of plateaus into the compression legs, and, as a consequence, isotherms that require larger area reductions before the minimal tensions are reached. Frequently, several slow compression-expansion cycles are required before the isotherms of the films containing BDP are

stabilized to produce the lowest tensions with minimal area reduction (see Q-static isotherms of NS in the presence of BDP). The higher hysteresis of Q-static isotherms of NS and OE in the presence of BDP is likely associated with a compression-driven progressive exclusion of the drug from the interface, because the rapid dynamic compression-expansion cycles carried out afterwards produce non-hysteretic isotherms indistinguishable in the absence and presence of the drug.

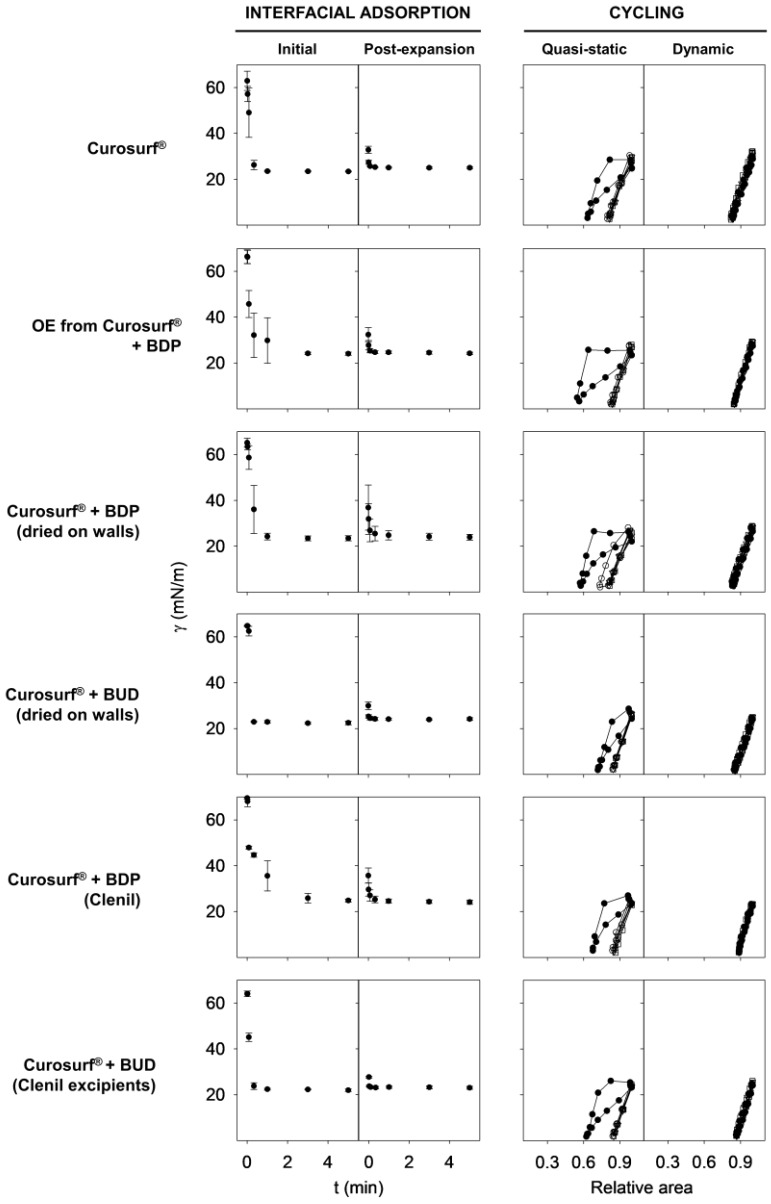

Figure 16: ***Effect of corticosteroids on the functional behaviour of Poractant alfa.*** Interfacial adsorption either upon initial injection at the surface of an air bubble at the CBS or upon bubble expansion has been compared for Poractant alfa alone (first row) or loaded with 10% (w/w with respect to phospholipid) BDP (2nd, 3rd and 5th rows) or BUD (4th and 6th rows) through different protocols. Plotted in the left panels are mean data with standard deviation after averaging three different adsorption experiments. Right panels show illustrative isotherms for cycles 1-4 under quasi-static and cycles 1, 10 and 20 under rapid dynamic compression-expansion regimes applied to the different films.

In **Figure 16** the functional behaviour in the CBS of the clinical surfactant Poractant alfa is evaluated in the absence or presence of the corticosteroids BDP or BUD. The figure also compares the effect of the drugs incorporated by the different protocols. As observed in the adsorption and compression-expansion isotherms of NS and OE, the presence of any of the corticosteroid, incorporated by any of the tested protocols, minimally affected the performance of surface films formed by Poractant alfa once subjected to compression-expansion dynamics. Initial adsorption of Poractant alfa was slightly affected by the presence of BDP, particularly when the drug was premixed with the surfactant material in organic solutions, presumably because that maximizes the incorporation of the drug into deep regions of surfactant lipid-protein complexes. Initial adsorption was also somehow slightly slowed when BDP was incorporated into Poractant alfa as part of Clenil. This is likely a transient effect of Clenil excipients, as observed upon exposure of Poractant alfa to equivalent emulsions BDP-free Clenil excipients (see **Figure *17***). However, in all the experiments, and once the interface of the bubble was opened, post-expansion adsorption was equally rapid in the absence and in the presence of the drug, indicating that the inhibition mechanism is by competition for the interface, instead of altering the composition of any surfactant elements.

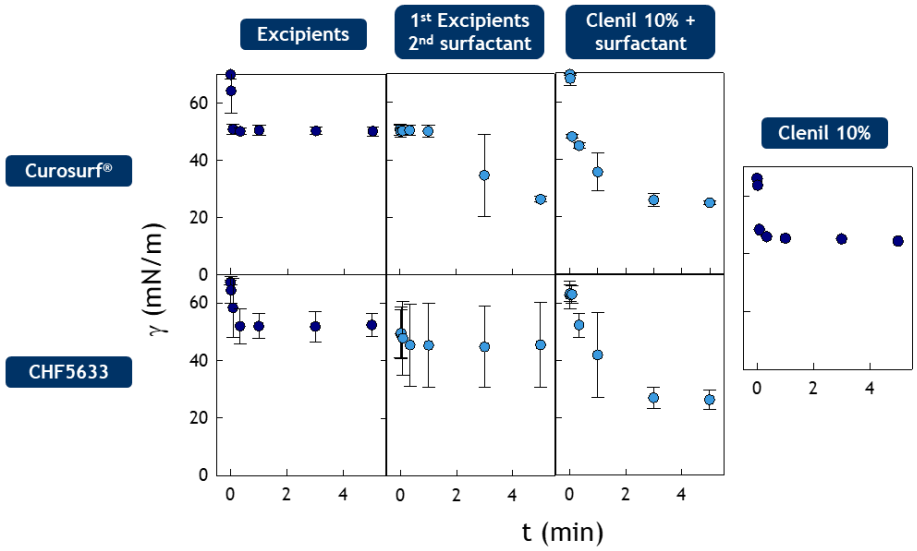

Figure 17: ***Excipients and Clenil effects on initial adsorption of Poractant alpha and CHF5633.*** Clenil® and its excipients clearly adsorb into the air-liquid interfase and affect the interfacial adsorption of both Poractant alpha and CHF5633, likely due to an inhibition by competition for the interface. This effect is more accentuated when the excipients are injected before surfactant than a mixture of both and CHF5633 seems to be more susceptible. Each plot represents the mean data with standard deviation after averaging three different experiments.

As illustrated in **Figure 18**, the reconstituted surfactant CHF5633 can also incorporate 10% by weight of BDP or BUD with respect to phospholipid without relevant impairment of its functional properties. Initial adsorption of CHF5633 alone often produces not very low surface tensions at

first instance. However, upon interfacial expansion, this surfactant almost instantaneously reduced surface tension to equilibrium tensions of aprox. 25 mN/m, indicating the ultimate efficient transfer of surface active lipids into the interface. CHF5633 films could then reduce surface tension further to very low values of around 2 mN/m upon repetitive compression-expansion cycling. Interestingly, corticosteroid-loaded CHF5633 samples exhibited improved interfacial adsorption from the initial contact with the air-water interface, likely as a consequence of the slight perturbation introduced by the incorporated drugs on membrane fluidity. Neither BDP nor BUD altered substantially compression-expansion isotherms of CHF5633 films, as observed in the quasi-static or dynamic -A isotherms in **Figure 18**.

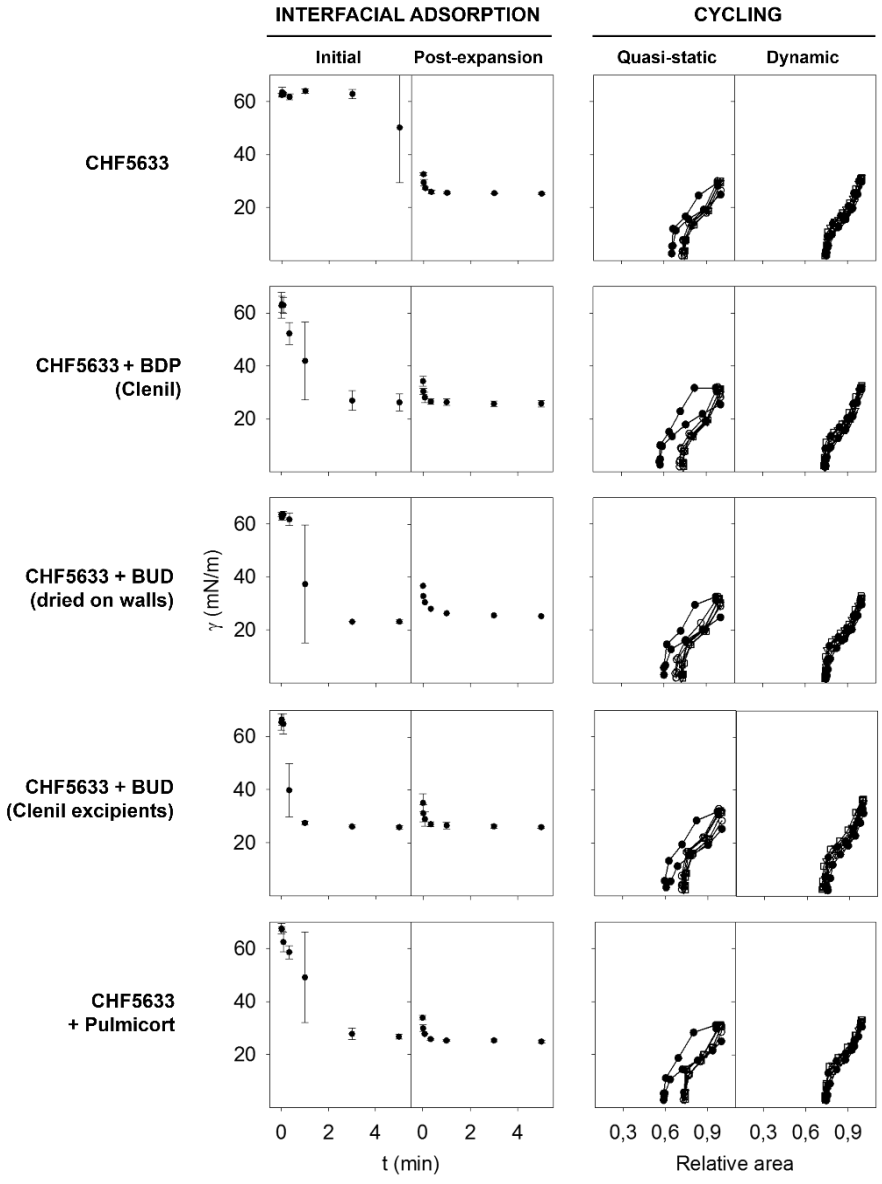

Figure 18: ***Effect of corticosteroids on the functional behaviour of CHF5633.*** Interfacial adsorption either upon initial injection at the surface of an air bubble at the CBS or upon bubble expansion has been compared for CHF5633 alone (first row) or loaded with BDP (2nd row) or BUD (3rd, 4th and 5th rows) through different protocols.

Plotted in the left panels are mean data with standard deviation after averaging three different adsorption experiments. Right panels show illustrative isotherms for cycles 1-4 under quasi-static and cycles 1, 10 and 20 under rapid dynamic compression-expansion regimes applied to the different films. The amount of drug in the different experiments was 10% (w/w with respect to phospholipids) except for BUD incorporated from Pulmicort, whose proportion was 1%, the maximal amount allowed by the dilution of CHF5633 with Pulmicort to reach the operational surfactant concentration.

Interfacial vehiculization of corticosteroids

To assess whether incorporation into surfactant allows an efficient transfer and spreading of the drugs, we used a novel custom-made experimental design. As described in the *Vehiculization troughs* section, two different troughs (donor and recipient) were connected, each monitored by a surface pressure sensor, by an interfacial bridge. PS samples, in the presence or in the absence of the drug, were introduced into the donor trough, and following the changes in surface pressure in both troughs we could monitor adsorption and movement of any surfactant material through the air-liquid interface.

Figure 19 summarizes the adsorption/spreading isotherms of different materials from the donor trough, where they were originally introduced, to reach the recipient compartment via diffusion through the air-liquid interface.

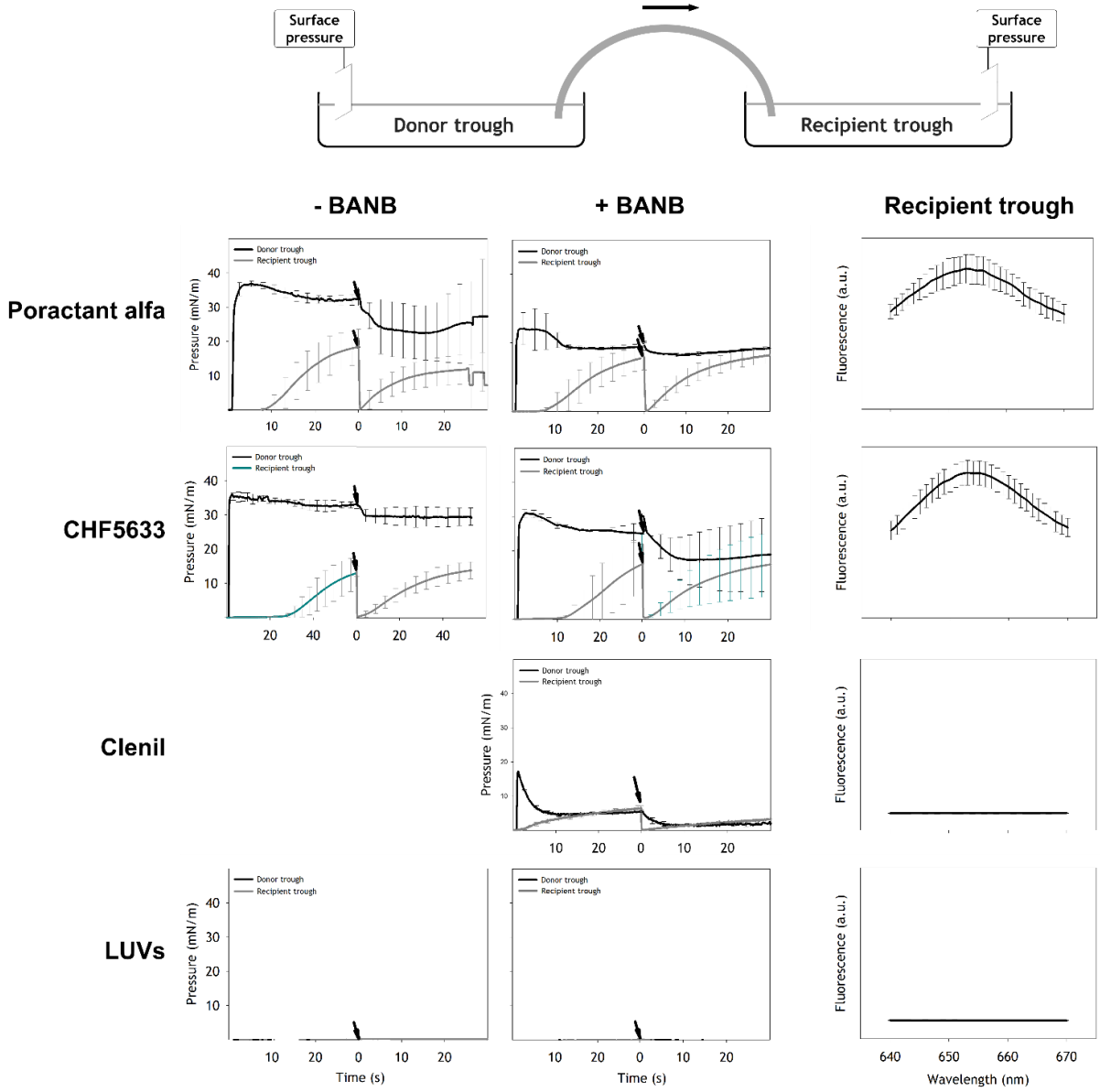

Figure 19: ***Pulmonary surfactant-assisted interfacial vehiculization of corticosteroids.*** Compared are adsorption/spreading isotherms of Poractant alfa (first row) and CHF5633 (second row) in the absence (left panels) or presence (central panels) of BDP/BANB (9% total drug/phospholipid, 1% fluorescent probe), as measured by the increase in surface pressure detected in the donor (black line) or in the recipient (grey line) trough of a setup such as the one illustrated in the upper cartoon. At the time indicated by the arrow, interfacial material was harvested by suction at the surface of the recipient trough and further changes with time of surface pressure were continuously followed as additional material was diffusing again from the donor trough. Data represent mean and standard deviation after averaging three different experiments. Compared are also adsorption/spreading isotherms of BDP/BANB Clenil (3rd row), or of a sample of DPPC/POPG (7:3, w/w) LUV liposomes (4th row) in the absence or presence of 10% BDP/BANB. On the right, the fluorescence emission spectra are compared of samples taken from the recipient trough at the end of the experiments.

When an aliquot of any of the two clinical surfactants tested, Poractant alfa or CHF5633, was deposited at the donor trough, an immediate increase of surface pressure up to around 35-38 mN/m was recorded. After a lag time of aprox. 5-7 min, surface pressure started to increase also at the recipient trough, once the material adsorbed into the air-water interface of the donor

chamber diffused along the interfacial connecting bridge. The increase in pressure in the recipient trough was accompanied by a slight decay in pressure at the donor chamber, indicating the transfer of material between the two compartments. However, surface pressure at the donor trough never dropped below 30 mN/m, indicating that transfer of material towards the recipient chamber was associated with a continuous adsorption and replenishment of further material from the donor subphase. At a given time during the experiment (indicated by an arrow in the panels of Figure 9), the interfacial material at the recipient trough was cleared by aspiration, which produced an immediate decay in surface pressure. However, this decay was rapid and subsequently compensated by new adsorption and transference from the donor trough. This □-t kinetics demonstrated that there is a rapid and continuous connection of the two chambers via the air-liquid interface, and that this interfacial space can be used for a rapid interface-driven spreading and diffusion of surfactant material. The interfacial transfer of material between the two troughs could be followed in a comparable way when either Poractant alfa or CHF5633 were introduced in the donor trough. Interfacial transfer kinetics of these two materials were not affected when either of the two clinical surfactants were preloaded with 10% of BDP (with 1 % (w/w) consisting of the fluorescent analogue BANB), confirming that the inclusion of the corticosteroids did not alter the ability of the surfactants to adsorb and spread along the interface. Interestingly, when the material spread at the interface of the recipient trough was collected and taken to the spectrofluorometer, the fluorescence spectrum of the probe could be easily detected (see right panels in Figure 9), indicating that the drug had diffused from the donor to the recipient chambers following the surfactant. The lower panels in Figure 9 illustrate how the introduction in the donor trough of a pure lipid sample (DPPC/POPG 7:3 w/w liposomes) produced a marginal increase in pressure, as a consequence of a poor adsorption of the lipids in the absence of any surfactant protein. The incorporation of BDP into those liposomes did not produce any improvement in interfacial adsorption and, as a consequence, very limited diffusion of material from the donor to the recipient trough. Therefore, we could not detect the fluorescence of BANB originally incorporated into the liposomes once material from the interfacial recipient compartment was extracted. Similarly, BANB was not transferred from the donor into the recipient chamber when the drug was introduced as a solution in Clenil excipients, the typical formulation in which BDP is administered to patients.

DISCUSSION

Several studies have reported the benefits of administering clinical steroids in combination with PS [120, 122, 171]. However, until now the ability of different surfactant formulations to incorporate

them, the potential impact of the drugs on PS function and its vehiculization capabilities along the air-liquid interface have not been investigated in detail. The data presented here support the concept that, provided a proper incorporation, PS is able to efficiently transport corticosteroids to long distances using the interface as a 'shuttle', without losing their ability to produce and sustain very low surface tensions along breathing-like compression-expansion dynamics.

Surfactant formulations seem very efficient in solubilizing poorly soluble drugs such as corticosteroids. In fact, all the surfactant preparations tested here have shown affinity to incorporate drugs such as BDP or BUD, regardless of the way the drugs were presented to the surfactant complexes. Both natural and clinical surfactants induced favourable partition of corticosteroids from dry films at the walls of glass tubes into their phospholipid-based membranes, and incorporating the drugs from their clinical formulations like Clenil or Pulmicort, typically used to deliver inhaled corticoids. We presume that corticosteroid molecules, somehow similar to cholesterol, a natural component of pulmonary surfactant in most species, likely integrate into phospholipid surfactant membranes simulating the way how cholesterol distributes between liquid-disordered and liquid-ordered regions [172, 173]. Pulmonary surfactant composition and structures are prepared to accept a certain proportion of steroids, at least up to ca. 15-20% (by weight with respect to phospholipids), without any impairment in surfactant function, as it has been demonstrated in the past [174, 175, 176]. Our drug incorporation experiments determined that both natural surfactant and clinical surfactants like Poractant alfa or CHF5633 can readily incorporate up to 10% by weight of corticosteroids, constituting a very efficient potential vehicle to convert the drugs into a deliverable formulation. Porcine natural surfactant already contains around 5-8% of cholesterol [42], while Poractant alfa and CHF5633 are produced in the absence of cholesterol. Taking into account that we are incorporating around 10% of additional steroid, none of the tested surfactant loadings goes beyond the potentially deleterious ratio of 20% steroid [174].

Detailed functional analysis in the captive bubble surfactometer, under conditions simulating the demanding conditions imposed by respiratory mechanics, confirm that corticosteroid incorporation does not alter the main properties of porcine natural surfactant or those of the clinical preparations, Poractant alfa and CHF5633. The three pulmonary surfactant preparations tested exhibit good interfacial adsorption, both upon initial contact with the air-liquid interface or upon expansion of an interface previously exposed to the surfactants, once loaded with the drugs. The synthetic surfactant CHF5633 even shows better initial adsorptive properties in the presence of BDP or BUD than in their absence. We think that this is consistent with a fluidifying effect of

the drug on the surfactant membranes, in a similar manner to what could be caused by a small percentage of cholesterol, thus promoting a more dynamic behaviour to interact and transfer surface active phospholipid molecules from the beginning, even before such dynamic transfer could be induced by an expanding interface. The main difference in the surface behaviour of corticosteroid-loaded surfactants compared with the corresponding drug-free preparations can be observed at the quasi-static compression expansion isotherms. In these experiments, a very slow compression can allow the reorganization of surfactant films to rearrange the distribution of the components that are less stable at the highest compressions, when the films are forced to adopt very high molecular packing. It seems that surfactant films, particularly those formed by the native surfactant, undergo a more extensive compression-driven reorganization in the presence of drugs, as noticed from the frequent larger plateaus, inducing an expansion of the q-static isotherms to large compression rates. For instance, NS films require 40-45% area reduction during the first q-static compression to reach minimal surface tension, whilst they reach a similar minimal tension with less than 20% area reduction in the second compression cycle. In contrast, and once loaded with 10% BDP, NS films require >50% area reduction to reach minimal tension in the first Q-static cycle, 40% in the second, and 25% in the third one. Only after four slow compression-expansion cycles the film is competent to produce minimal surface tension with less than 20% area reduction (see Figure 15). The increase in the hysteretic behaviour of NS films cycled at slow speed when the surfactant is bearing the corticosteroid could be interpreted as a consequence of the larger area reduction required during compression to produce the squeeze-out of the drug to surface-associated compartments that are likely out from the interface, and therefore do not interfere with reaching the maximal packing required to produce minimal tension at the end of compression. The drug could then be excluded from the interface in a similar manner to some of the natural surfactant components, such as unsaturated lipids or cholesterol [4, 177]. A similar behaviour has been also reported for NS films incorporating cholesterol or other spurious components such as those from meconium [177, 178, 179]. Interestingly, none of the clinical surfactantstested, Poractant alfa or CHF5633 do not show so marked increase in hysteresis as observed in the q-static isotherms of NS films. We think that this difference could be due to the different intrinsic content of cholesterol. The larger exclusion plateaus in NS isotherms could be a consequence of a proportion of steroid near to the limit accepted by films compressed at tight packing [180]. Clinical surfactants films, with no cholesterol, could still accept 10% of corticosteroid at their maximal pressures (minimal tensions).

The innocuous effect of corticosteroids such as BDP or BUD on the dynamic surface properties of PS complexes open new opportunities to use corticosteroid-loaded clinical surfactants as a basis of inhalable delivery strategies. Our double trough experiments demonstrate that corticosteroid-loaded surfactants can take the drug with them to adsorb onto peri-interfacial compartments, promoting its vehiculization to long distances through diffusion along the air-liquid interface. Surfactant could then be prepared to use the interface as a 'shuttle' to spread the drugs. This might change, the potentially exploitable concept of inhalable strategies intended to deliver drugs through the paediatric or neonatal airways [4]. Traditional drug delivery through the airways has been usually linked to the production of small enough vehiculizable entities, such as aerosolized or nebulized particles of less than 2 μm of diameter [181]. According to that idea, only the smallest particles, propelled with enough energy, could be able to reach the narrowest distal airways and the alveoli. This could be particularly important for drugs intended for a lung-mediated systemic delivery, because the alveolar-capillary barrier is the surface exhibiting more favourable transport capabilities. However, we show here that if drugs are properly integrated into a clinical PS, in the right amounts and using procedures that preserve the most favourable surfactant dynamic properties, drugs could readily adsorb into the air-liquid interface and along it, travel from the upper to the distal airways to efficiently spread along the whole lung.

CHAPTER II:

A structural trip through a dynamic interface

INTRODUCTION

Most studies analysing the interactions of different exogenous compounds with the respiratory system have been mainly focused on their potential toxicological effect on the lung epithelium. Few reports have included pulmonary surfactant as an important element that could be targeted in this regard and even less considering it as a drug delivery system. However, the consideration of this essential system as a key element in respiratory drug delivery is increasing in the recent years. Indeed, a deep understanding of how drugs or nanoparticles may affect the structure and surface behaviour of pulmonary surfactant is essential to optimize the design and production of improved drug delivery strategies targeting the airways, not only to avoid toxicological effects but also to get synergistic effects from their combination.

As aforementioned, pulmonary surfactant is secreted into the alveolar spaces where it accomplishes its main function: reducing the surface tension of the layer of water covering the whole respiratory surface. The lungs are continuously inflating and deflating during the process of breathing, a phenomenon that makes alveoli to be uninterruptedly dilating and contracting. This highly dynamic process is translated into a subsequent compression and expansion of the interface between that layer of water and the breathing air. As pulmonary surfactant is located as a film in this dynamic air-water interface, it has been optimized to adapt to such active environment, producing surface tensions below 2 mN/m (surface pressures above 70 mN/m). The 'squeeze-out' model is widely accepted to explain some of the transformations suffered by the surfactant films subjected to compression. It states that the interfacial film folds down to form 3D multi-layered structures enriched with unsaturated phospholipids, leaving the interface accumulating most of DPPC. This mechanism allows surfactant films to form compression-driven transient metastable structures, excluding material that cannot be packed enough to sustain the minimal tensions, below 1–2 mN/m [65]. These 3D structures maintain stable the association with the interface presumably thanks to proteins SP-C and SP-B. Moreover, they can reinsert into the interface during expansion, ensuring the integrity of the film along successive breathing cycles [47].

Since Dr. Irving Langmuir [182, 183] and Dr. Katherine Blodgett improved the device developed by the German and 'independent-for-obligation' scientist Agnes Pockels to study the behaviour of oils in air-water interfaces, many surface active components have been tested. However, it was not until 1957 when Dr. John Allen Clements proposed the Langmuir and Blodgett method to study the interfacial behaviour of pulmonary surfactants. The possibility of studying this system under compression and expansion conditions, modelling somehow the alveolar dynamics, makes

the Langmuir-Blodgett trough the most extensive technique to study the structural insights of pulmonary surfactant and the effects that different compounds could have on it.

Particularly in this chapter, an improvement of this technique is proposed to study the interfacial behaviour of hydrophobic drugs, focusing on the structural effects that they could produce on pulmonary surfactants films. This novel setup allows to highlight the importance of interfacial dynamics to enhance both drug delivery and its subsequent release from the air-liquid interface. Proper surfactants and simpler models consisting of lipid-protein mixtures or pure lipids can be used to perform experiments and better understand the role of each lipid-protein component. In particular, DPPC (the simplest model), purified porcine surfactants (emulating endogenous surfactant) and their organic fraction (mimicking clinical/exogenous surfactants) were assessed in combination with tacrolimus (TAC, FK-506 o Fujimycin). This compound is an immunosuppressive drug widely used during lung transplantation that can be considered as a good model for testing hydrophobic drugs.

This chapter pretends to explore from a structural and dynamic perspective how the drug travels over the interface and is released once in the desired location and the role of interfacial dynamics in the vehiculization and release processes.

KEY TECHNIQUE

Langmuir-Blodgett trough

The Langmuir-Blodgett trough allows for study the interfacial behaviour and the structural transformations of surface active materials in the presence or the absence of additional compounds, under dynamic conditions of compression and expansion. It consists of a thermostated Teflon trough filled with liquid (a water solution, generally), a surface pressure sensor, a transference system (dipper) and a barrier able to compress and expand the molecules confined at the air-liquid interface (see **Figure *20***). When the sample is applied on the interface (either in aqueous or organic solution), amphipathic molecules such as phospholipids spread along it forming a confined interfacial monolayer, also known as Langmuir film. Although there are several designs for the barriers, the barrier at the Langmuir-Blodgett trough used in this Thesis is a Teflon ribbon partially immersed into the aqueous subphase (purchased from NIMA technologies, Coventry, UK). This barrier is fixed forming an area-variable rectangle (from 185 cm^2 to 58 cm^2) with own-designed cylindrical pieces at vertexes that avoid the leakage of interfacial material at high compression rates.

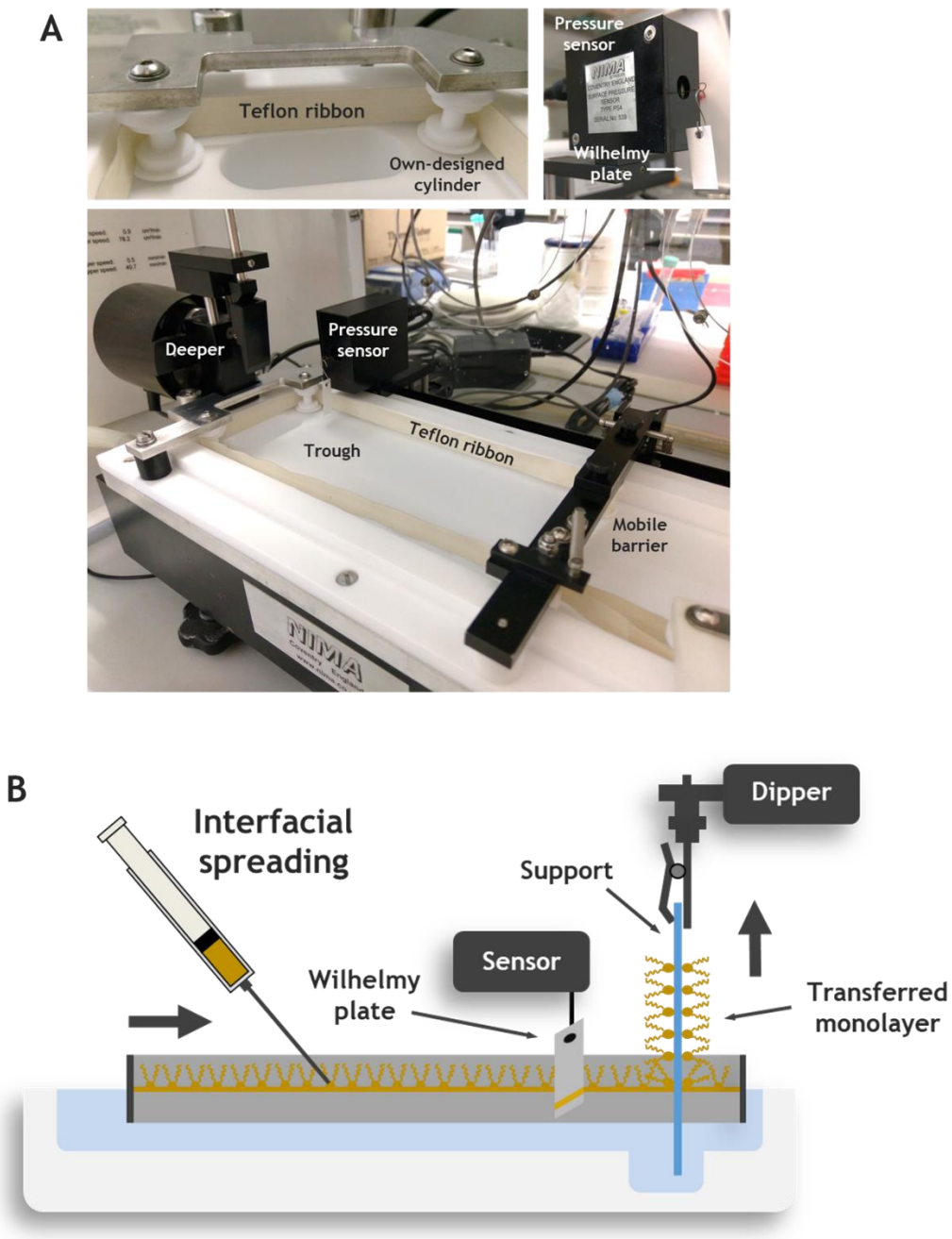

Figure 20: ***Langmuir-Blodgett trough.*** **A)** Images of characteristic parts of the Langmuir-Blodgett trough. **B)** Schematic representation.

When the barrier closes, the film is compressed and the phospholipids rearrange laterally in the interface, increasing the lateral pressure and reducing the area per molecule. After this, the barrier can be opened to study how the interfacial molecules behave during expansion. Additionally, it can also be repeatedly opened and closed to observe the effects of this dynamism on the films. The changes in surface pressure (π) are constantly monitored by a pressure sensor that transduces the signal to a computer. When the area per molecule is so low that promotes

intermolecular interactions, the surface pressure start to rise. These changes in surface pressure are usually represented with π-area isotherms and reflect how interfacial molecules are organised into the air-liquid interface. Low pressures indicate that molecules are completely dispersed along the interface, while high pressures are usually associated with highly ordered states characterized by tightly packed lipids at the air-liquid interface. At maximal compression, those molecules which cannot support such pressures are excluded from 2D to 3D planes (see **Figure *21***).

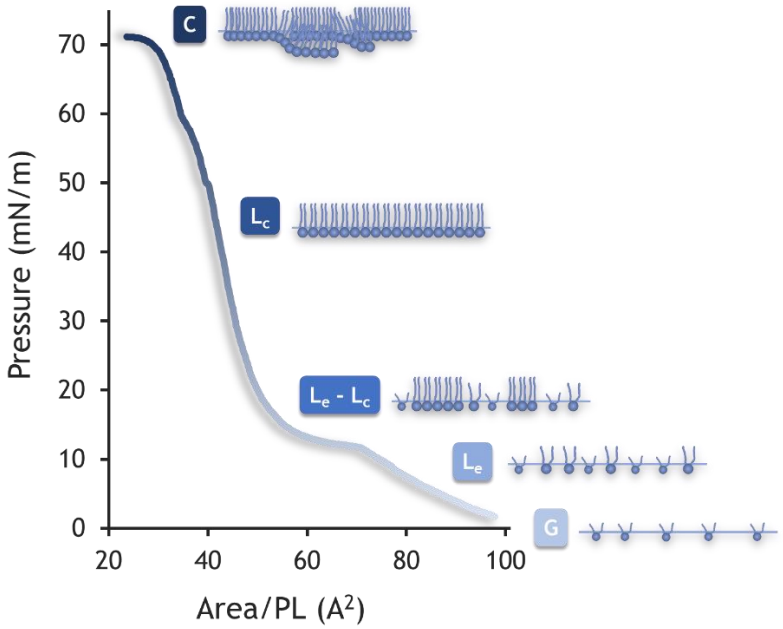

Figure 21: *π-area isotherm of a DPPC film at 25 °C with the associated interfacial lipid phases.* Taking the isotherm of DPPC as a model, five different packing states (lipid phases can be described). The gas phase (G) at low surface pressures, where phospholipids are dispersed along the interface and can move freely. Then liquid-expanded (L_e), where they occupy less area per molecule but still have free motion. Lipids start contacting each other and surface pressure rises. At the liquid-condensed (L_c) phase, where the acyl chains are orientated perpendicular to the interface and the molecules are tightly packed. The plateau at around 12 mN/m in DPPC represents a coexistence between L_e and L_c phases, where the work of compression is applied to achieve the ordered lateral packing of the interfacial molecules. If the lateral pressure is higher than the threshold that they cannot resist, the molecules are excluded out from the interface (collapse or C).

The presence of additional molecules intercalated between phospholipids can produce changes in the area occupied per molecule, the compressibility of the layer and the cooperativity, or modify completely how phospholipids organise into the interface. This can easily be detected by variations in the shape of the isotherm. Hence, this technique is very useful to study interfacial properties of pulmonary surfactant and how incorporated elements such as drugs, nanocarriers or pollutants interact with it. The possibility of compressing and expanding the interface also permits to evaluate whether this dynamism, analogous to that occuring in alveoli during breathing, enhances the depuration or release of those additional molecules from the interface.

Apart from evaluating the changes in surface pressure, the interfacial films can also be transferred onto solid supports to observe in detail their structure under a microscope (i.e. epifluorescence or AFM, as it is the case of this Thesis). The transference could be performed at constant pressure, where the barrier is automatically moved to compensate for the pressure reduction due to material loss during the transference. Alternatively, transference can be performed at continuously varying surface pressure (COVASP), where the film is transferred while closing the barrier to have the film at all possible pressures into the same sample [184, 185]. As shown in **Figure *22***, the methodology changes depending on the properties of the support, determining the orientation of the lipids in the transferred film.

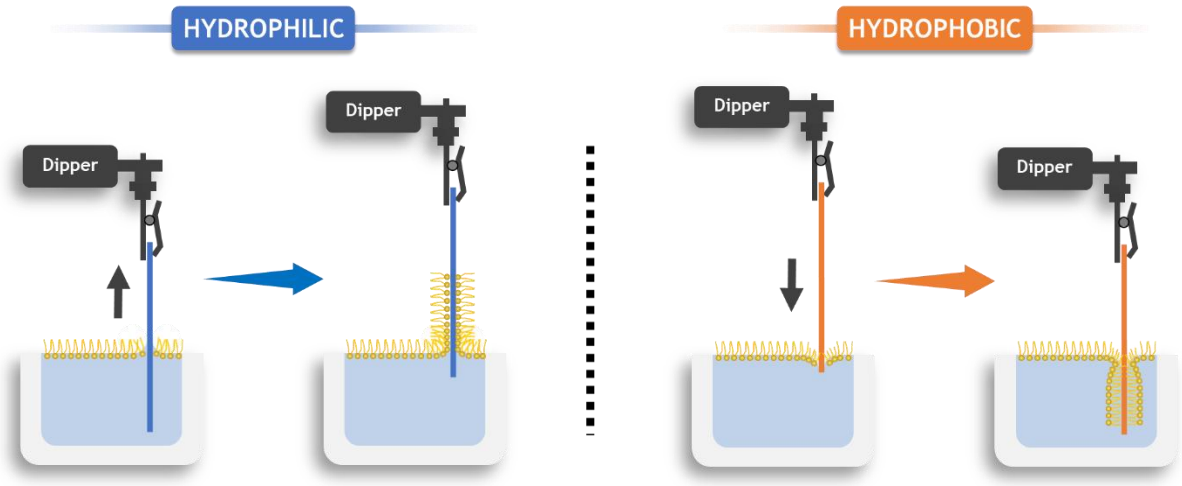

Figure 22: ***Protocol to transfer monolayers onto hydrophobic or hydrophilic supports, to form Langmuir-Blodgett films.***

In this Thesis, all the supports used to transfer the interfacial films were hydrophilic: glass for epifluorescence microscopy and mica for AFM. As AFM allows to scan the surface of samples, it is possible to observe different heights in interfacial films and analyse their 3D organization under compression-expansion dynamics. These different heights usually correspond to clusters of phospholipids (lipid domains) with different packing stages (lipid phases) or several layers of them (3D structures), as the height of phospholipid acyl chains increases during the packing of lipids upon compression. For epifluorescence analysis, samples have to be labelled with fluorescent dyes prior to their deposit onto the Langmuir-Blodgett trough. These probes are normally fluorescent molecules covalently attached to phospholipids (head or acyl chains). Thus, depending on the size and the position of the fluorescent group and the saturated or unsaturated nature of its acyl chains, such dyes can be employed to label packed domains or fluid phases. Having this in mind, it is possible to observe and described the lateral distribution of interfacial

molecules. When labelled phospholipid cannot support highly packaged status, as it is the case of the NBD-PC used in this Thesis, it will be excluded from the most condensed domains upon compression. This leads to detect the ordered phase as dark structures with growing sizes as the lateral pressure increases.

Looking at the possibilities of this technique, together with the vehiculizing trough developed in this project, we decided to go further and connect both the traditional Wilhelmy and Langmuir-Blodgett trough through interfacial bridges (see **Figure *23***). The former is still the donor, while the latter acts as the recipient. This novel dynamic *in vitro* model of the respiratory surface opens new possibilities to understand how surfactant and its passengers behave interfacially under compression and expansion conditions. The larger recipient surface also helps to collect more molecules improving the detection. The possibility of removing the interfacial bridge after travelling or cycling also increases the potential of this technique. Specifically, removing the bridge just before performing compression-expansion cycles, supposes an unprecedented strategy. The surfactant film that has already spread can be carefully analysed, avoiding the adsorption of new material coming from the surfactant reservoir in the subphase. When the cycles are performed in the presence of the bridge, it is possible to analyse how cycling enhances the surfactant trip along the interface. Additionally, the experiment can be continued beyond the dynamic cycles to evaluate the readsorption of interfacial-associated membranes (removing the bridge and monitoring the surface pressure for a certain period of time) or to check whether successive interfacial compression-expansion cycles favour the interfacial reposition of new material coming from the donor reservoir (leaving the bridge and monitoring the surface pressure for some additional time).

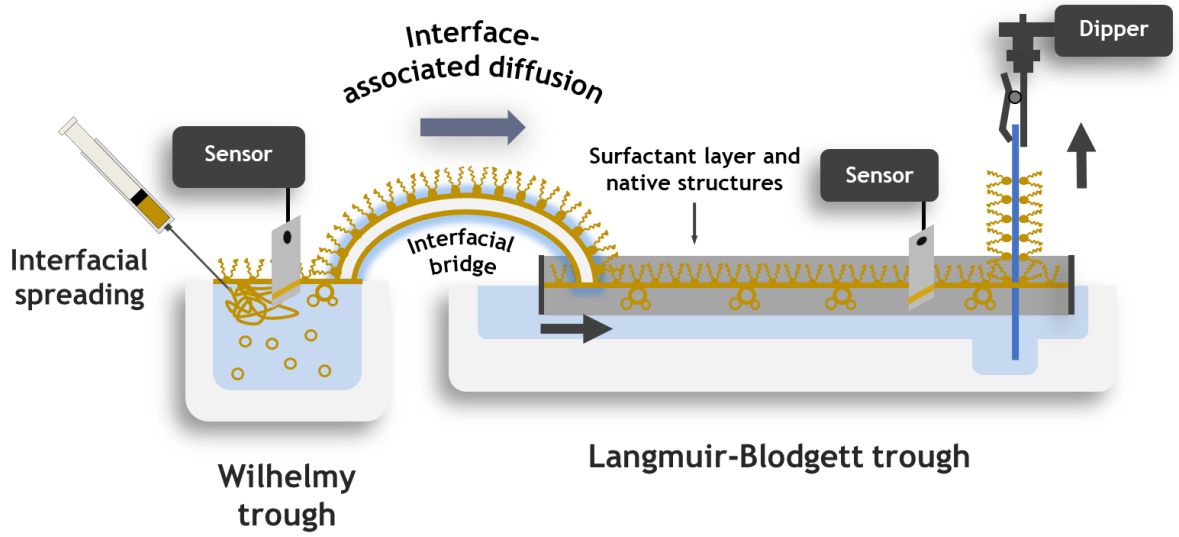

Figure 23: ***Schematic representation of the dynamic vehiculization trough.***

RESULTS

Traditional models in a classical technique: Exploring how a hydrophobic drug interacts with pulmonary surfactant and behaves interfacially

DPPP monolayers and hydrophobic drugs: the simplest model of pulmonary surfactant to study interfacial distribution

To study how hydrophobic drugs are distributed laterally in interfacial monolayers of DPPC and to elucidate how they could interact with pulmonary surfactant, three different proportions (1%, 5% and 10% w/w with respect to DPPC) of Tacrolimus have been assessed. Each DPPC/drug combination, dissolved in Chloroform/Methanol (2:1 v/v), was directly distributed into the air-liquid interface to form a simple monolayer. After 10 minutes, waiting for organic solvents to evaporate, the compression isotherm (barrier speed: 25 cm^2/min) for each Tacrolimus proportion was obtained while transferring the monolayers to a glass plate (deeper speed: 5 mm/min). As shown in **Figure *24***, the crescent addition of TAC alters the lateral structure of DPPC impeding the formation of compression-driven domains. At lower surface pressures, the area per molecule of phospholipid increases upon the addition of TAC, indicating that the drug actually intercalates between DPPC molecules at the interfase. At a surface pressure of around 10-12 mN/m and a temperature of 25 °C, when DPPC begins to undergo a lateral reorganization with its resulting characteristic plateau in the isotherm, the size of both micro- and nano-domains is clearly reduced (observed by epifluorescence microscopy and AFM). The formers are not even formed when the highest amount of TAC is assessed. This effect is also possible to observe looking at the isotherms, where the plateau is shifted among the increasing amounts of TAC. These effects may indicate that tacrolimus is interacting with DPPC molecules and obstructing their lateral reorganization in the interface. At pressures higher than the exclusion surface pressure of TAC in DPPC monolayers (around 30 mN/m), the isotherms remain similar suggesting that tacrolimus is being excluded from the interface at a level that does not affect the DPPC behaviour.

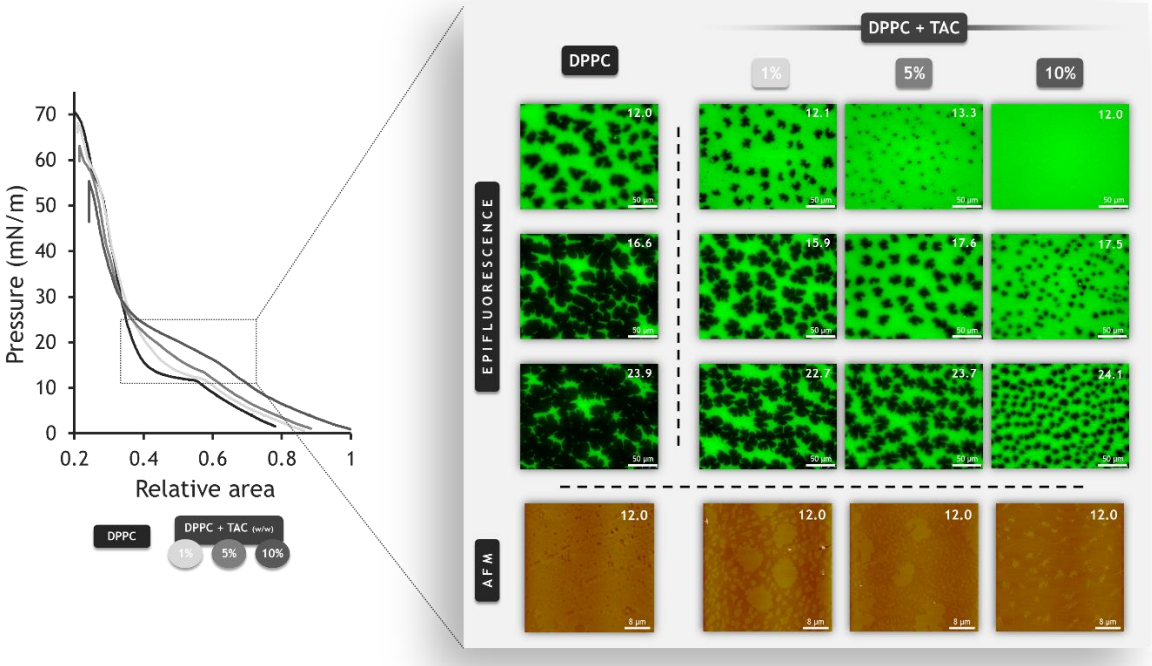

Figure 24: ***Effect of increasing amounts of tacrolimus on DPPC interfacial monolayers.*** The graph represents the transference isotherms of DPPC at 25 °C in the presence of increasing amounts of TAC (1%, 5% and 10% by mass with respect to DPPC). Samples were spread over the surface disolved in Clorodorm/MetOH (2:1 v/v). After 10 min, the barrier was closed at 25 cm^2/min and the deeper 5 mm/min to ensure a proper transference of the monolayers. The plateau observed at around 12 mN/m corresponds to the coexistance of two differentes lipid phases (liquid expanded (L_e) and liquid condensed (L_c)). *Epifluorescence images* show the lateral distribution of DPPC and how the growing addition of TAC alters the formation of macro-domains of highly packed DPPC (L_c; black regions); the green color corresponds to L_e where phosphatidylcoline labelled with the fluorescent probe nitrobenzoxadiazole (NBD) is located as a consequence of its lateral exclusion from the high ordered domains at high levels of packing. *Atomic force microscopy (AFM) images* represents how TAC affects the lateral arrangement of DPPC molecules in nano-domains. Bars: Epifluorescence = 50 µm; AFM = 8 µm.

In order to track where TAC localises along the air-liquid interface in the presence of DPPC and its interfacial behaviour during compression, the same experiments were performed using a fluorescent tacrolimus labelled with NileBlue (TAC·NileBlue). Only the 1% by mass of TAC·NileBlue were added as a trace; the rest amount to complete the three assessed proportions was intact TAC to minimize the possible additional effect of the dye. As shown in **Figure *25***, the size of domains was different depending on the filter used to observe the fluorescence of NBD-PC or TAC·NileBlue under the epifluorescence microscope. Particularly, the domains observed with the NBD-PC filter were consistently smaller than the same detected by the TAC·NileBlue one. However, these differences decrease upon compression, suggesting that the lateral exclusion is a gradual process where the drug molecules are laterally excluded at lower surface pressures than NBD-PC. *Figure 25B* also shows how at the highest TAC·NileBlue concentration the effect of altering the lateral

phase transition is taking place at higher surface pressures, indicating that TAC is broadening the phase transition of DPPC even until pressures near to the exclusion of TAC, as it is also observable in **Figure *24***.

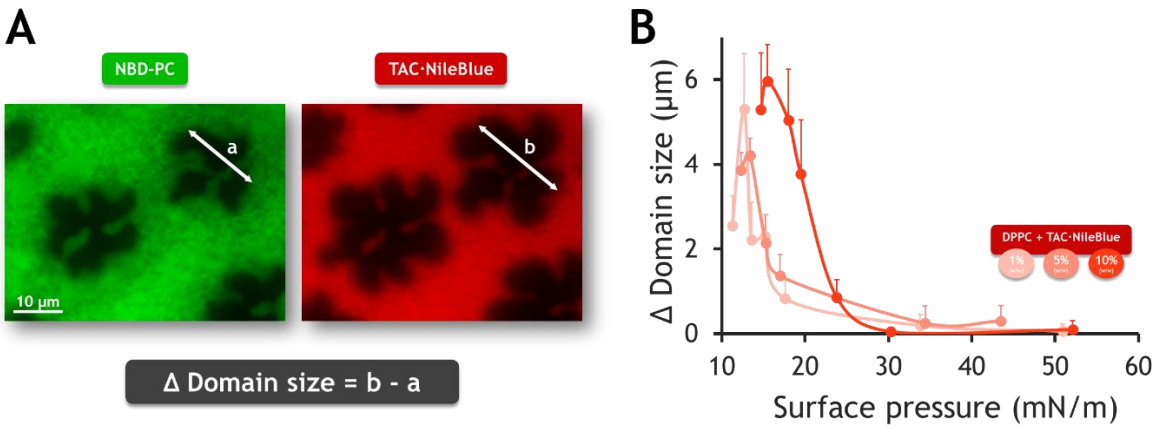

Figure 25: ***Lateral exclusion of TAC from highly packed DPPC domains.*** A) The same domains seen under different filters (representative colours; green: NBD-PC; red: TAC·NileBlue). White arrows indicate the strategy used to measure their difference in size. Bar = 10 µm.

Figure *26* represents the distribution of the total amount of pixels along the 256 levels of grey from row images taken by the epifluorescence microscope to continuous-pressure transferences. Interestingly, the images corresponding to TAC·NileBlue show a progressive displacement of the whole pixels to the darker levels upon compression. This shifting can be traduced into a reduction of intensity derived from fluorescence loss. Considering that all samples were handled equally and images were taken maintaining the same exposure times (200ms) at higher lamp intensity, it can be supposed that this loss of fluorescence may be associated to an exclusion of fluorescent molecules from the interface. Regardless the amount of TAC, at surface pressures below the plateau, the pixels were accumulated in slightly darker levels than the same observed just at the beginning of the plateau, suggesting that molecules at the interface are somehow laterally clustering, resulting in brighter images. Although this clustering is more evident at pressures above the plateau due to the presence of bigger domains, all the pixels are concentrated in considerable darker levels, suggesting that TAC could not only be excluded laterally but also interfacially during compression.

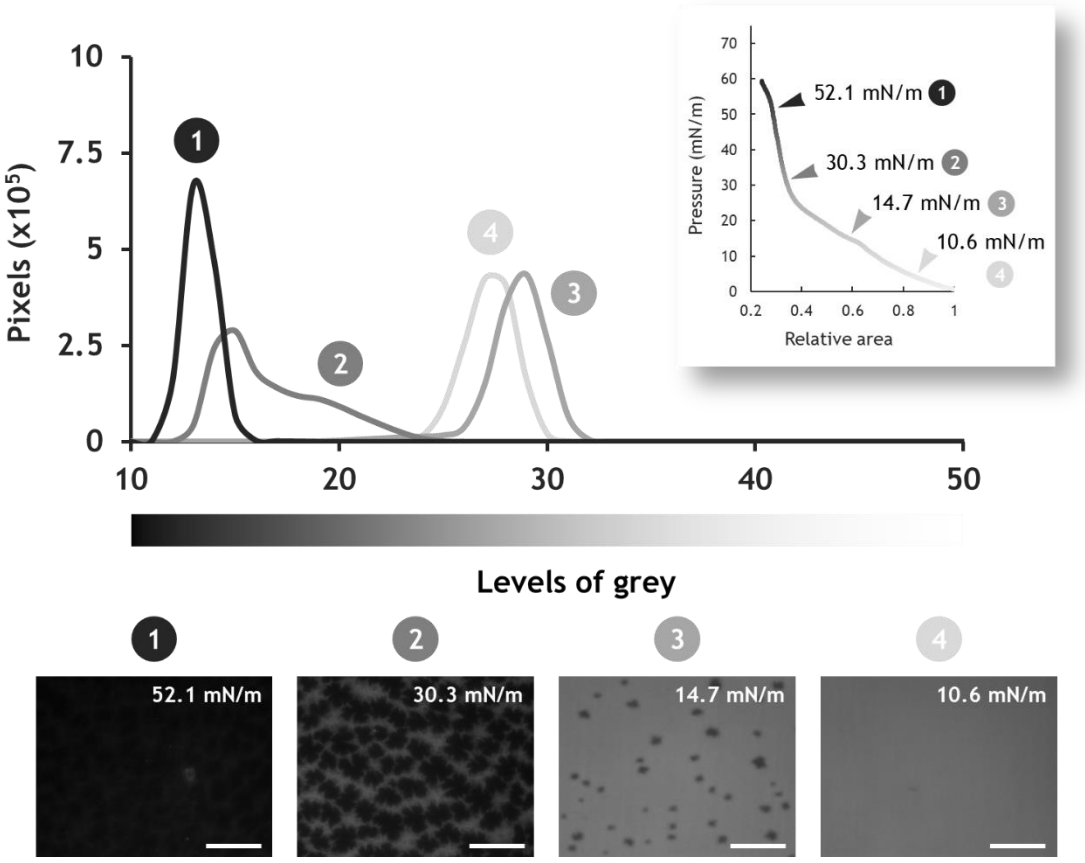

Figure 26: ***Representative histograms of images showing how TAC () is excluded from the air-liquid interface over compression.*** Each histogram corresponds to one of the images below at the indicated lateral pressure. Raw images. Bar = 50 µm.

To further explore the potential interfacial depuration, the monolayers were subjected to five compression and expansion cycles. Figure *27* shows that after cycles the effect of TAC is apparently reverted. When the sample is mixed with TAC at 10% w/w, it is evident that DPPC starts generating domains at higher pressures than pure DPPC. However, after five compression-expansion cycles, this effect is partially reverted and DPPC forms domains.

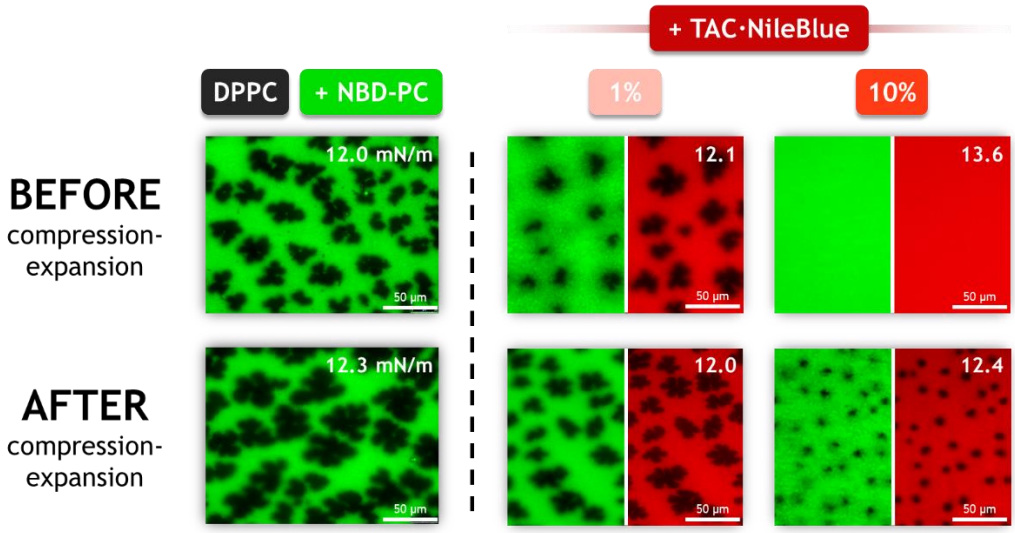

Figure 27: ***Epifluorescence images showing how compression-expansion cycles promote the interfacial exclusion of TAC.*** Representative images taken before and after five compression-expansion cycles at the pressures indicated on each image. Representative colours; green: NBD-PC; red: TAC·NileBlue. The histogram of each image was adjusted to better differentiate the structures in the image (fluorescence of each dye after cycles was reduced as a consequence of interfacial exclusion). Bar = 50 µm.

In **Figure *28*** the release process during the compression-expansion cycles is represented. The isotherms clearly show how the area per molecule, especially with the maximum amount of TAC, is decreasing over the cycles. This reduction of area at the lowest pressures indicates that the monolayer is likely losing material (DPPC, TAC or both) from the interface during interfacial dynamics. When focusing on the plateau, the same process can be observed as a progressive shifting to the left. Once again, looking at the shape of the whole isotherms after the cycles, they resemble pure DPPC. These results indicate that the monolayer could be mainly losing TAC, confirming that TAC is not only excluded laterally but also three-dimensionally from the interface towards the aqueous subphase upon high pressures.

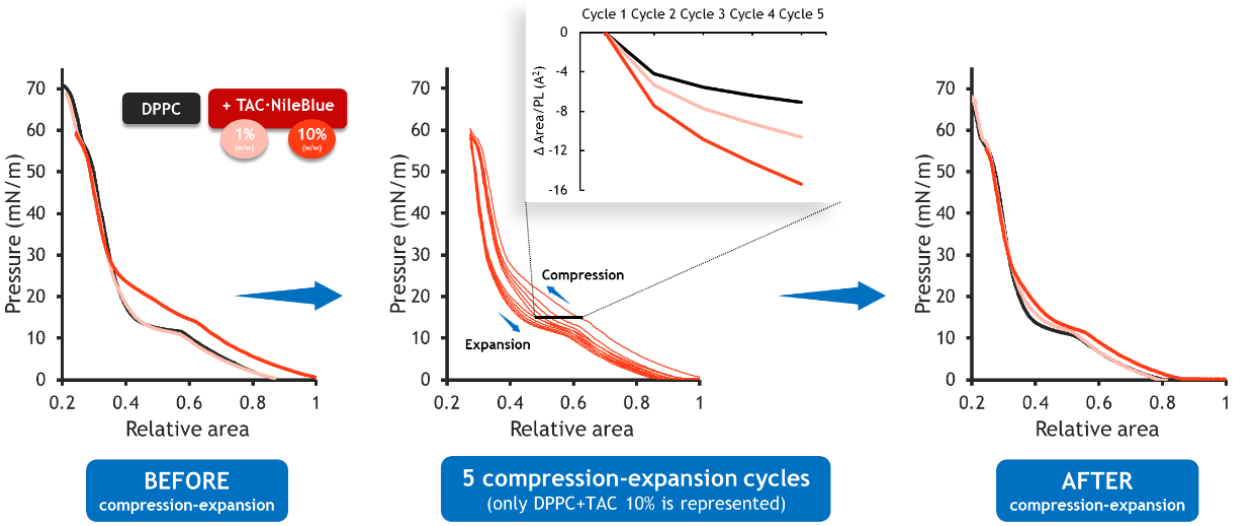

Figure 28: ***Interfacial exclusion process in DPPC monolayers.*** π-area isotherms of DPPC in the presence of crescent amounts of TAC (1% and 10% w/w) before, during and after five compression-expansion cycles. The zoom-like graph in the middle represents the reduction of area per molecule at 15 mN/m, which corresponds to the amount of material released over the cycles.

Dissecting the interfacial exclusion from surfactant monolayers

As mentioned above, TAC was able to colocalise with the liquid-expanded phase of DPPC at the air-liquid interface and the interfacial dynamics promotes its exclusion from there. Hence, the next step was to test whether a similar behaviour occurs in combination with pulmonary surfactants. In this case, the organic fraction (OE) of a self-purified porcine surfactant was combined with the TAC proportions used in the previous experiments with DPPC (1%, 5% and 10% w/w). Each OE/drug combination, dissolved in Chloroform/Methanol (2:1 v/v), was directly distributed into the air-liquid interface of the Langmuir-Blodgett trough. Then, the compression isotherms and interfacial transferences were obtained before and after five compression-expansion cycles. **Figure *29*** shows the isotherms before, during and after the dynamic process, revealing how the surfactant located at the interface is subjected to depuration during cycling. Specifically, before the cycles, it is clear that crescent amounts of TAC reduce the characteristic plateau of surfactant at around 40-45 mN/m. The slope upon compression is also reduced at lower pressures, meaning that the same area compression produces lower increase of pressure reducing the cooperativity. This induces to think that TAC is intercalating between surfactant elements and could somehow promote the exclusion of additional surfactant components at the same time of its exclusion upon compression. During cycles, a major reduction of area to reach the same surface pressure can be observed as TAC proportion is increasing. This is evident especially at lower pressures when it is expected to be excluded. Although this area is gradually reduced during cycles, this reduction is more evident upon the first compression. Moreover, after

the dynamic process, the surface pressure at the maximum surface area is considerably less than before. It may suggest that interfacial dynamics induces liberation of some surfactant components and enhances TAC release from the interface.

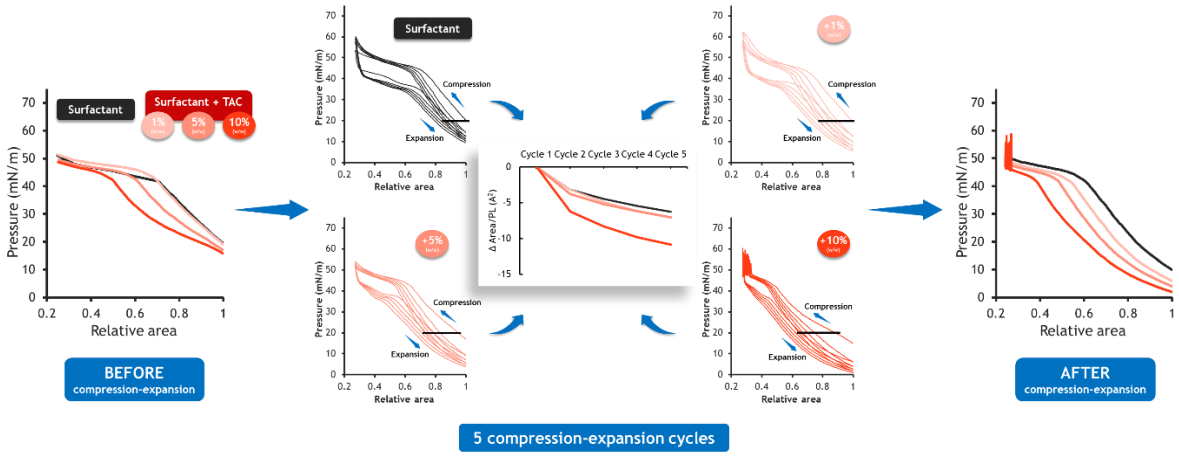

Figure 29: ***Interfacial exclusion process in surfactant monolayers.*** π-area isotherms of surfactant in the presence of crescent amounts of TAC (1% and 10% w/w) before, during and after five compression-expansion cycles. The zoom-like graph in the middle represents the reduction of area per molecule at 15 mN/m, which corresponds to the relative amount of material released over the cycles.

In an attempt to characterise this process graphically, **Figure *30*** shows a representative image of a surfactant monolayer containing 5% of TAC at a surface pressure near the end of the plateau (47.5 mN/m). In this image, which is a merge between the filter using to detect the fluorescence of NBD-PC and TAC·NileBlue, different regions can be observed. The darker area that mainly covers the whole image corresponds to surfactant clusters from where both fluorescent dyes have been laterally excluded. Then, a green brighter crack containing some yellow circular structures that remains to vesicles can be observed. Knowing that NBD-PC is represented in green and TAC·NileBlue in red it is possible to interpret that those vesicle-like structures are composed by both NBD-PC and TAC·NileBlue. This could demonstrate that during compression there is a rearrangement of surfactant components and the drug, which generates different clusters. These can be later squeezed-out from the interface in the form of vesicles-like arrangements at certain surface pressures that cannot resist at high pressure states.

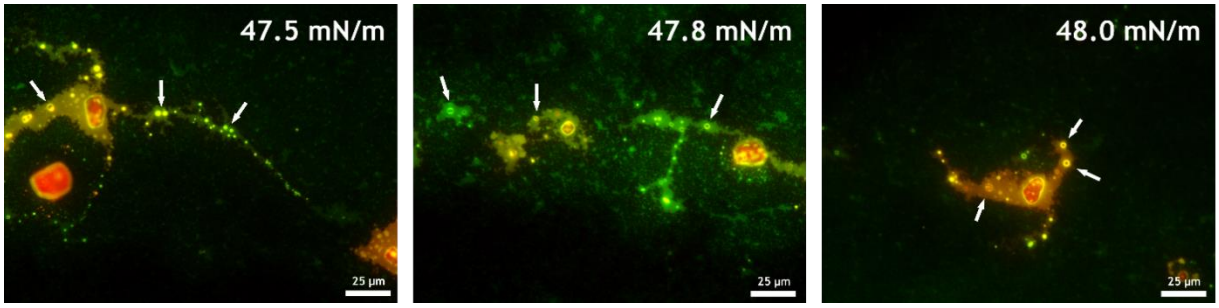

Figure 30: ***Squeezing out of TAC·NileBlue and NBD-PC.*** The images show an interface saturated with the organic fraction of a self-purified surfactant corresponding to pressures at the end of the plateau. The majority of the interface is covered by dark regions from where both dyes have been laterally excluded. They correspond to condensed phases, likely enriched with DPPC. White arrows indicate vesicles-like structures full of TAC·NileBlue and NBD-PC already excluded from the interface. The histogram of each images was firstly shortened and then contrasted to better differentiate the structures in the images. Merge is shown (Red: TAC·NileBlue; Green: NBD-PC). Bar = 25 µm

Dynamic vehiculization

Setting up

As observed in the previous experiments, pulmonary surfactant can incorporate TAC into its membranes with no significant effects on its functionality (see Figure S… in supplementary). Knowing that interfacial dynamics could also define the behaviour and destiny of the drug, the dynamic vehiculization of additional passengers was studied kinetically and structurally. As mentioned above, to perform these experiments, the double trough used in the Chapter I was modified. Instead of being a static system, the substitution of the recipient trough by a Langmuir-Blodgett trough allows to convert this respiratory surface model into a dynamic system. This change permits to better simulate the alveolar dynamism and evaluate the vehiculization capabilities of pulmonary surfactant considering additional parameters as never before.

Before starting the experiments, the dynamic vehiculization trough was tested to ensure that instrumental variability would not affect the experiments. The adsorption and spreading capabilities were parallelly tested in both static and dynamic vehiculization troughs to confirm that both were able to produce similar results. A sample of the organic fraction obtained from purified porcine surfactant (15 µL at 50 mg/mL) was spread into both donor troughs in the form of an aqueous suspension. In **Figure *31***, which compares the changes in surface pressure over time in both donor and recipient troughs, no substantial differences were observed. When the aliquot of surfactant was added at either donor troughs, the same immediate increase of surface pressure up to around 41-42 mN/m was recorded (surfactant π_{eq}). Once the material adsorbed into both donor air-water interfaces, it diffused equally along the interfacial connecting bridge. The lag time for surface pressure to start raising at the recipient trough was slightly superior in the dynamic

system due to the bigger surface area. However, this time difference did not impede to reach the maximum surface pressure at the same time (after 25 min). These results guaranteed that the experiments performed with the new set up were totally reproducible and no other instrumental variability more than the lag time affected them.

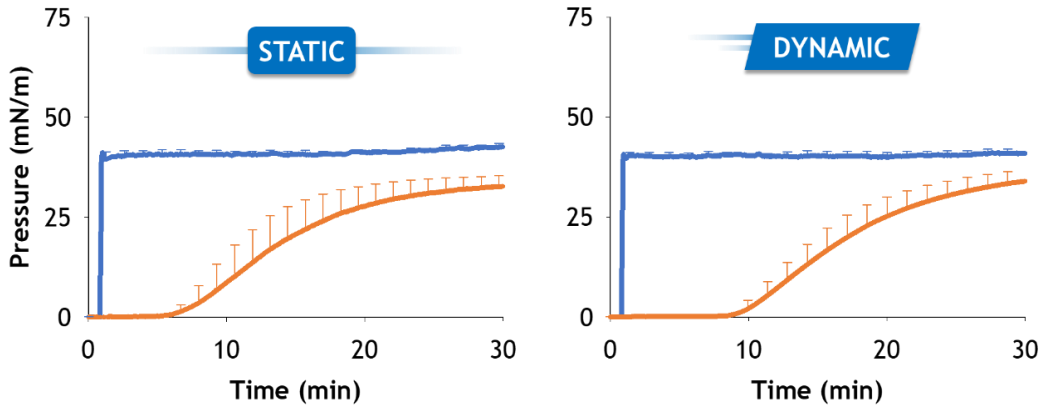

Figure 31: ***π-time inotherms measured in both static (left) and dynamic (right) vehiculization troughs.*** Adsorption and spreading capabilities of pulmonary surfactant have been analysed to evaluate instrumental variability between both vehiculization troughs.

Interfacial dynamics promotes TAC release

The previous experiments confirmed the ability of surfactant to transport drugs through an air-liquid interface. The next step was to determine how these drugs are released from the interface to play its therapeutic effect and whether dynamic cycles enhance this process after travelling interfacially. To demonstrate it, an aqueous aliquot (15 µL at 50 mg/mL) of OE in combination with 10% TAC (8% TAC + 2% TAC·NileBlue by mass) was deposited in the donor trough and subjected to 10 compression-expansion cycles in the recipient. These cycles were performed in the presence and in the absence of an interfacial bridge, maintaining both interfaces connected or disconnected, respectively. These strategies allow to study a) release of TAC over the cycles avoiding the possible material coming from the donor trough (with no bridge) and b) whether dynamics promotes the interfacial trip (with bridge).

The π-time and π-area isotherms represented in **Figure *32*** illustrate several differences when the cycles are performed with donor and recipient interfaces either connected or disconnected. The continuous fluctuations observed in the donor isotherm (blue) during the cycles in the presence of the bridge (**Figure *32*** B) evidences that both interfaces are continuously connected. Therefore, every change in the interfacial film of the recipient trough is being transmitted to the donor via air-liquid interface. In the π-area isotherms, a progressive reduction of the characteristic

plateau of pulmonary surfactant at around 40-45 mN/m is observed in both situations. After this plateau, compressibility also decreases over the cycles, meaning that the interfacial film is progressively depurated from those components that cannot support such pressures, likely enriching the layer with DPPC. The major reduction of this plateau is observed during the first compression, regardless of the connection of both interfaces. Then, this reduction is more gradual, suggesting that the main depuration occurs at this moment. Upon removing the interfacial bridge before cycling (**Figure *32***A), the maximum pressure slightly decreases over the cycles, compared to the situation when both interfaces are connected. In the case of the minimum pressures, this difference is more accentuated, confirming that the material lost during the compression is not replenished during the expansion. When both interfaces are connected, this decrease in lateral pressure is not that obvious after the subsequent expansions, though during the first cycle is similar.

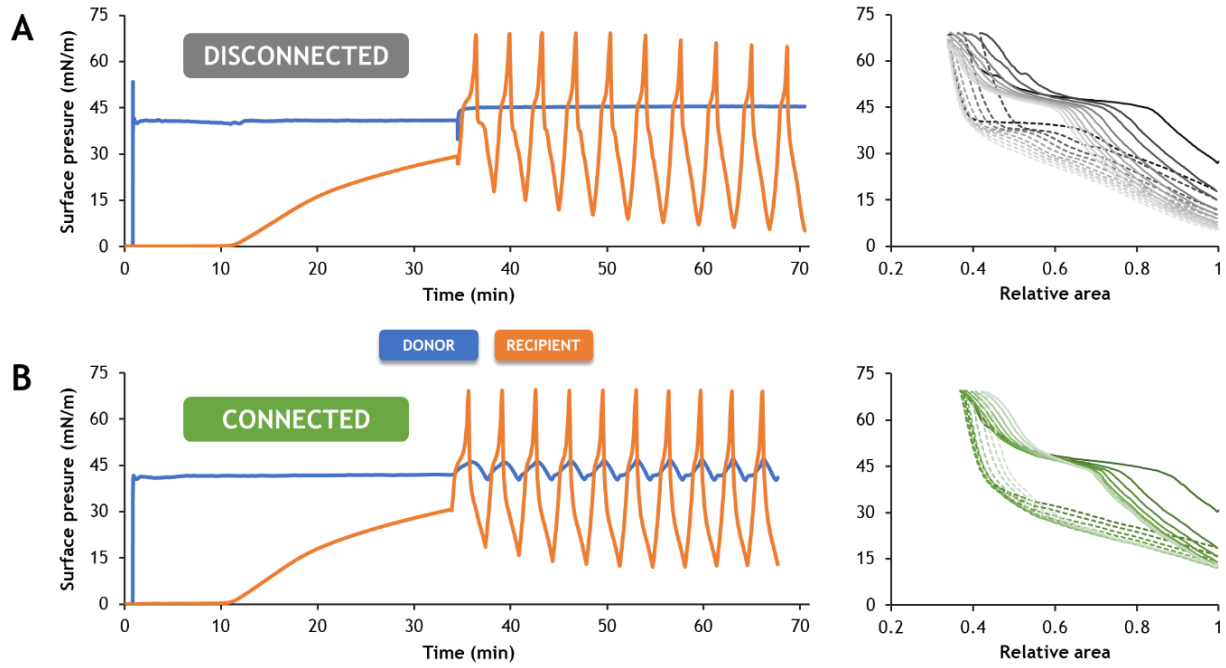

Figure 32: *π-time and π-area isotherms showing that compression-expansion dynamics promotes the interfacial trip.* A) Removing the interfacial bridge just before the cycles (disconnected). B) Leaving the bridge during the whole experiment (connected).

Comparing the isotherms during the first and last compression with pure DPPC (**Figure *33***), it is clear that surfactant films only resemble DPPC behaviour after the exclusion plateau, when surface pressure can reach values close to 72 mN/m (only feasible by DPPC monolayers). After dynamic cycles, the isotherms show more reduced plateaus allowing surfactant films for reaching these higher surface pressures with lower changes in surface areas. In comparison with

disconnected interfaces (**Figure *33***A), when they are connected (**Figure *33***B) the last compression isotherm is shifted to the right and start at higher pressures, indicating that there is more material in the interphase, and the plateau is more reduced. This is, less area compression is needed to overtake the plateau and reach higher pressure. This is advancing that more material could be present in the interface and likely enriched with DPPC. Although the pressure at the beginning of the last compression (end of 9th expansion) is clearly reduced in both cases, it is more evident when the bridge is absent, meaning that less material is in the interface and resulting in the shift of the isotherm (**Figure *33***C). Clearly, the loss of material is compensated with the surfactant reservoir coming from the donor, which is constantly adsorbing into the air-liquid interface and travelling along it. Focusing on the isotherm above the plateau in the presence of the bridge, it is possible to observe that it is even more right-shifted than the plateau in the first compression. This is another evidence that the material remained in the interface could be progressively enriching with DPPC.

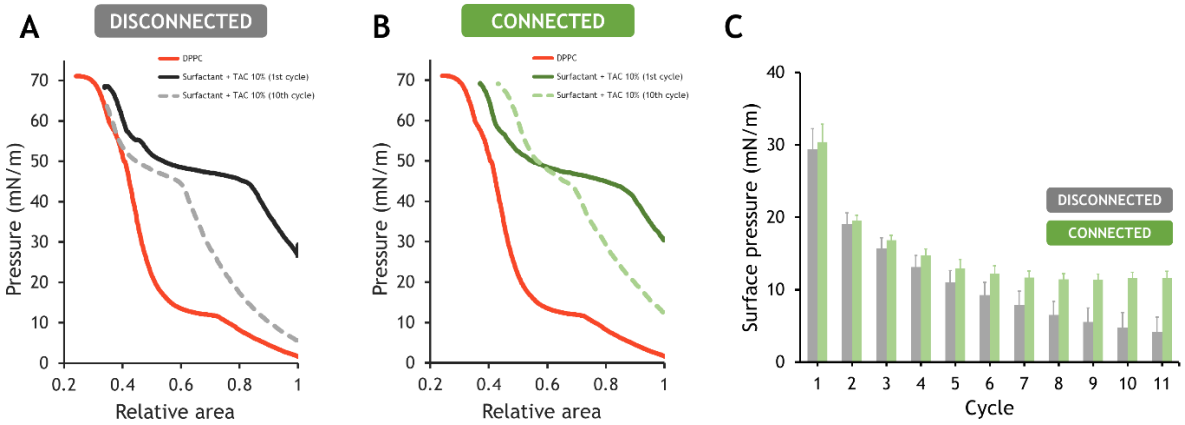

Figure 33: *π-area isotherms comparing the first and last compression with pure DPPC.* A) and B) representative π-area isotherms comparing the first and last compression with pure DPPC with the interfaces disconnected and connected, respectively. C) Minimal surface pressures after each expansion. Error bars correspond to standard deviation (n=3).

After each experiment, the recipient interface was collected and fluorescence of TAC·NileBlue was measured at three different moments: before and after 10 compression-expansion cycles and after the first compression. *Figure 34A* shows that fluorescence decays dramatically after the cycles, in accordance with the situation observed in the π-area isotherms. The same decrease can be observed after the first compression, confirming that the major exclusion is happening at that moment. Interestingly, when the cycles are performed with both interfaces connected, the fluorescence is considerably higher than the signal detected in the absence of the interfacial bridge (see *Figure 34B*). These results insinuate that, although TAC is

being excluded during the cycles, the presence of the bridge allows the continuous transference of material from the donor to the recipient trough.

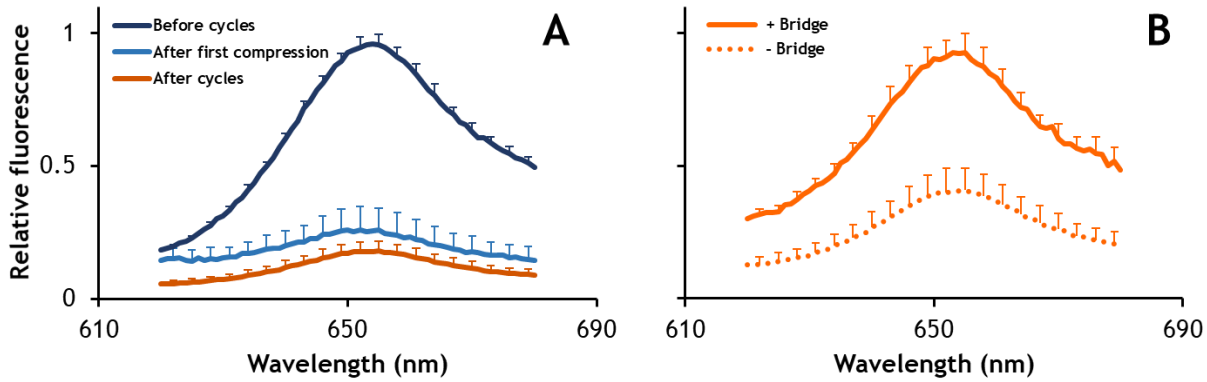

Figure 34: ***Fluorescence spectra.*** A) Measured in the recipient trough before and after the cycles and just after the first compression (different experiments) to highlight the exclusion of TAC after interfacial dynamics without the bridge. B) Comparison between cycling with or without the interfacial bridge. Relative fluorescence was calculated independently with respect to the maximum on each graph considering all replicates. Error bars correspond to standard deviation calculated in accordance to the measurement of relative fluorescence (n=3).

3D structures: interfacial paths to scape

Once knowing that interfacial dynamics promotes drug release from the interface, it wanted to be elucidated how this process takes place. Consequently, interfacial films derived from the previous experiments were transferred to mica and glass plates and imaged under atomic force and epifluorescence microscopes. Attending to the "squeeze-out" model [47, 65], three-dimensional structures associated to the interface were expected under compression conditions. Therefore, topographical analysis of the AFM images was performed and several representative are shown in **Figure *35***. Micro (1-2 μm) and nanodomains (70-120 nm) of liquid-condensed phases (L_c) can be observed at surface pressures just before reaching the plateau values. Some higher spots and worm-like structures of around 4 nm height are apparently formed on top of these nano and microdomains (arrows in **Figure *35*** A.1), though they are likely L_e phases confined in L_c domains, as described in the literature [65]. These structures, which are probably bilayers, confirmed the formation of 3D structures during compression of the interfacial film. At higher pressures on the plateau (see **Figure *35*** A.2 and A.3), these structures increase in height (up to 20 nm) and extension (up to 5 μm). The graphs below each image in **Figure *35*** represent the height of one section (white dashed lines) and give information about which kind of structures are forming. Knowing that a phospholipid monolayer measures around 1.5-2 nm and the difference in lipid phases is around 0.5-0.8 nm [186, 187], these results induce to think that the interface-associated

structures are monolayers and bilayers stacked on top of each other, reaching in some cases up to five bilayers.

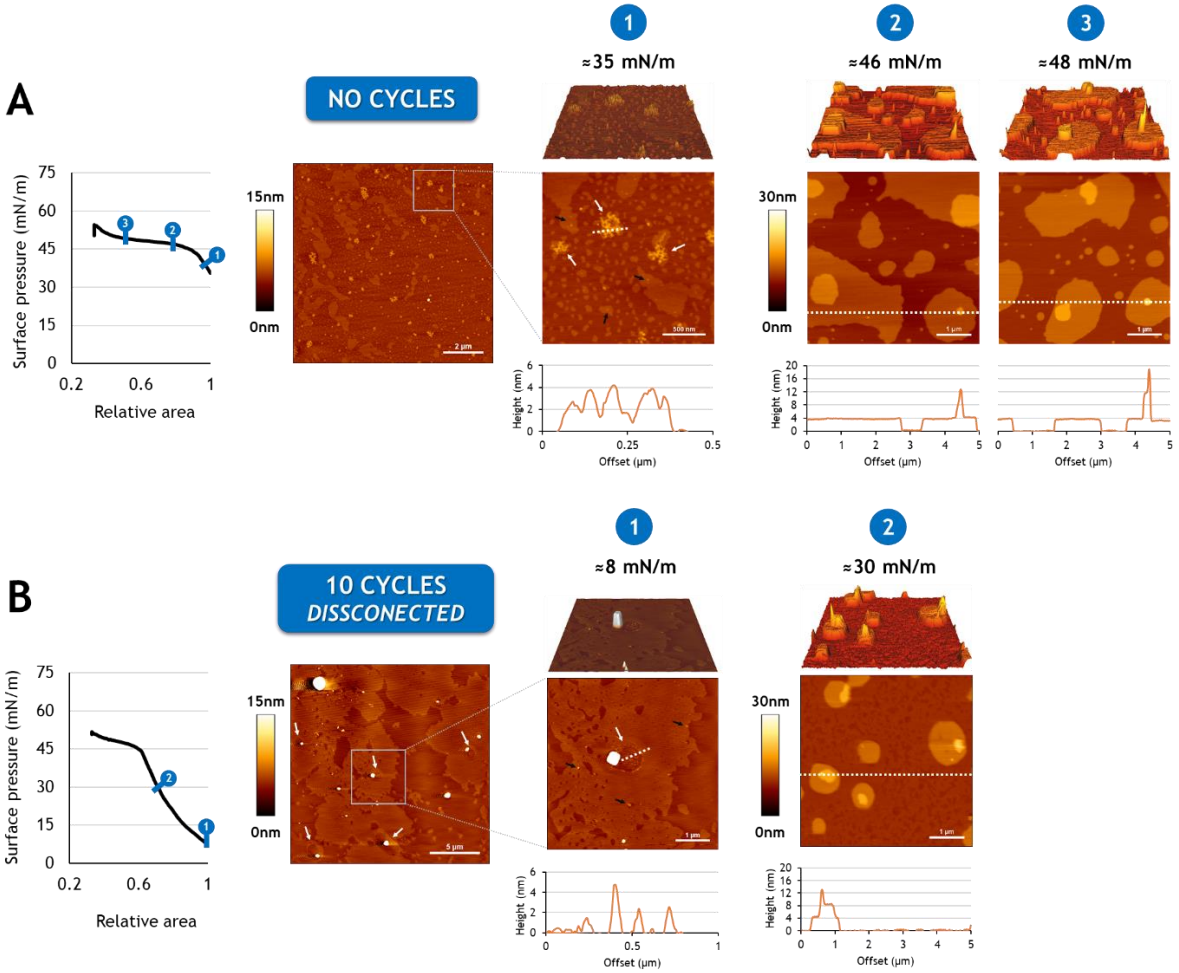

Figure 35: ***Topographical images taken with AFM before (A) and after (B) interfacial dynamics.*** 3D representation is located on top of the corresponding image. The graph on the left represents the π-area isotherm and indicates the pressure at which images were taken. Graphs below each image represents the height of one section (dashed lines). Arrows: A) white: worm-like structures (4 nm height); black: little spots (4 nm height). B) white: crater-like structures with little spots inside (4 nm height); black: little spots (100nm width and 4-8 nm height).

Surprisingly, **Figure *35*** *B.1* shows that at low pressures after the cycles (≈8 mN/m), when liquid-expanded (L_e) phases are expected to be bigger and more abundant, a more homogeneous and apparently more condensed phase is observed, instead. Little spots of up to 100 nm diameter and 4-8 nm in height can also be observed on top of those L_c phases (black arrows in **Figure *35*** B.1). Bigger crater-like structures (1-1.5 µm diameter) with plenty of those little spots inside and around, are also observed with a huge erection (up to 220 nm height) placed on the side. At higher pressures below the plateau (≈30 mN/m; Figure *35* B.2), the structures showing several stacked monolayers and bilayers are observed again. However, they appear at lower pressures

than the same obtained before the interfacial dynamics. Interestingly, their diameter coincides with the crater-like structures measured at low pressures. These results likely suggest that once the 3D structures are formed during the first compression, some could remain over the expansions acting as nucleation sites during the next successive cycles.

When the interfacial films were observed under the epifluorescence microscope (see **Figure *36***), highly intense spots were found in all assessed experimental conditions. They correspond to high concentration of fluorescent dyes NBD-PC and NileBlue which rearrange forming clusters during compression. After the cycles, the spots are smaller and the areas around completely dark. The intensity of fluorescence also decreases over compression and after the cycles. This suppose another evidence to confirm a possible lateral reorganization of the film during interfacial dynamics which leads to the accumulation of fluorescent dyes in specific locations before being excluded from the interface.

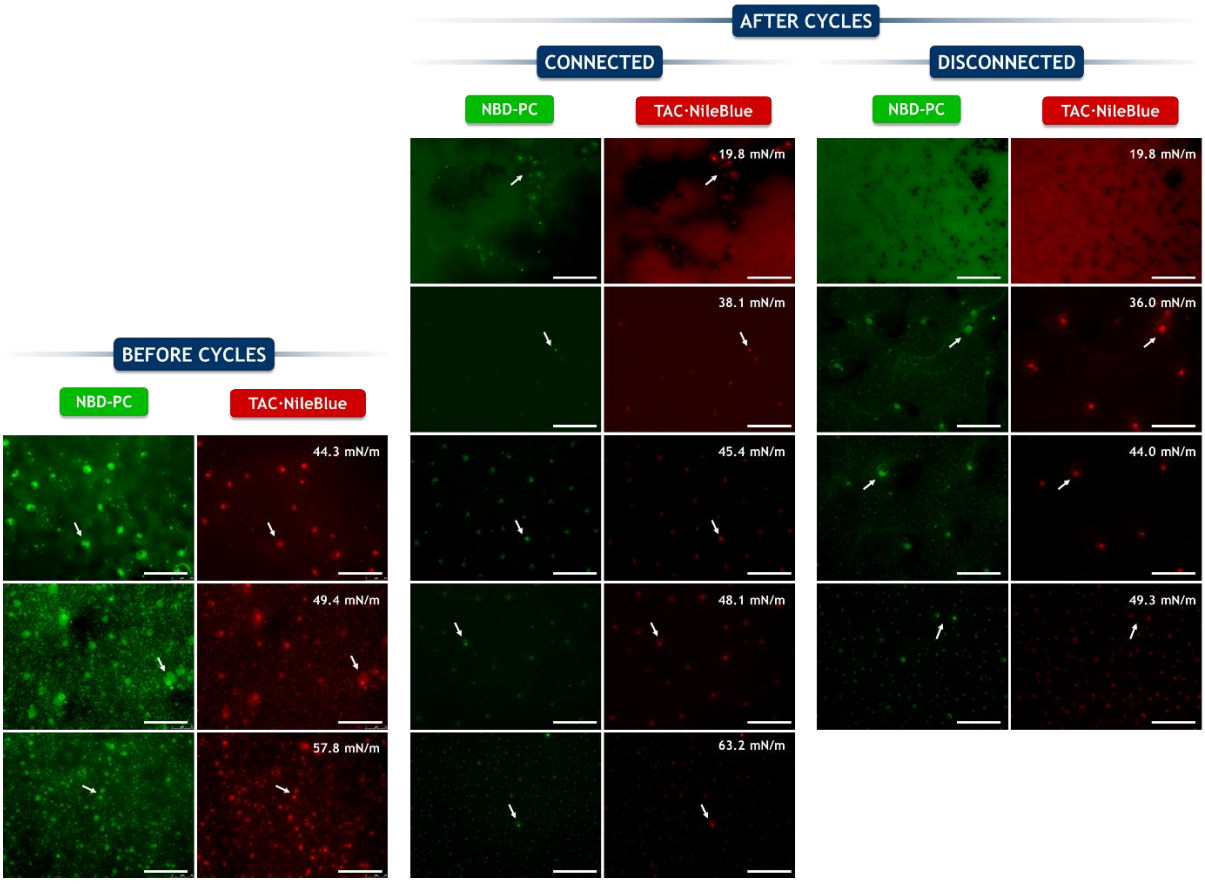

Figure 36: ***Main structures formed in the surfactant film transferred from the recipient compartment.*** Images taken under an epifluorescence microscope from transferences of OE·NBD-PC + TAC·NileBlue films, before or after dynamic cycles with or without the interfacial bridge. White arrows indicate some examples of presumably excluded three-dimensional structures. The histogram was shortened to better differentiate the structures in the images. Red: TAC·NileBlue; Green: NBD-PC. Bar = 50 µm.

Surprisingly, comparing these images with those obtained using the AFM (see **Figure *37***), the fluorescent clusters coincide with the compression-driven three-dimensional structures, insinuating that TAC is being firstly accumulated those specific locations and then excluded from the interface through them, as if they were membranes tunnels connected to the interface.

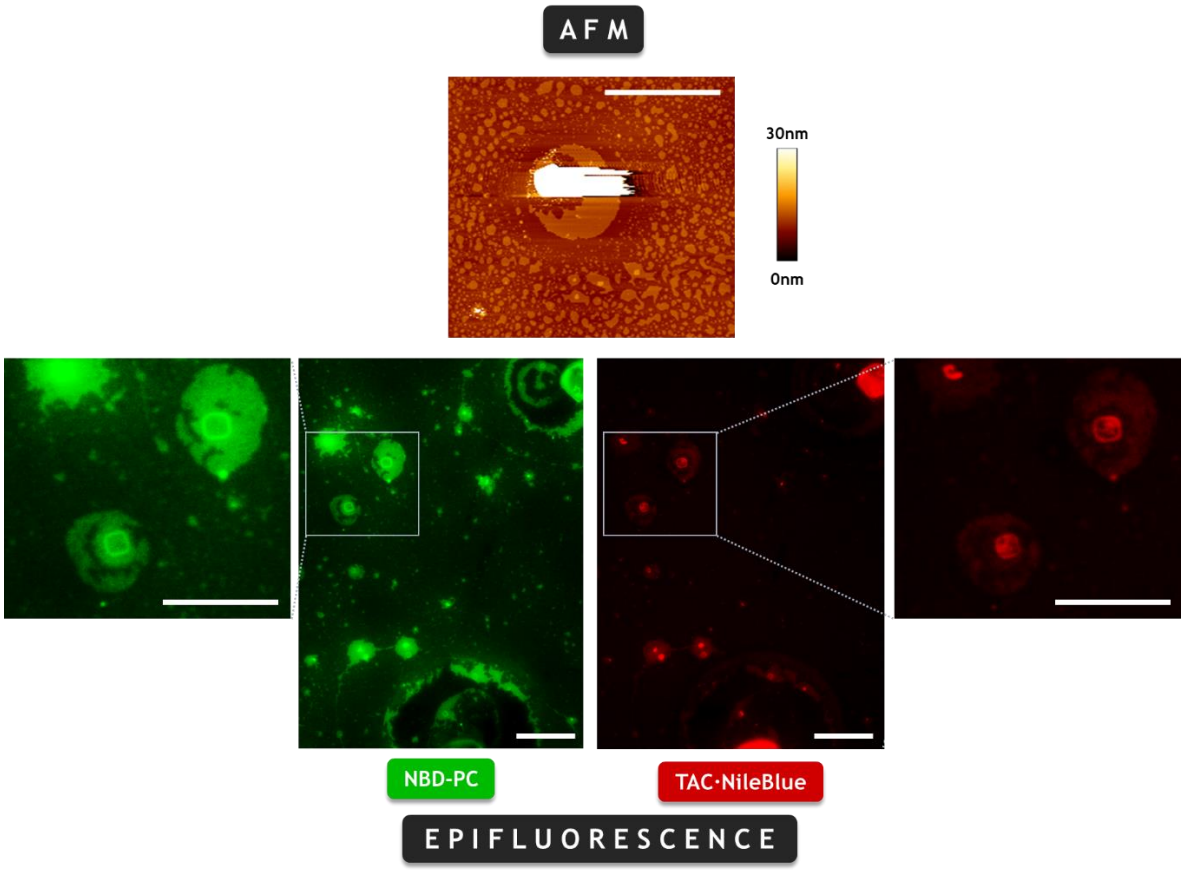

Figure 37: ***3D structures seen in AFM corresponds to the brighter domains in epifluorescence.*** In epifluorescence, the histogram of each image was firstly shortened and then contrasted to better differentiate the fluorescent structures. Merge is shown (Red: TAC·NileBlue; Green: NBD-PC). Bar = 25 µm.

Vehiculization in occupied interfaces

All the previous experiments were performed in clean air-liquid interfaces. However, to approximate the experiments even more to what happens in the lung, vehiculization was analysed in previously occupied interfaces. Emulating the endogenous surfactant, the interface was firstly coated with limited amounts of NS (1 µL labelled with 1% mol BODIPY-PC at 50 mg/mL) to minimize the formation of surface-associated reservoirs in both donor and recipient troughs. After 35 min to allow NS to coat both donor and recipient interfaces, a second addition of surfactant was applied (14µL at 50mg/mL). In this case, the sample was a combination of OE and 10% TAC (8% TAC + 2% TAC·NileBlue by mass), emulating the vehiculizing surfactant. The addition of drug/surfactant mixture was conducted following two different strategies: a) at static conditions

to know whether surfactant can also travel and transport TAC through an already surfactant-coated interface, and b) during compression-expansion cycles to evaluate if interfacial dynamics enhances the interfacial trip and the replenish of used surfactant.

As illustrated in **Figure *38***, the initial addition of surfactant produced the typical jump in surface pressure up to 41-42 mN/m. However, after the first 5 minutes it plunges to 10-12 mN/m. This sharp reduction coincides with the beginning of the increase in the recipient before reaching the equilibrium at 10-12 mN/m. This suggests that surfactant that leaves the donor to travel to the recipient is not replenished due to the limited amounts of material applied to the donor. At the moment of adding the vehiculizing surfactant in static conditions (**Figure *38***A), the surface pressure surges again up to 41-42 mN/m in the donor trough and surfactant starts traveling interfacially until equilibrating at the same pressure in the recipient. Under dynamic conditions, the vehiculizing surfactant was added during the fifth expansion, but when surface pressure in the donor trough was still increasing (35 mN/m) due to the transmission of the compression of the recipient trough along the paper bridge. This addition of new material results in a notable increase in surface pressure at the donor trough, and a reduction in the previously-observed sharp fluctuations (**Figure *38***B). At the same time, the minimum and maximum pressures of each cycle start to increase at the recipient trough. These results evidence that interfacial dynamics enhances not only depuration of interfacial films and enrichment of high-compressible phospholipids, but also the incorporation of new material coming from the donor reservoir, regardless the presence of surfactant occupying the interface.

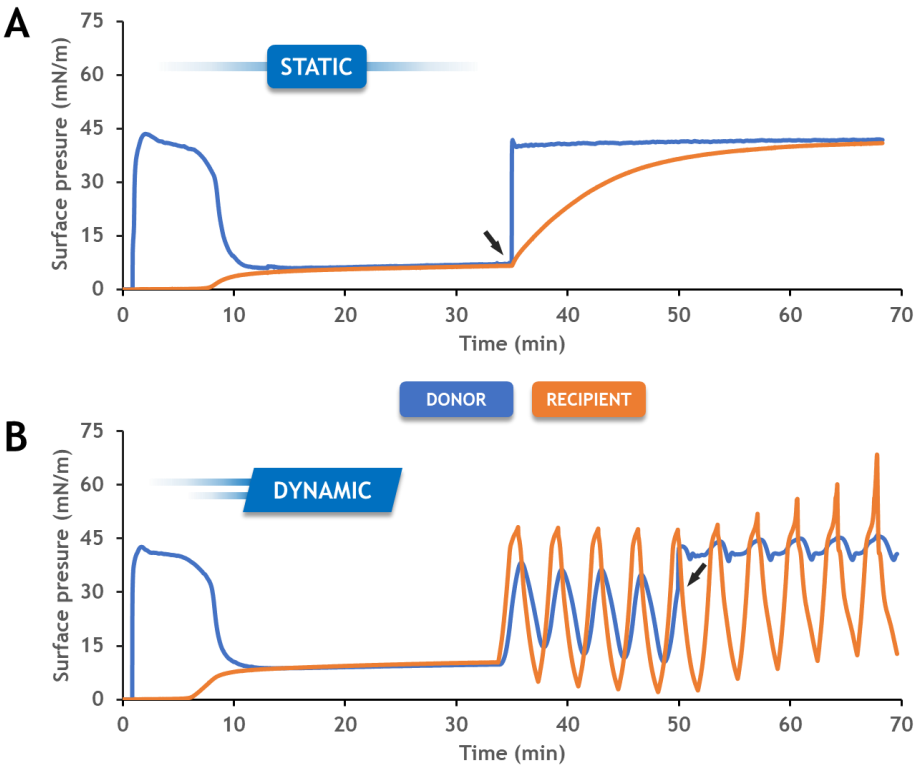

Figure 38: ***Interfacial vehiculization of Tacrolimus into a surfactant-coated interface.*** Surface pressure has been monitored into donor and recipient troughs after covering the interface with NS·BODIPY-PC and posteriorly adding OE + TAC·NileBlue. The second surfactant addition was: (A) after 35 min in static conditions (black arrow), and (B) during fifth expansion (black arrow) leaving the experiment for five more cycles.

Parallelly, images of each experiment were taken under the epifluorescence microscope. The idea was to observe how an exogenous-like surfactant behaves when it contacts with the endogenous-like surfactant which was previously applied, to confirm that surfactant transports TAC through a previously-coated interface and to see how TAC is distributed. Images in **Figure *39*** illustrate how, regardless the strategy followed, the exogenous-like surfactant (red) reaches the recipient trough and mixes with the endogenous-like (green) at surface pressures below 45mN/m. At higher pressures green fluorescence is not observed while red is clustered in brighter spots. This presumably results from the lateral exclusion of the drug from highly packed domains and the subsequent interfacial exclusion as happening in the experiments performed with clean interfaces.

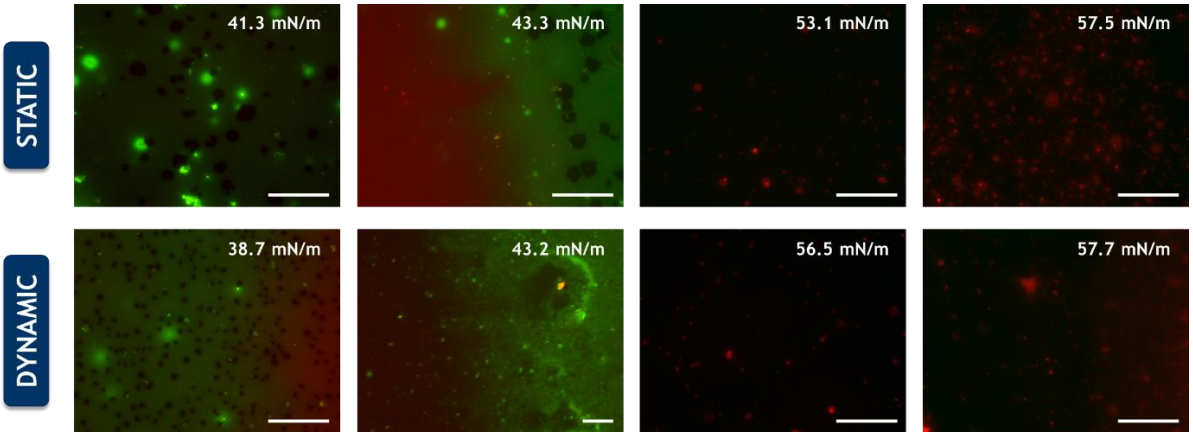

Figure 39: ***Main structures formed due to the diffusion of OE/TAC·NileBlue mixtures into a NS·BODIPY-PC coated interface.*** Epifluorescence images from the experiments adding surfactant suspensions before and during cycles. The histogram was shortened to better differentiate the structures in the images. Merge is shown (Red: TAC·NileBlue; Green: NBD-PC). Bar = 50 µm.

A fluorescence overview

In order to better interpret the former experiments, TAC·NileBlue fluorescence spectra of each experimental condition measured in the recipient trough, are represented together in **Figure *40***. As clearly observed, the major fluorescence was obtained before performing interfacial dynamics. After the cycles, fluorescence decays considerable. However, this decrease is less noticeable when both interfaces are connected, indicating that although TAC is being excluded, new dye is coming from the donor reservoirs. Interestingly, even with the interfaces connected, fluorescence was slightly higher just after interfacial dynamics than 30 minutes later.

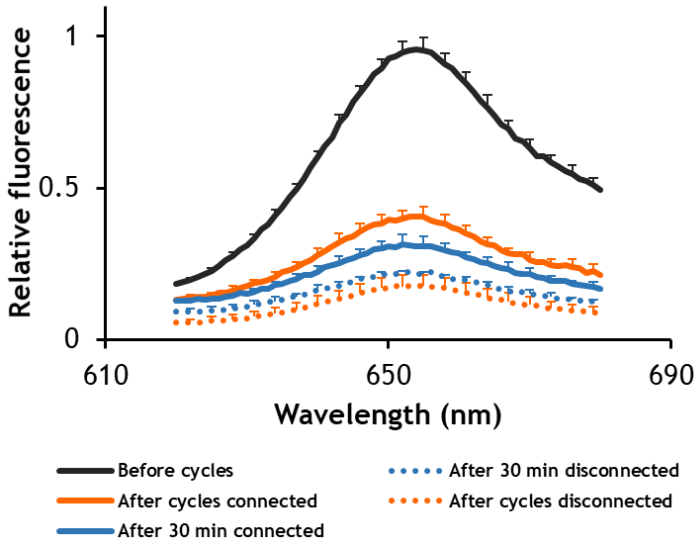

Figure 40: ***Fluorescence spectra of TAC·NileBlue measured in the recipient trough after each experimental condition.*** Relative fluorescence was calculated independently with respect to the maximum on each graph considering all replicates. Error bars correspond to standard deviation calculated in accordance to the measurement of relative fluorescence (n=3).

DISCUSSION

Few studies have addressed the mechanisms supporting the ability of PS to transport drugs through the air-liquid interface and, even lees, to know which are the insights involved in the release process. The previous chapter focused on the idea of vehiculizing hydrophobic drugs and how they could alter the interfacial functionality of different surfactant formulations. Nevertheless, as important as vehiculizing drugs is to release them in the desired locations. The squeeze-out model could give indirect evidences that the exclusion of drugs is happening through the interface-associated 3D structures [47], as occurring with unsaturated phospholipids [65] or meconium components [188]. However, no direct proofs are available showing the real mechanism behind the vehiculizing and exclusion process under dynamic conditions. The data presented here support the idea that the breathing-like compression and expansion dynamism, at which the respiratory surface is continuously subjected during the process of breathing, enhances the vehiculization of therapeutic passengers towards the alveoli and, once there, it promotes their exclusion via interfacial-associated 3D pathways.

Exploring how a hydrophobic drug interacts with pulmonary surfactant and behaves interfacially

Although the use of DPPC monolayers as a model of pulmonary surfactant cannot properly cover the entire insights of such a complex system, it could advance several essential cues to elucidate how TAC is interacting with it and behaves interfacially. The assays performed with monolayers of DPPC demonstrated that Tacrolimus is actually able to intercalate between DPPC molecules and somehow affects their lateral distribution under compression circumstances. The former can be interpreted as a positive sign since it is suggesting that pulmonary surfactant could contain certain amounts of TAC in its membranes to be vehiculized. The latter, on the other hand, could be interpreted as a negative effect since it is altering one of its most useful characteristics for the interfacial activity of pulmonary surfactant: the capacity of self-packing very tightly to form a solid-like phase able to displace water molecules from the interface reducing the surface tension. Nevertheless, deeply analysing the behaviour of DPPC monolayers in the presence of TAC upon compression, it emerges that TAC is excluded laterally first and then interfacially. The increase of lateral pressure undergoes a lateral rearrangement of the interfacial molecules in different clusters, attending basically to its size and capacity of packing. The presence of domains upon compression confirms that at certain lateral pressure, TAC cannot sterically resist and is laterally excluded to the fluid phase. The slight increase of fluorescence observed in the fluorescence images at the beginning of compression confirmed that, upon the lateral organization of the monolayer, the drug is firstly accumulated in the fluid phase. Then, at higher pressures, the drug is interfacially excluded

as the fluorescence of the fluid phase is considerable less upon this process. However, some signal is still detectable, indicating that not all the durg is excluded during the first compression. We additionally propose that during the lateral exclusion of TAC, the already-formed domain containing DPPC and NBD-PC around is disturbed, evidenced by a darker halo around the domains seen in **Figure *25***. In **Figure *41*** this exclusion model is proposed. This could be determinant for the interfacial rheology impairing its interfacial functions.

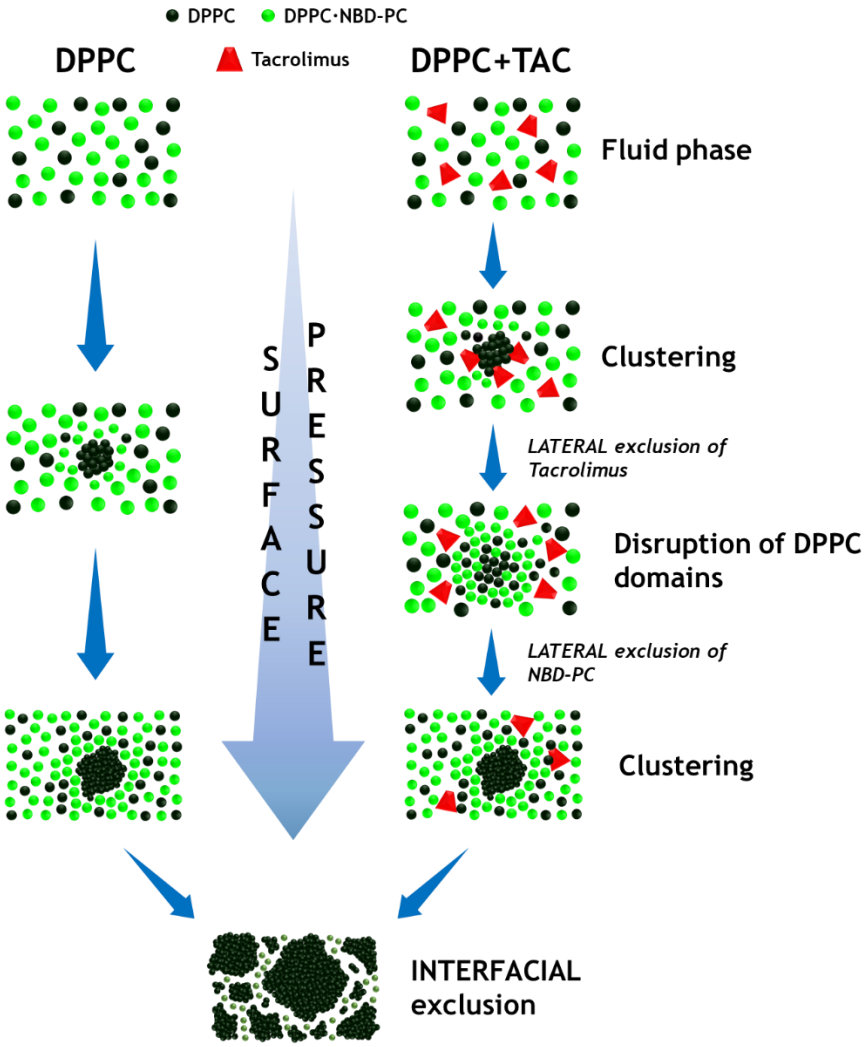

Figure 41: ***Lateral and interfacial exclusion model.*** This model shows the compression-triggered lateral exclusion of TAC and NBD·PC from the highly packed domains of DPPC. At low surface pressures molecules at the interface have free movement and occupy more area (Fluid phase). Over compression, molecules start clustering and Tacrolimus (TAC), which cannot be compressed, is firstly excluded, disturbing the already-formed DPPC domain. At higher pressures, DPPC molecules pack tighter and NBD-PC is also excluded. Finally, the extremely high lateral pressure forces TAC and NBD-PC to leave the interface in a merely steric process.

Having this in mind, we thought that if TAC is excluded from the interface over compression, the exclusion would be even higher making consecutive compression-expansion cycles. Effectively, although the major exclusion takes place during the first compression, the remaining TAC is

progressively excluded upon the cycles. This is a such depuration that leads DPPC to start packing at the same pressures than in the absence of the drug, forming the condense domains again. Nevertheless, in DPPC monolayers where no other elements leading this process are present (i.e. SP-B or SP-C), this exclusion is produced from fluid phases following an uncontrolled steric process. At this point, knowing that DPPC can hold TAC and the compression-expansion dynamics is promoting its exclusion, it becomes appropriate to introduce the rest of the elements in the system. Similarly, the experiments preformed using organic solutions of surfactant and following the Langmuir protocol to prepare interfacial monolayers confirmed the lateral clustering prior to the exclusion from the interface, as observed in the fluorescence images where the drug is localised in specific regions surrounded by highly packed domains. Additionally, the broader transition plateau observed during the first compression at maximum amount of TAC evidences that the presence of the drug at pressures bellow 30 mN/m affects the phase transition of the lipid and triggers the depuration of the interfacial film during the first compression, likely disturbing the surroundings of condensed regions as observed in pure DPPC monolayers.

In presence of organic extracts of surfactant, when unsaturated lipids and proteins are present also in the interface together with surfactant, the presence of vesicles-like full of TAC and NBD-PC out of the condense regions over the exclusion plateau above 34 mN/m is advancing that this exclusion is taking place at specific locations. Therefore, this process, still being a steric issue, seems to be accurately orchestrated. In fact, the characteristic plateau of surfactant supposes an indicative of the existence of structural transitions, where predominantly non-compressible material folds down to reduce the surface tensions to values below 2mN/m. This structural transitions, which have been well studied, will be discussed in the next section.

Dynamic vehiculization

The experiments proposed in this section, where traditional Wilhelmy and Langmuir-Blodgett troughs are connected, allow to study surfactant films as never before. Since Dr. Clements proposed the Langmuir-Blodgett trough to study the structure of pulmonary surfactants, it has been one of the most used method. Traditionally, the way of forming monolayers and surfactant films has been by spreading an organic solution or aqueous suspension directly on the Langmuir-Blodgett trough. Even applying the sample in organic solvents, which is widely thought that it ensures the formation of simple monolayers, exist the risk to unintentionally generate subjacent structures that could incur in erroneous interpretations. Levering the spreading properties of pulmonary surfactant, only the fraction absorbed into the interface of an independent trough and then spontaneously spread through an interfacial bridge to the Langmuir-Blodgett trough can be

studied using this method. Apart from this, it is possible to reach the equilibrium surface pressure in this trough without reducing the area and study the native structures, avoiding the possible formation of them derived from compression-driven lateral segregation and allowing reaching minimal surface tensions close to physiological (2 mN/m) under compression. More importantly, once formed the surfactant film, the possibility of removing the bridge also allows to study this native-like film independently of any surfactant reservoir, which could also lead to erroneous interpretations.

The assays carried out in the presence or in the absence of the interfacial bridge have demonstrated that the loss of interfacial material over interfacial dynamics in the recipient trough, and consequently in the donor due to the continuous spreading towards the recipient, activates the adsorption and interfacial trip of new material. Only in limiting conditions of surfactant, as there is not enough new surfactant accumulated in the subphase, the material that is being transferred from the donor to the recipient trough is not replaced. However, unrestricted amounts of surfactant added to the donor trough maintain the interface completely saturated, even when the material is traveling. This highlights the necessity of a continuous network of new and operative surfactant at the alveolar lining fluid in the lung to ensure a constant transference of material into the interface. When the recipient trough has no reservoirs with new surfactant (interfaces disconnected), all the material that was lost during the interfacial dynamics is not replaced, bringing to light that the excluded material is unable to readsorb, even after half an hour after the compression and expansion dynamics. However, in the presence of the bridge the material lost during the cycles is unequivocally replenished by new coming from the donor. This put on the table that the normal breathing cycles enhance the diffusion of PS towards the alveolar region and, consequently, the vehiculized passengers. It has been well established that the particular composition of PS, especially the presence of the hydrophobic surfactant proteins (SP-B and SP-C), optimizes the interfacial behaviour of surfactant films during compression-expansion dynamics [47] and facilitates the spreading of exogenous formulations. During compression, part of the material already at the interface folds down and is excluded from it to be recycled; during expansion, that released surfactant likely generates surface tension gradients. Leveraging such gradients, mostly towards the alveoli, and attending to the Marangoni effects [189], we speculate that exogenous surfactant and additional passengers that are properly associated could hook the endogenous surfactant and spread independently of fluid flows induced by the ciliated bronchial epithelia. Interfacial surfactant-associated phenomena could therefore allow reaching the alveolar region, with surfactant sharing the trip with additional elements, such as allergens, drugs or

nanocarriers. However, further studies are required to evaluate the potential effect of fluid flows induced by the mucociliary escalator.

The topographical and epifluorescence observations confirmed that the interfacial dynamics promotes the selective exclusion of material from the interface. As mentioned, this selectivity arises from a mere steric matter, where every molecule that cannot resist high lateral pressures is simply excluded from the interface. However, this loss of material far from taking place aleatory, is perfectly orchestrated and localized in specific locations at the interface. Transitions structures have been detected at pressures coinciding with the conspicuous plateau observed just above the equilibrium surface pressure (42-45 mN/m). This metastable 3D structures have been well studied, and it is widely accepted that they consist in an equilibrium coexistence between L_e, L_c and collapsed phases [190]. These collapsed phases, presumably formed under the coordination of the hydrophobic proteins SP-B and SP-C [191], are monolayers and bilayers stacked on top of each other [47, 192, 193]. It is widely accepted that these multilayered 3D structures, through which part of the excluded material remain closely associated to the interface to ensure a proper amount of surfactant over the subsequent compressions, are enriched of unsaturated phospholipids [65]. As observed in the topographical images, the 3D structures formed during the cycles seem to re-extend again along the interface. However, little higher spots remain. Knowing that SP-B and SP-C are critical to form, stabilise and re-expand these kind of structures, we suggest that these spots could be accumulations of these proteins. They cluster during compression and act as nucleation points from where unsaturated lipids and other molecules will be excluded from the interface during the subsequent compressions.

Following the "squeeze-out" model, this work stablishes that, in a similar manner to unsaturated phospholipids, additional therapeutic passengers as TAC or corticoids are excluded to the subphase through these multilayered structures in the form of three-dimensional structures. In fact, observing these structures under the epifluorescence microscope, we realised that both small and bigger 3D formations were completely full of TAC and NBD-PC, which labels the fluid phases where unsaturated phospholipids are expected to be. The TAC fluorescent spectra measurements revealed that fluorescence decayed after interfacial dynamics, concretely during compressions. Hence, the drug is unequivocally excluded from the interface. However, the excluded material is not able to readsorb, confirming *in situ* the existence of small aggregates of "used" surfactant unable to readsorb once excluded. These small aggregates has been reported to be enriched with unsaturated phospholipids and need to be removed from the alveolar lining fluid for recycling [65].

Attending to the fact that interfacial dynamics activates the adsorption and interfacial trip, one could anticipate that more TAC must be vehiculized and hence more should be detected over the cycles when both troughs are connected, especially after 30 minutes. Nonetheless, the fluorescence readings did not show the same. In an attempt to explain this, we speculate that over compression, non-compressible molecules form continuous pathways of fluid phases that converge into those 3D structures. Like interfacial rivers that merge in the subphase ocean. As shown in the literature [47] and in the topographical profiles of this work, the condensed micro and nanodomains coexist with a continuous network of L_e phases, revealing the existence of these interfacial pathways. Once at the recipient trough, as TAC cannot intercalate between the already-formed condensed phase, it could comfortably flow along the interfacial pathways to reach the 3D structures, where it could diffuse to the subphase. So that it likely goes directly to the subphase and only the remaining in the interface can be detected.

Regarding the material that remains at the interface, it seems to be refined. Judging by the shape of the isotherms after the cycles, which progressively reminds to DPPC, not only in the absence but also in the presence of the interfacial bridge, the material that stays at the interface tend to be DPPC. Although the initial amount of surfactant at the interface is not replaced completely (evidenced by the pressures at the end of the expansions), the high lateral pressures reached during compressions confirm that DPPC is not being excluded, or at least the majority. Additionally, several evidences suggest an enrichment of DPPC and simultaneous depuration of the material coming from donor reservoir: the reduction of necessary area to reach the maximum pressures, the concomitant shortening of the exclusion plateau and the fact that the pressures at the end of the expansions in the presence of the bridge do not change excessively. Conversely, in the absence of the bridge, the necessary area to reach the maximum pressures increases and the pressures at the end of the expansions decreased considerably. Therefore, this is another prove confirming that the interfacial material is being lost but DPPC still remains there. This makes sense from a biophysical and physiological point of view because DPPC is the main phospholipid able to resist the lateral pressures reached in the alveoli and then reducing the surface tension to values near 0 mN/m. It has been theorised in the literature that both a "selective adsorption" of DPPC [65, 194, 195, 196] or "selective exclusion" of non-DPPC lipids could be occurring. It has been proposed that this "selective adsorption" is due to the combined action of SP-B and SP-A [195], but the experiments performed in this thesis were made using the organic fraction of surfactant, where SP-A is absent. However, even though these experiments do not contradict the existence of a selective adsorption, we propose that the progressive enrichment of DPPC is due to a presumable

simpler continuous "selective exclusion". The interfacial film is simultaneously depurated from uncompressible molecules constantly adsorbing with no other option than accumulate DPPC. The interesting and still unsolved question, common in both proposals, is how the amounts of DPPC in the interface are controlled. Is there a "selective exclusion" of DPPC orchestrated by surfactant proteins? Can cholesterol and SP-C be the ones involved in such a process?

Therefore, this chapter clearly provides a robust understanding of the elementary processes involved in the interfacial pulmonary drug delivery. It demonstrates that interfacial dynamics favours even further the transference of material from the donor to the recipient trough and promotes the release of carried drugs from the interface towards the aqueous subphase, regardless a previous saturation of the interface with pulmonary surfactant. Nevertheless, to properly transfer the generated knowledge to clinics, it is necessary to perform further experiments, taking into account the native context that the desired therapy will encounter in the lungs. Therefore, the next chapter addresses the pulmonary surfactant-promoted drug delivery approach directly on lungs using *in vivo* systems.

The experiments included in the present chapter were performed during a short-term stay in the Lung Biology Laboratory (Department of Physiology and Cellular Biology, Columbia University Medical Center, New York, USA) supervised and assisted by of Prof. Jahar Bhattacharya and Prof. Sunita Bhattacharya.

COLUMBIA UNIVERSITY
MEDICAL CENTER

CHAPTER III:

Surfing the in vivo interface

INTRODUCTION

The earlier *in vitro* biophysical studies demonstrated the potential use of pulmonary surfactant as a drug delivery system. This membrane-based lipid-protein material is able to pick up hydrophobic drugs, transport them long distances using air-liquid interfaces as a motorway and drop them off over the continuous interfacial compression and expansion dynamics. However, the relevance of these findings in intact lungs is poorly understood. Especially since the presence of mucus, immune system, pathogens, particles or the air and liquid flows produced during lung expansion and relaxation may impair this strategy drastically. Several *in vivo* studies have already demonstrated the synergistic effects of different surfactant/drug combinations such as antibiotics [114, 115, 116], corticosteroids [120, 121, 122] or even nanoparticles containing siRNA [197]. Nevertheless, none investigated how. Therefore, this chapter focuses on observing, describing and demonstrating the vehiculizing potential of pulmonary surfactant directly on lungs using *in vivo* systems. Consequently, it has been determined the distribution and efficacy of tacrolimus (also known as FK506 or TAC) as an airway-delivered drug model in a lipo-polysaccharide (LPS)-induced mouse model of acute lung injury. The idea was to detect synergistic anti-inflammatory effects when TAC is vehiculized in combination with exogenous pulmonary surfactant.

Lipopolysaccharide, also known as endotoxin, is the invariant virulence factor present in the outer cell membrane of Gram-negative bacteria (i.e. *Escherichia coli* and *Salmonella enterica*) [198]. It is one of the most potent activators of innate immune responses that triggers the activation of the inflammation process binding to Toll-like receptors (TLR), especially TLR-4 [199, 200]. Therefore, it has been extensively used to induce the inflammation process in lungs, generating *in vivo* models of ALI. LPS-induced ALI is mainly due to the disruption of the air-blood barrier integrity with the consequent extravasation of fluid, proteins and inflammatory cells (mostly neutrophils) into lungs [201]. The resulting protein leakage and ROS production completely destroy the alveolar balance, nourishing the overall inflammation [108]. The treatment with anti-inflammatory drugs could reduce the extensive oedema and contribute to counteract the inflammatory process.

In this regard, Tacrolimus (TAC) may be a good candidate. It is a hydrophobic immunomodulator firstly found in *Streptomyces tsukubaensis* [202], which has been widely used in transplantation of human lungs [203, 204] and other solid organs [205, 206] to prevent and treat allograft rejection. It has been extensively demonstrated that TAC supposes an effective treatment to lessen neutrophil activity and equilibrates the balance of pro-/anti-inflammatory cytokines, reducing the inflammation process [207]. Conjugated with FK binding proteins, TAC inhibits calcineurin, a phosphatase involved in intracellular signal transduction and blocks mitogen-activated protein

kinases (MAPKs) cascade and NF-κB. This inhibits pro-inflammatory cytokines production (i.e. IL-1β and IL-6) and NOS, and triggers the expression of anti-inflammatory cytokines (i.e. IL-10, TGF-β and TNF-β) [208, 209, 210].

The majority of the studies elucidating the effect of tacrolimus on inflammatory cells has been focused on T-cells and the adaptive immune responses. However, few evidences have demonstrated the effects of TAC on innate immune responses and the cells involved in this process. Some studies suggest that TAC firstly induces the activation of steady-state macrophages blocking the constitutively inhibition of TLRs by calcineurin [211, 212]; then, it seems to trigger a process of tolerance to subsequent challenge with LPS, providing some protection against *in vivo* LPS-induced endotoxin shock [213, 214]. With regard to the MAPKs pathway, TAC predominantly regulates cytokine production in activated macrophages through extracellular signal-regulated kinases (ERK) [212, 215, 216] , instead of c-Jun amino-terminal kinases (JNK) and p38 MAPKs, as occurring in T-cells. Additionally, TAC also induces apoptosis in inflammatory cells via caspases 3 and 9, shifting to an anti-inflammatory environment [210]. Moreover, apart from the anti-inflammatory effects on T-cells [217], macrophages [218] and neutrophils, it has also been reported that TAC could act as an antifibrotic drug inhibiting the TGF-β-induced collagen synthesis in human lung fibroblastic cells [219], showing better prognosis in patients [220].

THE *IN VIVO* MODEL

In order to explore the feasibility of the new and non-invasive drug delivery strategy proposed in this thesis, *in vivo* models have been used. As aforementioned, TAC has anti-inflammatory effects, then LPS-induced mice models for inflammation have been proposed to assess the potential synergistic effects of delivering the drug in combination with pulmonary surfactant and whether it enhances the distribution through the respiratory surface. Accordingly, in anesthetized Swiss Webster mice (8-10 week old and 30-40g weight), different solutions were sequentially intranasally instilled (see **Figure *42***): a) PBS (30 µL) at 0 and 1 h for control; b) PBS (30 µL) and LPS (5 mg/Kg; Lipopolysaccharides from Escherichia coli O111:B4 from Sigma-Aldrich) at 0 and 1 h, respectively for a pro-inflammatory group; c) own-purified porcine surfactant (50 µL; 10 mg/mL) and LPS (5 mg/Kg) at 0 and 1 h, respectively to test non-specific surfactant effects; d) TAC·NileBlue (50 µL; 15 µg) and LPS (5 mg/Kg) at 0 and 1 h, respectively to examine specific anti-inflammatory effects derived from the drug; and e) 50 µL of a combination of Surfactant (10mg/mL) + TAC·NileBlue (15µg; 1.5% wt), respectively to evaluate the synergistic anti-inflammatory effects. TAC was fluorescently labelled with NileBlue to track the distribution. Five hours after the last instillation, the mice were anesthetized and exsanguinated through the

heart. Then, 1 mL of ice-cold PBS was intra-tracheally instilled and withdrawn the bronchoalveolar lavage (BAL). Additionally, the same experiments were carried out in mice whose macrophages were previously depleted by clodronate. An aqueous suspension (60 µL; 7 mg/mL) of liposome-encapsulated clodronate (Clodrosome® from Encapsula NanoSciences LLC, USA) was intranasally instilled (15 mg/kg) to anesthetised mice. After two days, mice were treated as described in **Figure *42***.

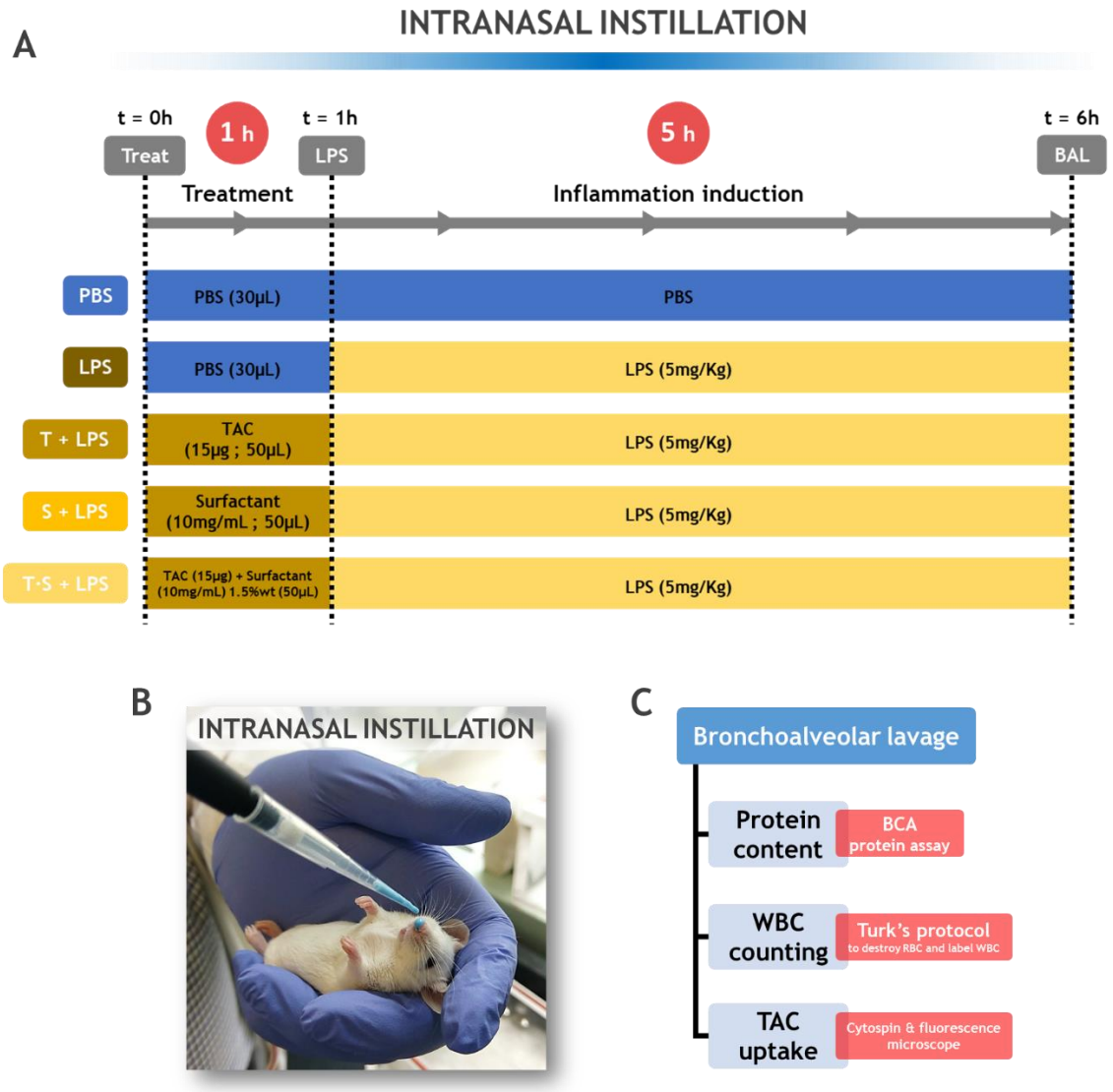

Figure 42: ***Experiment protocol.*** **A)** Experimental conditions. **B)** Example of intranasal instillation. **C)** Performed experiments using bronchoalveolar lavages to evaluate the anti-inflammatory effects and distribution of TAC trough the respiratory surface.

In a 9 µL BAL aliquot, Turk's solution (1:10 v/v) was added, in which acetic acid (1-2%) destroys RBCs and gentian violet stains nuclei making cells visible for counting on the haemocytometer (counted in four different squares of 0.04 mm^2; four aliquots per mouse BAL).

Then, the remaining BAL was centrifuged to separate cells (15 min; 4 °C; 800 G). The supernatant was used to determine the protein content by the bicinchoninic acid (BCA) assay to determine the existence of edema, while the pellet to directly observe the presence of red blood cells (RBC), as a sign of pulmonary edema, and determine which BAL cells uptake TAC. For the latter, the pellet was resuspended in PBS (1 mL) and conveniently diluted before centrifuging in a Cytospin™ 4 Cytocentrifuge (5 min; 4 °C; 2000 rpm) to deposit the appropriate number of cells in a glass slide. Then, the cells were fixed with methanol (99%) to observe them under the fluorescence microscope (Olympus IX81) in search of those that uptake TAC. Additionally, the cells were stained with Giemsa solution (30 min) to morphologically distinguish the different cell populations in BAL. The samples stained with Giemsa could not be observed to evaluate the TAC uptake, as this colourant is also visible with the same filter used for TAC·NileBlue, complicating the correct interpretation of the images by inducing false positives (see **Figure *43***). Therefore, it is necessary to prepare the samples separately to distinguish the cell populations (Giemsa staining) and observe the TAC·NileBlue fluorescence (no stain, just the fluorescently labelled TAC).

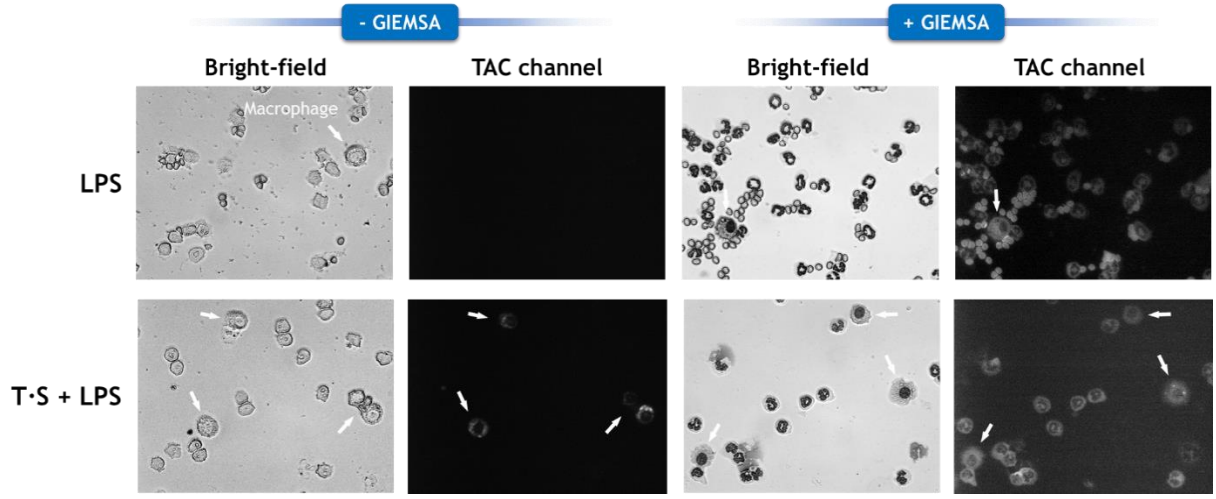

Figure 43: ***Giemsa emits fluorescence in a similar wavelength to TAC·NileBlue.*** The images correspond to bronchoalveolar cells observed under bright-field and fluorescence microscopy. After the cytospin, cells were directly fixed with methanol (- GIEMSA) or stained with Giemsa (+ GIEMSA). LPS samples (up) correspond to a negative control for TAC·NileBlue, while T·S + LPS (down) represents the positive control. When the cells were stained with Giemsa, a fluorescence signal can be observed even in the absence of TAC·NileBlue (LPS, + GIEMSA, TAC channel). If they are not stained (LPS, - GIEMSA, TAC channel) a fluorescence signal is not observed. In the case of T·S + LPS samples, TAC·NileBlue fluorescence is detected inside some cells (T·S + LPS, - GIEMSA, TAC channel), as expected. When they were stained with Giemsa (T·S + LPS, + GIEMSA, TAC channel) all the cells emit fluorescence. Although the fluorescence pattern is slightly different in those cells where TAC is expected to be (macrophages; white arrows), Giemsa stain complicates the correct interpretation of images.

RESULTS

To determine the anti-inflammatory effects of TAC and explore the possible synergistic effects of delivering it in combination with pulmonary surfactant, very basic inflammatory indicators

were evaluated from bronchoalveolar lavages (BALs) of five different groups of mice as described below. First, the amount of white blood cells (WBC) was calculated among the several conditions to determine the anti-inflammatory effect of the different formulations. Then, the presence of pulmonary oedema was analysed by observing the presence of red blood cells (RBC) and measuring the total protein content in the BAL. Finally, the TAC uptake in BAL cells were observed under the epifluorescence microscope.

Surfactant/TAC combinations produce synergistic effects

Figure *44* shows that the amount of WBC increased significantly in LPS-induced inflammation (LPS; 1.71±0.29 million/mL; mean ± SD, n=4) in comparison with the control group (PBS; 0.21±0.04 million/mL; mean ± SD, n=4). The treatment with only tacrolimus (T + LPS) or surfactant (S + LPS) did not counteract the LPS-mediated WBC increase (2.20±0.52 and 2.29±0.21 million/mL, respectively; mean ± SD, n=4). Nevertheless, when mice were pre-treated with tacrolimus vehiculized with pulmonary surfactant (T·S + LPS), the amount of WBC was greatly reduced (0.64±0.12 million/mL; mean ± SD, n=4), revealing that surfactant/TAC combinations have, somehow, synergistic effects.

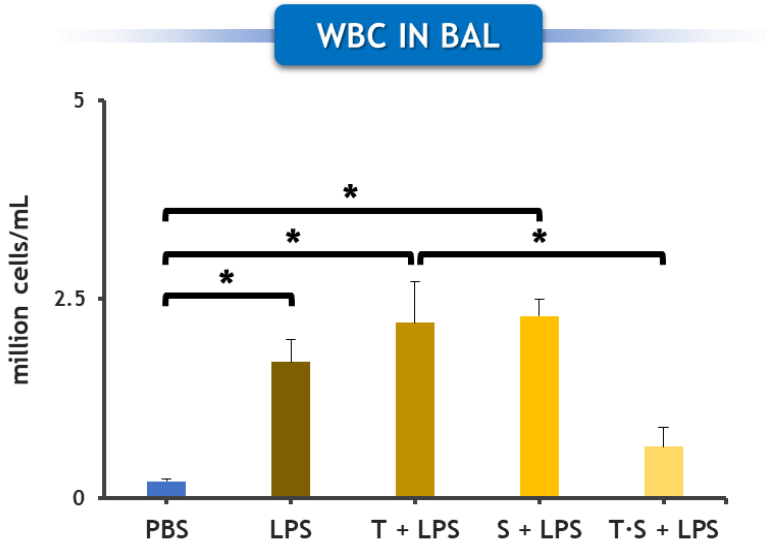

Figure 44: ***White blood cells (WBC) count in bronchoalveolar lavages (BALs).*** Mean of four mice is represented for each condition (four different squares of 0.04 mm^2 were observed; four aliquots per mouse BAL were counted). Error bars represent the standard deviation. (*) $p<0.01$ (One Way ANOVA, Holm-Sidak method).

The pellets obtained after centrifuging the BALs were merely observed (see **Figure *45***). The group of mice treated with LPS (LPS) clearly showed a reddish colour, evidencing the presence of red blood cells in the alveolar spaces, which usually suggests pulmonary edema. Those groups pre-treated with only TAC (T + LPS) or pulmonary surfactant (S + LPS) also presented a red

colour. However, when mice were pre-treated with TAC in combination with pulmonary surfactant (T·S + LPS), the pellet presented a yellowish colour like the control group (PBS), indicating that the extravasation of blood components to alveolar spaces was reduced.

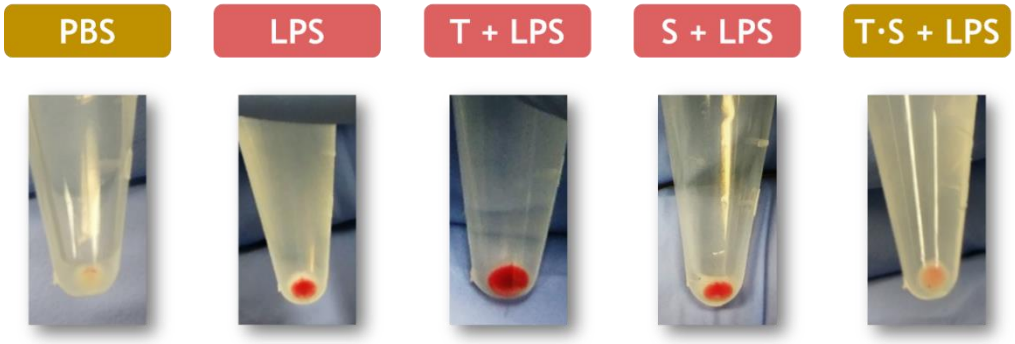

Figure 45: ***Pellets obtained after centrifuging BALs.*** Representative images of n=4 for each condition.

Something similar occurred when the total protein content was measured in the different bronchoalveolar lavages. As shown in **Figure *46***, the protein content in the LPS and T + LPS groups (0.70±0.38 and 0.86±0.55 mg/mL, respectively; mean ± SD, n=4) is significantly higher than the control (0.22±0.04 mg/mL; mean ± SD, n=4), evidencing that the LPS-promoted edema is not counteracted by the administered doses of tacrolimus. In the case of those mice pre-treated only with surfactant (S + LPS), the total protein content seems to be reduced (0.37±0.16 mg/mL; mean ± SD, n=4), although the differences with respect to LPS group are not statistically significant. On the other hand, the treatment with surfactant/tacrolimus combination clearly shows a great reduction of BAL proteins (0.20±0.04 mg/mL; mean ± SD, n=4).

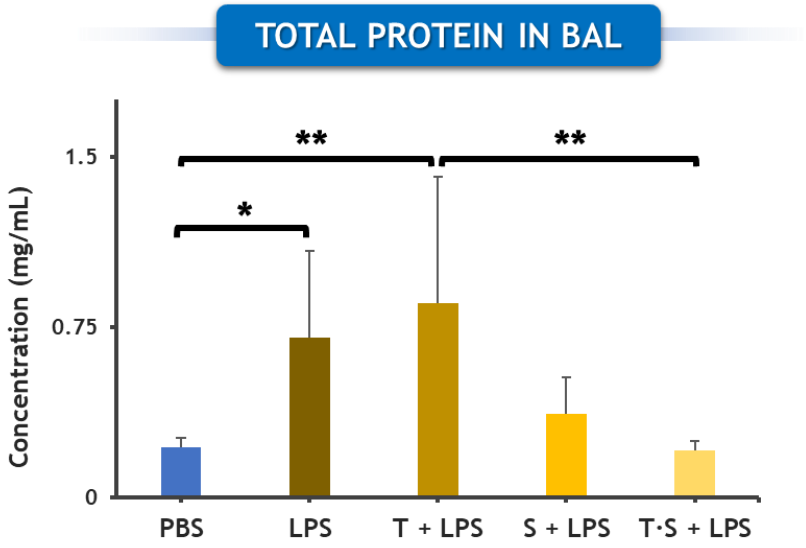

Figure 46: ***Total protein content in bronchoalveolar lavages (BALs).*** Mean of n=4 is represented for each condition. Error bars represent the standard deviation. (*) $p<0.05$ and (**) $p<0.01$ (Mann-Whitney Rank Sum Test).

TAC uptake as a proof of surfactant-mediated interfacial distribution

Before determining if TAC is captured by cells, it is convenient to characterise which types of cells are present in the different experimental conditions. Consequently, the pool of cells isolated from BALs was conveniently stained with Giemsa, which is a colouring agent widely used to morphologically differentiate blood and BAL cells [221]. **Figure *47*** shows the different cell populations that coexist in the airways in the absence and the presence of LPS-induced inflammation (A), and the proportion of macrophages in each experimental situations (B). In steady-state conditions (PBS group), the pool of bronchoalveolar cells is mainly composed by macrophages (97±2%; mean ± SD; n=3), ideally AMφ, characterised by big rounded deep blueish nuclei and granulized cytoplasm. However, in LPS-induced inflammatory conditions, the percentage of macrophages decreases (LPS: 9±4%; T + LPS: 5±3%; S + LPS: 13±9%; T·S + LPS: 9±6%; mean ± SD; n=3) as a consequence of a massive extravasation of blood elements, especially neutrophils (polymorphonucleated with deep blue-violet segmented-like nuclei) and erythrocytes (salmon-pink) (see Figure 47A). Although neutrophils remain in all LPS-induced conditions, erythrocytes decrease considerably in mice pre-treated with TAC in combination with surfactant (also showed in **Figure *45***).

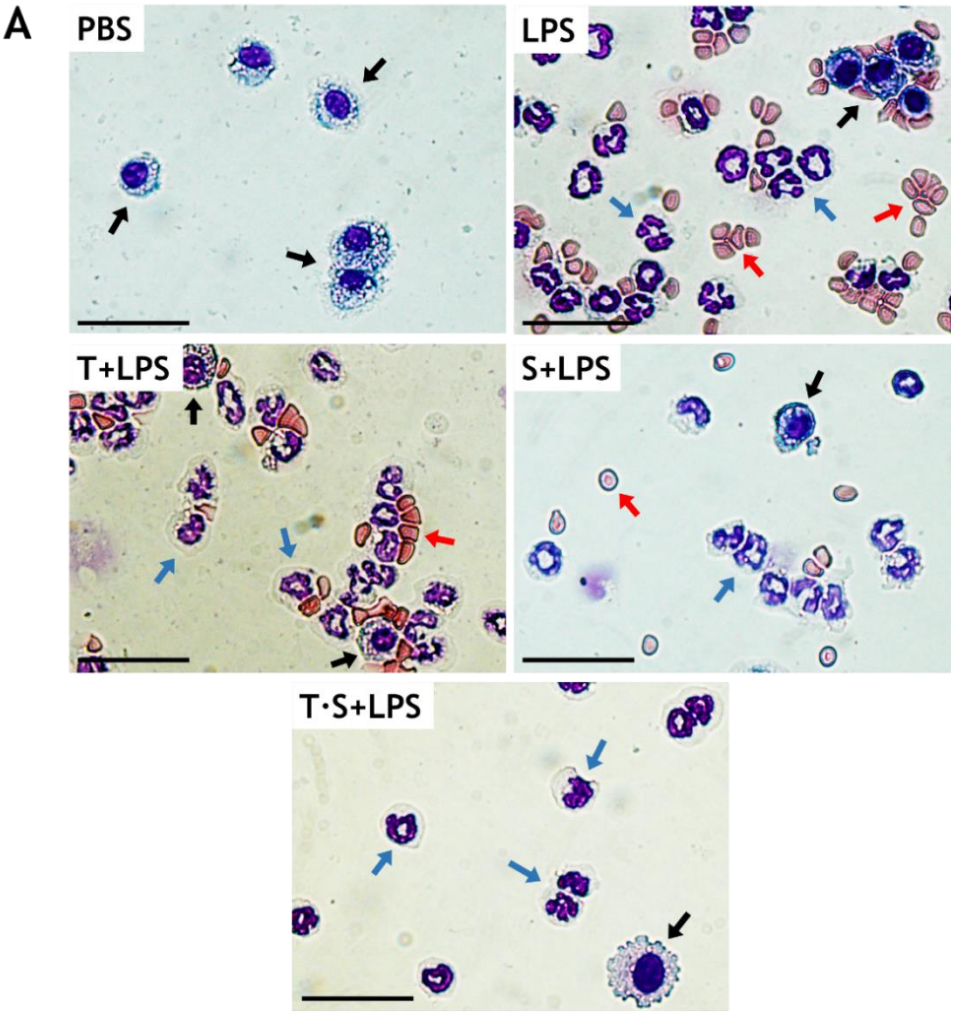

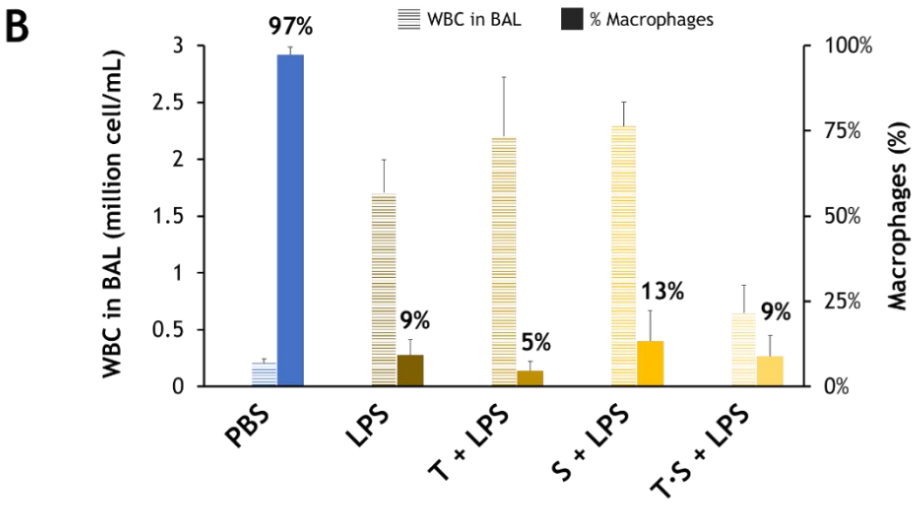

Figure 47: ***Cell populations in BALs.*** **A)** Representative images of each experimental condition are shown. Cells were stained with Giemsa to morphologically distinguish every cell population. **Black arrows**: macrophages; **blue arrows**: neutrophils; **red arrows**: erythrocytes. Bar = 100 µm. **B)** Percentage of macrophages with respect to total amount of WBC in BAL. The left axis represents the number of WBC expressed in million cells in 1 mL of BAL (stripped bars); the right axis corresponds to the percentage of macrophages with respect to WBC in BAL (smooth bars). Each percentage of macrophages was obtained by observing the slides stained with Giemsa. Bars represent mean of six different images per mice (n=3). Error bars represent the standard deviation.

In order to elucidate if TAC is internalised by alveolar cells and if pulmonary surfactant enhances this process, the WBC obtained from bronchoalveolar lavages were observed under the fluorescence microscope. **Figure *48*** shows representative images of the groups of mice pre-treated with TAC in the absence and in the presence of surfactant (A), the percentage of cells that uptake TAC (B) and the fluorescence intensity inside the cells as an indicator of internalised TAC (C). In the absence of TAC·NileBlue fluorescence was not detected, thus the images are not shown. The images clearly show that in combination with surfactant, TAC is internalised by many more cells. However, not every types of cells uptake TAC. Indeed, analysing their morphology, likely macrophages are the ones that internalise the drug. The percentage of cells that uptake TAC when it is vehiculized by pulmonary surfactant (7.9±5.1%; mean ± SD; n=3) is higher than delivering it alone (1.4±1.1%; mean ± SD; n=3) and coincides with the percentage of macrophages. These results suggest that macrophages internalise TAC and pulmonary surfactant seems to facilitate the process, either by improving the distribution along the respiratory surface or by leveraging the process of surfactant clearance. These evidences are coherent considering that alveolar macrophages are specialised in clearing surfactant from the alveolar spaces [15, 28, 62].

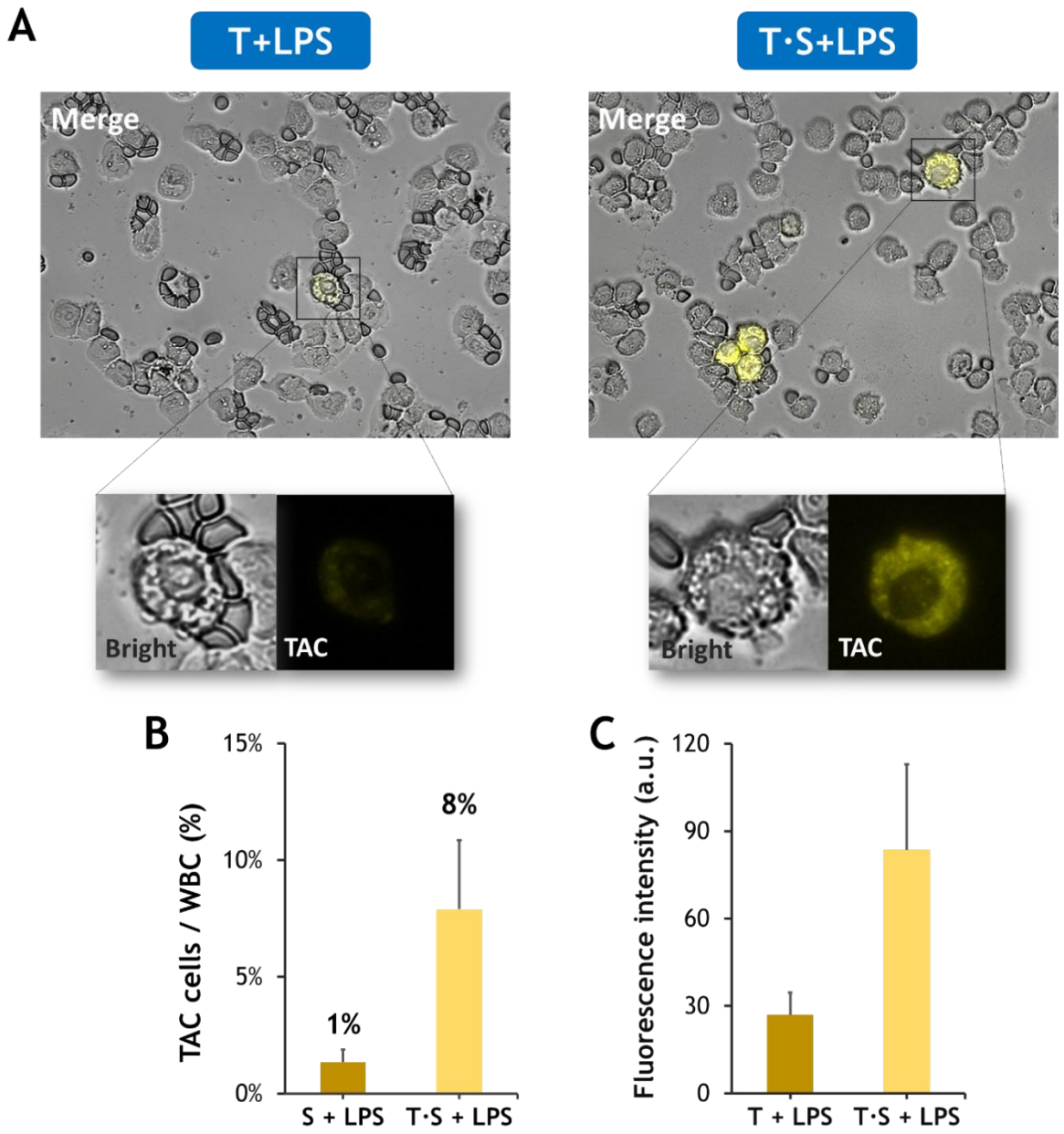

Figure 48: ***TAC uptake by BAL cells.*** **A)** Cells from BAL of LPS-induced inflammation mice models pre-treated with TAC·NileBlue in the presence and the absence of pulmonary surfactant. The bigger images correspond to a merge between bright field and fluorescence microscopy. Clearly, not all kinds of cells show TAC·NileBlue fluorescence. The amplifications correspond to an example of those cells that internalize TAC. Attending uniquely to the morphology, those cells seem to be macrophages. Notice that in the presence of surfactant the intensity of fluorescence is higher. The histogram of each image was equally adjusted to better differentiate the presence of TAC inside the cells. Bar = 100 µm. **B)** Percentage of cells that internalise TAC. In combination with pulmonary surfactant the amount of cells that uptake TAC is considerably higher. Each percentage was obtained by observing the slides previously fixed with MetOH and applying the same threshold to avoid background. The rest of conditions (PBS, LPS and S+LPS) are not shown, as no fluorescence was detected. Bars represent mean of six different images per mouse (n=3). Error bars represent the standard deviation. **C)** Fluorescence intensity of TAC·NileBlue inside cells. In combination with surfactant, cells internalize a higher amount of TAC. Fluorescence intensity was measured by ImageJ (Fiji). Three different regions of cytoplasm were aleatory measured from each cell on six images per mouse (n=3). T·S + LPS: 60 cells; T+LPS: 8 cells, as less cells uptake TAC. Mean is represented. Error bars correspond to standard deviation.

To further confirm the selective uptake of TAC inside macrophages and whether the anti-inflammatory effect of TAC is accomplished through them, mice were intranasally instilled with liposome-encapsulated clodronate (15 mg/kg), whose apoptotic effect on macrophages was widely demonstrated in the literature [93, 222, 223]. Two days after clodronate administration, mice were treated with different solutions following the same protocol for the previous experiments (see **Figure *42***). *Figure 49 A* shows the presence of neutrophils and cellular debris in the control group (Clod + PBS), a sign of pro-inflammatory and apoptotic processes. The evaluations of total protein content and WBC counting in BAL (see *Figure 49 B and C*, respectively) also showed a considerable increase of the inflammation process in the control group (Clod + PBS) and no signs of anti-inflammatory effects were observed in the TAC-treated groups. These results reveal that the depletion and loss of activity of AMφ induced by clodronate disrupt the pro-/anti-inflammatory balance. Therefore, the effect of Clodronate, whose pathway of action is completely different to LPS or TAC, hides the anti-inflammatory effects of TAC in LPS-induced lung injury mice. Thus, these models cannot be considered to evaluate the anti-inflammatory effects of TAC alone or in combination with pulmonary surfactant.

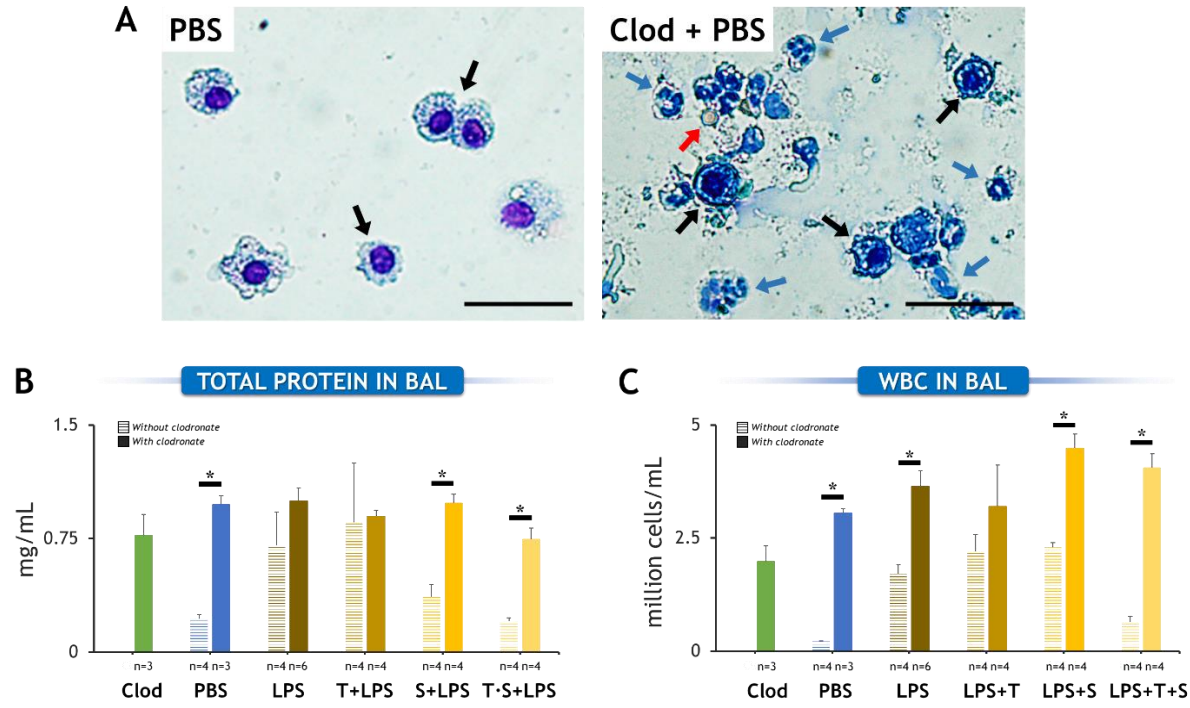

Figure 49: *Effect of clodronate (Clod) in bronchoalveolar fluid.* A) Representative images of control groups (PBS) in the presence and in the absence of clodronate. Cells were stained with Giemsa to morphologically distinguish every cell population. **Black arrows**: macrophages; **blue arrows**: neutrophils; **red arrows**: erythrocytes. Bar = 100 µm. **B)** Total protein content in BAL (stripped bars: without clodronate; smooth bars: with clodronate). Mean of n mice (indicated under the bars) is represented for each condition (stripped bars: without clodronate; smooth bars: with clodronate). Error bars represent the standard deviation. (*) $p<0.001$ (Mann-Whitney Rank Sum Test). **C)** WBC count in BAL (stripped bars: without clodronate; smooth bars: with clodronate). Mean of n mice (indicated under the bars) is represented for each condition (four different squares of 0.04 mm^2 were observed; four aliquots per mouse BAL were counted). Error bars represent the standard deviation. (*) $p<0.001$ (Mann-Whitney Rank Sum Test).

Nevertheless, the clodronate effect on AMφ is useful to further confirm that the cells which internalise TAC are macrophages. **Figure *50***A shows two representative images of LPS-induced mice pre-treated with surfactant/TAC combinations which have previously treated with clodronate

or not. The internalization of TAC in BAL cells is considerably reduced in those mice treated with clodronate, even in the remining macrophages (likely in an apoptotic state). This evidences that TAC, especially vehiculized in pulmonary surfactant, is actually internalised by no other type of cell than macrophages.

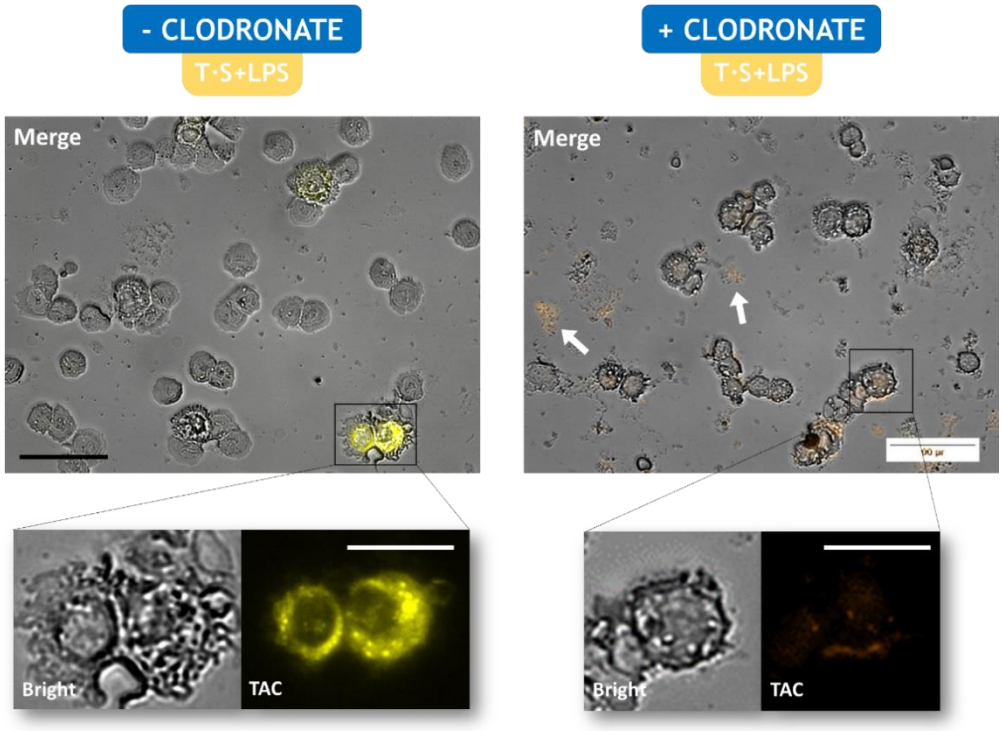

Figure 50: ***Effect of clodronate on bronchoalveolar cells.*** Cells from BAL of LPS-induced inflammation mice models pre-treated with TAC·NileBlue in the presence and the absence of pulmonary surfactant. The bigger images correspond to a merge between bright field and fluorescence microscopy. In the absence of clodronate, the TAC·NileBlue fluorescence is clearly detected inside macrophages, while in its presence the fluorescence signal is drastically reduced. Fluorescence associated to cellular debris is also observed, indicating that the integrity of BAL cells (likely macrophages) is compromised by clodronate. They cannot resist the centrifugation forces during the cytospin and finally burst (white arrows). The amplifications correspond to an example of those cells that internalize TAC. The histogram of each image was equally adjusted to better differentiate the presence of TAC inside the cells. Bar = 100 µm.

DISCUSSION

The previous chapters have demonstrated and characterised for the first time the possibilities of using pulmonary surfactant as a drug delivery system. It has been confirmed *in vitro* its ability to travel long distances along air-liquid interfaces and share this interfacial trip with additional passengers. Moreover, it has been observed how the breathing-like compression and expansion dynamics enhances the release process after travelling interfacially. However, these promising results obtained by using biophysical *in vitro* models did not simulate the entire barriers that the lungs have developed to prevent the entrance of foreign entities (i.e. branched structure, mucus, immune system or the air and liquid flows). Therefore, the inevitable following step was to prove the concept of surfactant-driven drug vehiculization *in vivo*. This was possible using a mouse model of LPS-induced ALI that allows to evaluate 1) the feasibility of this new and non-

invasive pulmonary drug delivery system, 2) the anti-inflammatory properties of tacrolimus vehiculized by pulmonary surfactant, 3) what occurs after reaching alveolar spaces and 4) which cells are involved in this novel strategy.

Certainly, TAC was selectively internalised in macrophages and the amount was considerably higher in combination with pulmonary surfactant. At the same time, the oedema as well as the amounts of WBC were visible reduced in LPS-challenged mice pre-treated with surfactant/drug combinations. These results induce to think that: 1) surfactant is an effective and efficient interfacial system, able to reach the alveolar spaces and transport TAC from the nose, 2) it enhances the availability and internalisation of TAC by alveolar macrophages and 3) it promotes the resulting anti-inflammatory effect possibly via macrophages.

It is extensively known that alveolar macrophages are specialised in removing and catabolising the 'used' surfactant excluded during the process of breathing in the form of small aggregates [62]. The previous *in vitro* results showed that TAC is excluded from the interface in small vesicles of surfactant components unable to readsorb, fruit of breathing-like interfacial compression/expansion dynamics. Therefore, the presence of higher amount of TAC in macrophages of surfactant-treated mice clearly induces to think that TAC is being excluded in small surfactant aggregates during breathing, and then phagocyted by alveolar macrophages. Thus, surfactant could be an efficient drug delivery system to carry hydrophobic compounds toward specific cells, allowing to reach precise lung targets such as alveolar macrophages. Additionally, apart from the aforementioned properties, attending to the spreading capabilities of pulmonary surfactant, it could enhance the distribution of the drug along the respiratory surface and reach more easily regions in the lungs that are difficult for the drug alone. Thus, more amount of drug can be available in the alveolar spaces to take its effect or cross the air-blood barrier.

Additionally, the treatment with only surfactant tends to prevent the protein leakage but not the WBC extravasation, likely as a consequence of the surface active properties of pulmonary surfactant. In fact, apart from the capillary blood pressure and plasma and tissue fluid osmotic pressure, surface tension is the other force that maintains the alveolar lining fluid stable impeding the ultra-filtration of fluid coming from the blood stream [224]. When the thin air-blood barrier is compromised by an inflammation process (i.e. LPS-induced), the permeability increases and blood components enter into the alveolar space. Some of the plasma components and inflammation-derived enzymes impair the function of pulmonary surfactant either by competing for the interface (i.e. albumin) or degrading its components (i.e. phospholipase A2) [108]. This inactivation, together

with the dilution of the pulmonary surfactant, leads to an increase in surface tension destabilising those forces with the consequent increase of oedema. The reduction of total proteins in BAL from mice pre-treated with exogenous surfactant seen in this study may be due to the fact that this surfactant counteracts the inhibition of the endogenous surfactant, either by replacing the used and inhibited one or inducing production of new and more active surfactant. This was the principle to start using the surfactant replacement therapy (SRT) in adults with ALI. Unfortunately, this therapeutic strategy was not as effective as expected in clinical trials [225]. Nevertheless, the surfactants used in those clinical trials had limitations in composition and functionality (Exosurf® [225], Survanta® [226] or Venticute® [111]). The way of delivery (aerosolization with ancient nebulizers) and dosage (only once or several intermittent) also limited the studies. The presence of surfactant inhibitors during inflammation, mainly phospholipase A2, finally inhibits the exogenous surfactant as well, especially when only one dose is administered and surfactants are not biophysically competent. Therefore, a multidose treatment with proper combinations of exogenous surfactants and anti-inflammatory drugs could empower the effect of SRT in ALI. Moreover, a continuous exposure to the treatment in nebulised formulations using the last generation of electrical nebulizers (i.e. based on Vibrating Mesh Technology) instead of intermittent intratracheal administration, could enhance even more the therapeutic efficacy and could contribute to reduce the high dosage needed in adults. This is possible not only leveraging the therapeutic properties of surfactant *per se*, but also using it to improve the distribution and targeting of the anti-inflammatory drug along the respiratory surface.

In summary, the use of pulmonary surfactant as a vehicle helps to distribute the drug along the respiratory surface from the upper airways to alveoli, enhancing at the same time the process of internalization into alveolar cells, apparently macrophages, and augmenting the anti-inflammatory response of the drug in LPS-challenged mice. All these evidences open novel avenues to treat diseases where the drug distribution and alveolar macrophages play a key role such as tuberculosis and pulmonary fibrosis or symptoms derived from acute lung injury. Nevertheless, this new drug delivery approach must be accompanied with the development and production of new surfactants that can improve the essential properties: good adsorption and spreading along the air-liquid interface and the ability to vehiculize and resist to inhibition. Such qualitative optimization, along to the creation of synthetic surfactants to control composition and produce larger quantities, of material a reasonable cost are the tendency nowadays.

GENERAL DISCUSSION & FUTURE PERSPECTIVES

One of the challenges in the last few years has been to design and develop new strategies in drug delivery. These strategies should allow overcoming different biological barriers in a non-invasive way and targeting specific locations in the body. In this sense, the respiratory system is proposed as a preferred pathway, principally because of the typical features of the respiratory surface (thin, large and highly vascularised) and the presence of pulmonary surfactant. The latter, historically considered a barrier and essential for the process of breathing, can be used as a carrier and to assist in solving different limitations of the current approaches, such as poor solubility of hydrophobic drugs, or to reach places in the lungs that are barely accessible, such as the alveolar spaces. Surfactant is an amphipathic material able to adsorb and localise into the interface between the layer of water covering the whole respiratory surface and the breathing air and, once there, to spread very efficiently over it. Considering these spreading capabilities, the main objective of this Thesis has been to assess the potential of pulmonary surfactant to deliver different drugs through the airways as a basis of a novel and non-invasive strategy, the 'interfacial therapy'. In order to explore this concept, an special *in vitro* setup was designed, mimicking somehow the connection through an air-liquid interface of upper and distal compartments of the airways. It consist in two different aqueous troughs connected by an interfacial bridge, so that pulmonary surfactant can travel from one to another only through the interface. Using this apparently simple device, it has been demonstrated *in vitro* for the first time the vehiculizing potential of pulmonary surfactant and that the compression and expansion breathing-like dynamics enhances the release of drugs from the air-liquid interface. Once the potential of this novel interfacial drug delivery strategy was demonstrated, it was also confirmed *in vivo*. Surprisingly, not only pulmonary surfactant was able to transport a drug like tacrolimus from the upper airways to distal alveoli, but also to deliver it towards the alveolar macrophages, which internalised the drug leading a synergistic anti-inflammatory effect in combination with pulmonary surfactant. The combination of biophysical and *in vivo* models has undoubtedly confirmed the extraordinary possibilities of pulmonary surfactant as a drug delivery system.

Nowadays, pulmonary surfactant is being widely used to treat the Respiratory Distress Syndrome in prematurely born babies. Unfortunately, clinical trials have failed to support the delivery of surfactant alone as a protective therapy in adult Acute Lung Injury (ALI) [108, 225]. However, those clinical trials presented important constraints with respect to the election of therapeutic surfactants, which had compositional and functional limitations, including uncertainties with respect to the delivery route and the specific dosages. The results of the present Thesis suggest that the combined administration of anti-inflammatory drugs and exogenous surfactants

might constitute an important adjuvant effect. This consideration is strongly supported by the unique interfacial properties of pulmonary surfactant, the advantages of using the respiratory surface as a way for drug delivery and the ongoing improvements in surfactant delivery strategies. The drug delivery capacities of pulmonary surfactant could go beyond the patients with surfactant problems, such as those of RDS. The challenge is to target local (lung) and peripheral pathologies, improving the delivery, targeting and effectiveness of different drugs through their association to pulmonary surfactant.

The results of this Thesis also illustrate the utility of biophysical models to analyse the elementary processes involved in the interfacial pulmonary drug distribution, which could be tailored to study the behaviour of any particular drug or therapeutic agent (peptides, proteins, RNA, DNA, etc.). They are a potent tool to design and optimize new surfactant vehiculization strategies prior to *in vivo* experimentation, which may reduce the use of animal models. Important aspects that can be optimised in a case-by-case basis include: 1) the incorporation of additional passengers (i.e. drugs, antibodies, siRNA or nanocarriers), 2) the maximal surfactant/passenger proportion that still maintain the integrity of surfactant biophysical properties, 3) the efficacy of the cmbined interfacial trip and 4) the interfacial behaviour under breathing-like dynamic conditions.

However, to properly transfer this knowledge to clinics, it is mandatory to consider the physiological context that the desired therapy will encounter in the lung. First of all, it is necessary to take into account that the distribution of clinical surfactant/drug combinations will not encounter an empty and clean interface at the lungs. In fact, the pulmonary interface will be already occupied by different materials, such as endogenous surfactant, or it would be extended on top of a thick layer of mucus layer at the upper airways. In this regard, additional experiments have been already carried out to analyse how the spreading of surfactant-loaded drugs over the interface is modulated in a surfactant-occupied interface. The obtained results suggest that the exogenous surfactant is able to interact with the endogenous surfactant film one without disturbing drug spreading. However, these promising data still need to be complemented with further experiments testing surfaces already coated with viscous complex solutions such as mucus [227]. On the other hand, the flow of fluid and particles into the upper airways is much influenced by the active participation of the mucociliary escalator, in charge of clearing accidentally inspired and potentially noxious entities [228]. Nevertheless, still under that particular environment, the fate of molecules firmly associated to the interfacial film likely differs from those molecules that move independently. It has been widely demonstrated that exogenous surfactant can efficiently distribute over the

airways and reach alveoli when delivered as an endotracheal bolus [229, 230, 231]. Thus, interfacial flows follow different movements than those involving the subphase. In this line, a preliminary study carried out at the laboratory of Prof. Jahar Bhattacharya´s laboratory in Columbia University, New York, has shown that surfactant is able to distribute TAC over mouse lungs reaching the alveolar spaces. In these preliminary experiments, a surfactant/TAC mixture was intranasally applied into the upper airways. Then, the isolated perfused lungs were observed under a confocal microscope showing that TAC·NileBlue fluorescence could be detected in alveoli. This result, pending of additional required controls, demonstrates the surfactant-assisted interfacial distribution over the respiratory surface. It also points out the idea that surfactant can flow against the mucociliary current and is competent to transport additional passengers with it.

The interfacial diffusion of surfactant/drug formulations could also be affected by the presence in the subphase and in the interface of different substances released as a consequence of lung injury, such as serum, or inflammatory mediators. These compounds may affect lung surfactant, impairing both its interfacial adsorption and spreading. In this regard, the combination of an efficient therapeutic surfactant with proper drugs could simultaneously address the intended pharmacological action and the restoration of the surfactant biophysical function. In this sense, different specific formulations of therapeutic surfactants could be designed for drug delivery depending on the clinical conditions of target lungs (properly aerated lungs or injured lungs requiring restoration of pulmonary surfactant inhibition). Additionally, the proper choice of the amounts of surfactant to be delivered along with the optimal surfactant/drug proportions could be crucial to allow for their rapid and efficient distribution over the interface. Up to now, the efficient clinical doses of the majority of approved therapeutic surfactants for SRT are above 50 mg/Kg at concentrations higher than 25 mg/mL [42, 108]. Nevertheless, the results obtained in the present Thesis have proven that lower doses of interfacial material can efficiently deliver drugs (15 mg/Kg at 10 mg/mL). This positive outcome is not surprising and the amount of surfactant could be further reduced in future experiments. Theoretically, only 3 mg/Kg is the estimated dose of exogenous surfactants to saturate the respiratory surface (1 m^2/Kg body weight) and reduce the surface tension to values below 2 mN/m^2.

A last important consideration is related to how pulmonary surfactant is usually delivered in exogenous therapies. Restoration of impaired surfactant function is frequently performed by applying clinical surfactants endotracheally in patients that are intubated as a consequence of their respiratory problems. Those patients could have better expectations if treated with a proper combination of surfactant and drugs. However, the strategies of non-invasive administration are

critical to obtain better and faster results. In this line, to be efficient, those approaches must still preserve the dynamic properties that make surfactant an extraordinary pharmacological agent with huge therapeutic delivery potential. The possibility of using aerosolised surfactant would face both the current problems related to patients intubation and reduce the hospitalization costs. Although several experiments performed in animals to date had no clear success, promising results were obtained by studying the vehiculizing capacity of lyophilised and nebulised clinical and synthetic surfactants. The used of a last generation of electrical nebulizers and current clinical and synthetic surfactants, is opening unprecedented avenues in surfactant and respiratory drug delivery.

The complexity of the pulmonary surfactant system and the necessity to maintain its biophysical properties intact, makes mandatory to evaluate each surfactant/drug combination in a case by case basis. In this thesis, only three different drugs have been studied to demonstrate and stablish the basis of the surfactant-driven interfacail vehiculization (beclomethasone dipropionate, budenoside and tacrolimus). Nevertheless, other molecules have also been tested, demonstrating that hydrophobicity is the most important aspect to consider. For instance, structural and functional preliminary experiments combining surfactant with amiodarone, a highly hydrophobic drug (AlogP = 6.94) used to treat and prevent irregular heartbeats that produces lung toxicity, showed that comparable amounts to those used for corticoids and tacrolimus (10% by mass) disturbed the interfacial properties of pulmonary surfactant drastically. Hydrophilic molecules, on the other hand, such as the antituberculotic drug isoniazid (AlogP = -0.77), have also been tested showing no interaction with pulmonary surfactant. This highlights the importance to design optimal carriers able to interact with pulmonary surfactant while encapsulating hydrophilic drugs and preventing the possible deleterious effects of hydrophobic therapeutics.

The potential use of liposomes in combination with pulmonary surfactant, which could be a promising way for delivering hydrophilic drugs, has also been explored. Unfortunately, the experiments carried out in our laboratory have shown disappointing results. These membrane-based nanocarriers resulted inefficient to transport hydrophilic molecules once contacting with surfactant components. Liposomes, as they are composed by phospholipids, easily fuse with surfactant membranes releasing the cargo even before it can be vehiculized. Some alternatives could be explored such as the use of polymeric micro or nanocarriers or viral capsids. The feasibility of functionalising the surface of these carriers with surfactant components, click-chemistry-based elements or antibodies could increase the range of possibilities, with a great potential to enhance the surfactant-promoted vehiculization of nanocarriers.

The increasing use of proteins as therapeutic agents, such as antibodies for the treatment of cancer, antibiotic peptides or antigen vaccination through the airways, highlights the importance of exploring the vehiculization of proteins in combination with pulmonary surfactant as well. In this sense, preliminary studies with SP-D have already demonstrated that pulmonary surfactant is able to interact and interfacially transport this hydrophilic surfactant protein. SP-D cannot travel on its own, thus confirming the importance of pulmonary surfactant to allow its distribution over the air-liquid interface. These data bring to light the possibilities of delivering proteins associated to pulmonary surfactant.

To summarize, the promising data exposed in this Thesis highlights the importance of continuing exploring the vehiculization capabilities of pulmonary surfactant, developing new and non-invasive ways for administering it, and elucidating how it can improve the distribution, target and effectiveness of any therapeutic agent (i.e. specific drugs, anti-bodies, siRNA or even cells) for both local diseases (i.e. fibrosis, ARDS or lung cancer) or peripheral delivery. Knowing that alveolar macrophages are the main actors in surfactant clearance, it will be also essential to have them into account and study their role on this delivery strategy and on local pathologies (how they migrate and get involved, how they could change or define new markers related with communication with epithelium and with other alveolar-resident/non-resident cells or how they can be modulated with therapeutic purposes, etc.). Additionally, it will be also of great potential to seek sophisticated *in vitro* models to: 1) design and optimize new synthetic surfactants specially tailored for vehiculization, 2) explore the diffusion through the air-blood barrier to treat peripheral diseases, and 3) investigate on how other barriers (i.e. mucus, air and liquid flows or immune system) could affect this novel strategy.

CONCLUSIONS

Pulmonary surfactant, a lipid-protein complex with high surface activity, is an efficient vehicle for transporting drugs over the whole respiratory surface. In this Thesis, an *in vitro* model of the respiratory air-liquid interface has been designed and optimised to study the potential use of pulmonary surfactant as a drug delivery system and the implications of compression-expansion breathing-like dynamics in surfactant-assisted drug diffusion through the air-liquid interface. Combining this biophysical model with an *in vivo* murine model, it has been demonstrated that:

1. Clinical and synthetic surfactants can incorporate hydrophobic drugs, such as corticosteroids or the anti-inflammatory tacrolimus, without affecting its functional properties.
2. Different surfactant formulations can transport drugs facilitating their distribution through *in vitro* and *in vivo* air-liquid interfaces.
3. Compression-expansion breathing-like dynamics enhance the interfacial trip and drug release from the air-liquid interface.
4. Pulmonary surfactant facilitates the distribution of drugs such as the hydrophobic anti-inflammatory tacrolimus *in vivo*, as observed in a murine model of endotoxin-caused lung injury.
5. Pulmonary surfactant facilitates vehiculization of drugs like tacrolimus toward the distal airways. Once at the alveolar spaces, the drug is liberated and taken by macrophages.
6. Surfactant/drug combinations have synergistic effects when administered *in vivo*, as observed in a model of administration of surfactant/tacrolimus in mice.

REFERENCES

1. Feynman, R. P. There's plenty of room at the bottom. *Engineering and science* 1960, *23* (5), 22-36.
2. ResearchAndMarkets. *Global Nanotechnology Market Outlook 2018-2024*; ResearchAndMarkets: https://www.researchandmarkets.com/reports/4536705/global-nanotechnology-market-outlook-2018-2024, December, 2018, p 160.
3. Evers, P. Nanotechnology in Medical Applications: The Global Market. BCC Research, 2017.
4. Hidalgo, A.; Cruz, A.; Perez-Gil, J. Barrier or carrier? Pulmonary surfactant and drug delivery. *Eur J Pharm Biopharm* 2015, *95* (Pt A), 117-27.
5. Kesisoglou, F.; Wu, Y. Understanding the Effect of API Properties on Bioavailability Through Absorption Modeling. *The AAPS Journal* 2008, *10* (4), 516-525.
6. Rubin, B. K.; Williams, R. W. Emerging aerosol drug delivery strategies: From bench to clinic. *Advanced drug delivery reviews* 2014.
7. Ungaro, F.; d'Angelo, I.; Miro, A.; La Rotonda, M. I.; Quaglia, F. Engineered PLGA nano- and micro-carriers for pulmonary delivery: challenges and promises. *The Journal of pharmacy and pharmacology* 2012, *64* (9), 1217-35.
8. Olsson, B.; Bondesson, E.; Borgström, L.; Edsbäcker, S.; Eirefelt, S.; Ekelund, K.; Gustavsson, L.; Hegelund-Myrbäck, T. Pulmonary drug metabolism, clearance, and absorption. In *Controlled Pulmonary Drug Delivery*, Springer, 2011, pp 21-50.
9. Hidalgo, A.; Cruz, A.; Perez-Gil, J. Pulmonary surfactant and nanocarriers: Toxicity versus combined nanomedical applications. *Biochimica et biophysica acta* 2017, *1859* (9 Pt B), 1740-1748.
10. Subbiah, R.; Veerapandian, M.; Yun, K. S. Nanoparticles: functionalization and multifunctional applications in biomedical sciences. *Current medicinal chemistry* 2010, *17* (36), 4559-77.
11. Loira-Pastoriza, C.; Todoroff, J.; Vanbever, R. Delivery strategies for sustained drug release in the lungs. *Adv Drug Deliv Rev* 2014, *75c*, 81-91.
12. Weber, S.; Zimmer, A.; Pardeike, J. Solid Lipid Nanoparticles (SLN) and Nanostructured Lipid Carriers (NLC) for pulmonary application: a review of the state of the art. *Eur J Pharm Biopharm* 2014, *86* (1), 7-22.
13. Gao, W.; Li, L.; Wang, Y.; Zhang, S.; Adcock, I. M.; Barnes, P. J.; Huang, M.; Yao, X. Bronchial epithelial cells: The key effector cells in the pathogenesis of chronic obstructive pulmonary disease? *Respirology* 2015, *20* (5), 722-9.
14. Bhattacharya, J.; Matthay, M. A. Regulation and repair of the alveolar-capillary barrier in acute lung injury. *Annual review of physiology* 2013, *75*, 593-615.
15. Lopez-Rodriguez, E.; Gay-Jordi, G.; Mucci, A.; Lachmann, N.; Serrano-Mollar, A. Lung surfactant metabolism: early in life, early in disease and target in cell therapy. *Cell Tissue Res* 2017, *367* (3), 721-735.
16. Byrne, A. J.; Mathie, S. A.; Gregory, L. G.; Lloyd, C. M. Pulmonary macrophages: key players in the innate defence of the airways. *Thorax* 2015, *70* (12), 1189-96.
17. Janssen, W. J.; Stefanski, A. L.; Bochner, B. S.; Evans, C. M. Control of lung defence by mucins and macrophages: ancient defence mechanisms with modern functions. *Eur Respir J* 2016, *48* (4), 1201-1214.
18. Aragao-Santiago, L.; Bohr, A.; Delaval, M.; Dalla-Bona, A. C.; Gessler, T.; Seeger, W.; Beck-Broichsitter, M. Innovative formulations for controlled drug delivery to the lungs and the technical and toxicological challenges to overcome(.). *Current pharmaceutical design* 2016, *22* (9), 1147-60.
19. Laube, B. L. Aerosolized Medications for Gene and Peptide Therapy. *Respir Care* 2015, *60* (6), 806-21; discussion 821-4.

20. Yang, W.; Peters, J. I.; Williams Iii, R. O. Inhaled nanoparticles—A current review. *International Journal of Pharmaceutics* 2008, *356* (1–2), 239-247.
21. Jaques, P. A.; Kim, C. S. Measurement of total lung deposition of inhaled ultrafine particles in healthy men and women. *Inhalation Toxicology* 2000, *12* (8), 715-731.
22. Patil, J.; Sarasija, S. Pulmonary drug delivery strategies: A concise, systematic review. *Lung India* 2012, *29* (1), 44-49.
23. Weber, S.; Zimmer, A.; Pardeike, J. Solid Lipid Nanoparticles (SLN) and Nanostructured Lipid Carriers (NLC) for pulmonary application: A review of the state of the art. *European Journal of Pharmaceutics and Biopharmaceutics* 2014, *86* (1), 7-22.
24. Smola, M.; Vandamme, T.; Sokolowski, A. Nanocarriers as pulmonary drug delivery systems to treat and to diagnose respiratory and nonrespiratory diseases. *International journal of nanomedicine* 2008, *3* (1), 1.
25. Labiris, N.; Dolovich, M. Pulmonary drug delivery. Part I: physiological factors affecting therapeutic effectiveness of aerosolized medications. *British journal of clinical pharmacology* 2003, *56* (6), 588-599.
26. Evans, C. M.; Koo, J. S. Airway mucus: the good, the bad, the sticky. *Pharmacology & therapeutics* 2009, *121* (3), 332-48.
27. Halliday, H. L. Surfactants: past, present and future. *Journal of perinatology : official journal of the California Perinatal Association* 2008, *28 Suppl 1*, S47-56.
28. Perez-Gil, J.; Weaver, T. E. Pulmonary surfactant pathophysiology: current models and open questions. *Physiology* 2010, *25* (3), 132-41.
29. Haitsma, J. J.; Lachmann, U.; Lachmann, B. Exogenous surfactant as a drug delivery agent. *Advanced Drug Delivery Reviews* 2001, *47* (2–3), 197-207.
30. Lopez-Rodriguez, E.; Perez-Gil, J. Structure-function relationships in pulmonary surfactant membranes: from biophysics to therapy. *Biochimica et biophysica acta* 2014, *1838* (6), 1568-85.
31. Vermehren, C.; Frokjaer, S.; Aurstad, T.; Hansen, J. Lung surfactant as a drug delivery system. *Int J Pharm* 2006, *307* (1), 89-92.
32. Parra, E.; Alcaraz, A.; Cruz, A.; Aguilella, V. M.; Perez-Gil, J. Hydrophobic pulmonary surfactant proteins SP-B and SP-C induce pore formation in planar lipid membranes: evidence for proteolipid pores. *Biophysical journal* 2013, *104* (1), 146-55.
33. Parra, E.; Moleiro, L. H.; Lopez-Montero, I.; Cruz, A.; Monroy, F.; Perez-Gil, J. A combined action of pulmonary surfactant proteins SP-B and SP-C modulates permeability and dynamics of phospholipid membranes. *The Biochemical journal* 2011, *438* (3), 555-64.
34. Haitsma, J. J.; Lachmann, U.; Lachmann, B. Exogenous surfactant as a drug delivery agent. *Advanced drug delivery reviews* 2001, *47* (2-3), 197-207.
35. Goerke, J. Pulmonary surfactant: functions and molecular composition. *Biochimica et biophysica acta* 1998, *1408* (2-3), 79-89.
36. Shelley, S. A.; Paciga, J. E.; Balis, J. U. Lung surfactant phospholipids in different animal species. *Lipids* 1984, *19* (11), 857-862.
37. Orgeig, S.; Hiemstra, P. S.; Veldhuizen, E. J.; Casals, C.; Clark, H. W.; Haczku, A.; Knudsen, L.; Possmayer, F. Recent advances in alveolar biology: evolution and function of alveolar proteins. *Respiratory physiology & neurobiology* 2010, *173*, S43-S54.
38. Orgeig, S.; Bernhard, W.; Biswas, S. C.; Daniels, C. B.; Hall, S. B.; Hetz, S. K.; Lang, C. J.; Maina, J. N.; Panda, A. K.; Perez-Gil, J. The anatomy, physics, and physiology of gas exchange surfaces: is there a universal function for pulmonary surfactant in animal respiratory structures? *Integrative and comparative biology* 2007, *47* (4), 610-627.

39. Suri, L. N. M.; Cruz, A.; Veldhuizen, R. A. W.; Staples, J. F.; Possmayer, F.; Orgeig, S.; Perez-Gil, J. Adaptations to hibernation in lung surfactant composition of 13-lined ground squirrels influence surfactant lipid phase segregation properties. *Biochimica et Biophysica Acta (BBA) - Biomembranes* 2013, *1828* (8), 1707-1714.
40. Veldhuizen, R.; Nag, K.; Orgeig, S.; Possmayer, F. The role of lipids in pulmonary surfactant. *Biochimica et Biophysica Acta (BBA)-Molecular Basis of Disease* 1998, *1408* (2), 90-108.
41. Brogden, K. A. Changes in pulmonary surfactant during bacterial pneumonia. *Antonie van Leeuwenhoek* 1991, *59* (4), 215-23.
42. Blanco, O.; Perez-Gil, J. Biochemical and pharmacological differences between preparations of exogenous natural surfactant used to treat Respiratory Distress Syndrome: role of the different components in an efficient pulmonary surfactant. *European journal of pharmacology* 2007, *568* (1-3), 1-15.
43. Ariki, S.; Nishitani, C.; Kuroki, Y. Diverse functions of pulmonary collectins in host defense of the lung. *BioMed Research International* 2012, *2012*.
44. Hussell, T.; Bell, T. J. Alveolar macrophages: plasticity in a tissue-specific context. *Nature reviews immunology* 2014, *14* (2), 81.
45. Nie, X.; Nishitani, C.; Yamazoe, M.; Ariki, S.; Takahashi, M.; Shimizu, T.; Mitsuzawa, H.; Sawada, K.; Smith, K.; Crouch, E. Pulmonary surfactant protein D binds MD-2 through the carbohydrate recognition domain. *Biochemistry* 2008, *47* (48), 12878-12885.
46. Ohya, M.; Nishitani, C.; Sano, H.; Yamada, C.; Mitsuzawa, H.; Shimizu, T.; Saito, T.; Smith, K.; Crouch, E.; Kuroki, Y. Human pulmonary surfactant protein D binds the extracellular domains of Toll-like receptors 2 and 4 through the carbohydrate recognition domain by a mechanism different from its binding to phosphatidylinositol and lipopolysaccharide. *Biochemistry* 2006, *45* (28), 8657-8664.
47. Perez-Gil, J. Structure of pulmonary surfactant membranes and films: the role of proteins and lipid-protein interactions. *Biochimica et biophysica acta* 2008, *1778* (7-8), 1676-95.
48. Goerke, J. Pulmonary surfactant: functions and molecular composition. *Biochimica et Biophysica Acta (BBA) - Molecular Basis of Disease* 1998, *1408* (2), 79-89.
49. Dietl, P.; Haller, T. Exocytosis of lung surfactant: from the secretory vesicle to the air-liquid interface. *Annual review of physiology* 2005, *67*, 595-621.
50. Suzuki, Y.; Fujita, Y.; Kogishi, K. Reconstitution of tubular myelin from synthetic lipids and proteins associated with pig pulmonary surfactant. *Am Rev Respir Dis* 1989, *140* (1), 75-81.
51. Nag, K.; Munro, J. G.; Hearn, S. A.; Rasmusson, J.; Petersen, N. O.; Possmayer, F. Correlated Atomic Force and Transmission Electron Microscopy of Nanotubular Structures in Pulmonary Surfactant. *Journal of Structural Biology* 1999, *126* (1), 1-15.
52. Korfhagen, T. R.; LeVine, A. M.; Whitsett, J. A. Surfactant protein A (SP-A) gene targeted mice. *Biochimica et Biophysica Acta (BBA) - Molecular Basis of Disease* 1998, *1408* (2), 296-302.
53. McCormack, F. X.; Whitsett, J. A. The pulmonary collectins, SP-A and SP-D, orchestrate innate immunity in the lung. *The Journal of Clinical Investigation* 2002, *109* (6), 707-712.
54. Parra, E.; Perez-Gil, J. Composition, structure and mechanical properties define performance of pulmonary surfactant membranes and films. *Chemistry and physics of lipids* 2015, *185*, 153-75.
55. Williams, M. C. Conversion of lamellar body membranes into tubular myelin in alveoli of fetal rat lungs. *The Journal of cell biology* 1977, *72* (2), 260-77.

56. Olmeda, B.; Villén, L.; Cruz, A.; Orellana, G.; Perez-Gil, J. Pulmonary surfactant layers accelerate O2 diffusion through the air-water interface. *Biochimica et Biophysica Acta (BBA) - Biomembranes* 2010, *1798* (6), 1281-1284.
57. Serrano, A. G.; Perez-Gil, J. Protein-lipid interactions and surface activity in the pulmonary surfactant system. *Chemistry and physics of lipids* 2006, *141* (1-2), 105-18.
58. Roldan, N.; Nyholm, T. K. M.; Slotte, J. P.; Perez-Gil, J.; Garcia-Alvarez, B. Effect of Lung Surfactant Protein SP-C and SP-C-Promoted Membrane Fragmentation on Cholesterol Dynamics. *Biophysical journal* 2016, *111* (8), 1703-1713.
59. Bernardino de la Serna, J.; Vargas, R.; Picardi, V.; Cruz, A.; Arranz, R.; Valpuesta, J. M.; Mateu, L.; Perez-Gil, J. Segregated ordered lipid phases and protein-promoted membrane cohesivity are required for pulmonary surfactant films to stabilize and protect the respiratory surface. *Faraday discussions* 2013, *161*, 535-48; discussion 563-89.
60. Cabre, E. J.; Malmstrom, J.; Sutherland, D.; Perez-Gil, J.; Otzen, D. E. Surfactant protein SP-B strongly modifies surface collapse of phospholipid vesicles: insights from a quartz crystal microbalance with dissipation. *Biophysical journal* 2009, *97* (3), 768-76.
61. Olmeda, B.; Garcia-Alvarez, B.; Gomez, M. J.; Martinez-Calle, M.; Cruz, A.; Perez-Gil, J. A model for the structure and mechanism of action of pulmonary surfactant protein B. *FASEB journal : official publication of the Federation of American Societies for Experimental Biology* 2015, *29* (10), 4236-47.
62. Olmeda, B.; Martinez-Calle, M.; Perez-Gil, J. Pulmonary surfactant metabolism in the alveolar airspace: Biogenesis, extracellular conversions, recycling. *Ann Anat* 2017, *209*, 78-92.
63. Ueda, T.; Ikegami, M.; Jobe, A. Surfactant subtypes. In vitro conversion, in vivo function, and effects of serum proteins. *Am J Respir Crit Care Med* 1994, *149* (5), 1254-9.
64. Gunther, A.; Schmidt, R.; Feustel, A.; Meier, U.; Pucker, C.; Ermert, M.; Seeger, W. Surfactant subtype conversion is related to loss of surfactant apoprotein B and surface activity in large surfactant aggregates: experimental and clinical studies. *American journal of respiratory and critical care medicine* 1999, *159* (1), 244-251.
65. Keating, E.; Zuo, Y. Y.; Tadayyon, S. M.; Petersen, N. O.; Possmayer, F.; Veldhuizen, R. A. A modified squeeze-out mechanism for generating high surface pressures with pulmonary surfactant. *Biochimica et Biophysica Acta (BBA)-Biomembranes* 2012, *1818* (5), 1225-1234.
66. Wright, J. Clearance and recycling of pulmonary surfactant. *American Journal of Physiology-Lung Cellular and Molecular Physiology* 1990, *259* (2), L1-L12.
67. Rider, E. D.; Ikegami, M.; Jobe, A. H. Localization of alveolar surfactant clearance in rabbit lung cells. *American Journal of Physiology-Lung Cellular and Molecular Physiology* 1992, *263* (2), L201-L209.
68. Wright, J. R.; Youmans, D. C. Degradation of surfactant lipids and surfactant protein A by alveolar macrophages in vitro. *The American journal of physiology* 1995, *268* (5 Pt 1), L772-80.
69. Pettenazzo, A.; Jobe, A.; Humme, J.; Seidner, S.; Ikegami, M. Clearance of surfactant phosphatidylcholine via the upper airways in rabbits. *Journal of Applied Physiology* 1988, *65* (5), 2151-2155.
70. Ikegami, M.; Grant, S.; Korfhagen, T.; Scheule, R. K.; Whitsett, J. A. Surfactant protein-D regulates the postnatal maturation of pulmonary surfactant lipid pool sizes. *Journal of applied physiology* 2009, *106* (5), 1545-1552.

71. Ikegami, M.; Na, C.-L.; Korfhagen, T. R.; Whitsett, J. A. Surfactant protein D influences surfactant ultrastructure and uptake by alveolar type II cells. *American Journal of Physiology-Lung Cellular and Molecular Physiology* 2005, *288* (3), L552-L561.
72. Bates, S. P63 (CKAP4) as an SP-A receptor: implications for surfactant turnover. *Cellular Physiology and Biochemistry* 2010, *25* (1), 41-54.
73. Wissel, H.; Lehfeldt, A.; Klein, P.; Muller, T.; Stevens, P. A. Endocytosed SP-A and surfactant lipids are sorted to different organelles in rat type II pneumocytes. *American journal of physiology. Lung cellular and molecular physiology* 2001, *281* (2), L345-60.
74. Bates, S. R.; Dodia, C.; Tao, J.-Q.; Fisher, A. B. Surfactant protein-A plays an important role in lung surfactant clearance: evidence using the surfactant protein-A gene-targeted mouse. *American Journal of Physiology-Lung Cellular and Molecular Physiology* 2008, *294* (2), L325-L333.
75. Ogasawara, Y.; Kuroki, Y.; Akino, T. Pulmonary surfactant protein D specifically binds to phosphatidylinositol. *The Journal of biological chemistry* 1992, *267* (29), 21244-9.
76. Persson, A. V.; Gibbons, B. J.; Shoemaker, J. D.; Moxley, M. A.; Longmore, W. J. The major glycolipid recognized by SP-D in surfactant is phosphatidylinositol. *Biochemistry* 1992, *31* (48), 12183-12189.
77. Fukuzawa, T.; Ishida, J.; Kato, A.; Ichinose, T.; Ariestanti, D. M.; Takahashi, T.; Ito, K.; Abe, J.; Suzuki, T.; Wakana, S.; Fukamizu, A.; Nakamura, N.; Hirose, S. Lung Surfactant Levels are Regulated by Ig-Hepta/GPR116 by Monitoring Surfactant Protein D. *PLoS One* 2013, *8* (7), e69451.
78. Joshi, N.; Walter, J. M.; Misharin, A. V. Alveolar Macrophages. *Cellular Immunology* 2018.
79. Garbi, N.; Lambrecht, B. N. Location, function, and ontogeny of pulmonary macrophages during the steady state. *Pflügers Archiv-European Journal of Physiology* 2017, *469* (3-4), 561-572.
80. Epelman, S.; Lavine, K. J.; Randolph, G. J. Origin and functions of tissue macrophages. *Immunity* 2014, *41* (1), 21-35.
81. Ginhoux, F.; Jung, S. Monocytes and macrophages: developmental pathways and tissue homeostasis. *Nature Reviews Immunology* 2014, *14*, 392.
82. Todd, E. M.; Zhou, J. Y.; Szasz, T. P.; Deady, L. E.; D'Angelo, J. A.; Cheung, M. D.; Kim, A. H.; Morley, S. C. Alveolar macrophage development in mice requires L-plastin for cellular localization and retention within alveoli. *Blood* 2016, blood-2016-03-705962.
83. Guilliams, M.; Scott, C. L. Does niche competition determine the origin of tissue-resident macrophages? *Nature Reviews Immunology* 2017, *17*, 451.
84. Guilliams, M.; De Kleer, I.; Henri, S.; Post, S.; Vanhoutte, L.; De Prijck, S.; Deswarte, K.; Malissen, B.; Hammad, H.; Lambrecht, B. N. Alveolar macrophages develop from fetal monocytes that differentiate into long-lived cells in the first week of life via GM-CSF. *The Journal of Experimental Medicine* 2013, *210* (10), 1977-1992.
85. Mass, E.; Ballesteros, I.; Farlik, M.; Halbritter, F.; Günther, P.; Crozet, L.; Jacome-Galarza, C. E.; Händler, K.; Klughammer, J.; Kobayashi, Y.; Gomez-Perdiguero, E.; Schultze, J. L.; Beyer, M.; Bock, C.; Geissmann, F. Specification of tissue-resident macrophages during organogenesis. *Science* 2016, *353* (6304).
86. Schneider, C.; Nobs, S. P.; Kurrer, M.; Rehrauer, H.; Thiele, C.; Kopf, M. Induction of the nuclear receptor PPAR-**γ** by the cytokine GM-CSF is critical for the differentiation of fetal monocytes into alveolar macrophages. *Nature Immunology* 2014, *15*, 1026.

87. Baker, A. D.; Malur, A.; Barna, B. P.; Kavuru, M. S.; Malur, A. G.; Thomassen, M. J. PPARγ regulates the expression of cholesterol metabolism genes in alveolar macrophages. *Biochemical and Biophysical Research Communications* 2010, *393* (4), 682-687.
88. Nakamura, A.; Ebina-Shibuya, R.; Itoh-Nakadai, A.; Muto, A.; Shima, H.; Saigusa, D.; Aoki, J.; Ebina, M.; Nukiwa, T.; Igarashi, K. Transcription repressor Bach2 is required for pulmonary surfactant homeostasis and alveolar macrophage function. *The Journal of Experimental Medicine* 2013, *210* (11), 2191-2204.
89. Cain, D. W.; O'Koren, E. G.; Kan, M. J.; Womble, M.; Sempowski, G. D.; Hopper, K.; Gunn, M. D.; Kelsoe, G. Identification of a Tissue-Specific, C/EBPβ-Dependent Pathway of Differentiation for Murine Peritoneal Macrophages. *The Journal of Immunology* 2013, *191* (9), 4665-4675.
90. Yu, X.; Buttgereit, A.; Lelios, I.; Utz, S. G.; Cansever, D.; Becher, B.; Greter, M. The cytokine TGF-β promotes the development and homeostasis of alveolar macrophages. *Immunity* 2017, *47* (5), 903-912. e4.
91. Westphalen, K.; Gusarova, G. A.; Islam, M. N.; Subramanian, M.; Cohen, T. S.; Prince, A. S.; Bhattacharya, J. Sessile alveolar macrophages communicate with alveolar epithelium to modulate immunity. *Nature* 2014, *506*, 503.
92. Hussell, T.; Bell, T. J. Alveolar macrophages: plasticity in a tissue-specific context. *Nature Reviews Immunology* 2014, *14*, 81.
93. Bhattacharya, J.; Westphalen, K. In *Macrophage-epithelial interactions in pulmonary alveoli*, Seminars in immunopathology, 2016; Springer, pp 461-469.
94. Willart, M. A.; Deswarte, K.; Pouliot, P.; Braun, H.; Beyaert, R.; Lambrecht, B. N.; Hammad, H. Interleukin-1α controls allergic sensitization to inhaled house dust mite via the epithelial release of GM-CSF and IL-33. *Journal of Experimental Medicine* 2012, *209* (8), 1505-1517.
95. Unkel, B.; Hoegner, K.; Clausen, B. E.; Lewe-Schlosser, P.; Bodner, J.; Gattenloehner, S.; Janßen, H.; Seeger, W.; Lohmeyer, J.; Herold, S. Alveolar epithelial cells orchestrate DC function in murine viral pneumonia. *The Journal of clinical investigation* 2012, *122* (10), 3652-3664.
96. De Luca, D.; van Kaam, A. H.; Tingay, D. G.; Courtney, S. E.; Danhaive, O.; Carnielli, V. P.; Zimmermann, L. J.; Kneyber, M. C.; Tissieres, P.; Brierley, J. The Montreux definition of neonatal ARDS: biological and clinical background behind the description of a new entity. *The Lancet Respiratory Medicine* 2017, *5* (8), 657-666.
97. Whitsett, J. A.; Wert, S. E.; Weaver, T. E. Diseases of pulmonary surfactant homeostasis. *Annual Review of Pathology: Mechanisms of Disease* 2015, *10*, 371-393.
98. Iyengar, J. N.; BKK, R. R. Pulmonary alveolar proteinosis in children: An unusual presentation with significant clinical impact. *Indian journal of pathology & microbiology* 2018, *61* (3), 418-420.
99. Happle, C.; Lachmann, N.; Škuljec, J.; Wetzke, M.; Ackermann, M.; Brennig, S.; Mucci, A.; Jirmo, A. C.; Groos, S.; Mirenska, A. Pulmonary transplantation of macrophage progenitors as effective and long-lasting therapy for hereditary pulmonary alveolar proteinosis. *Science translational medicine* 2014, *6* (250), 250ra113-250ra113.
100. Mucci, A.; Lopez-Rodriguez, E.; Hetzel, M.; Liu, S.; Suzuki, T.; Happle, C.; Ackermann, M.; Kempf, H.; Hillje, R.; Kunkiel, J.; Janosz, E.; Brennig, S.; Glage, S.; Bankstahl, J. P.; Dettmer, S.; Rodt, T.; Gohring, G.; Trapnell, B.; Hansen, G.; Trapnell, C.; Knudsen, L.; Lachmann, N.; Moritz, T. iPSC-Derived Macrophages Effectively Treat Pulmonary Alveolar Proteinosis in Csf2rb-Deficient Mice. *Stem cell reports* 2018.

101. Avery, M. E.; Mead, J. Surface properties in relation to atelectasis and hyaline membrane disease. *A.M.A. journal of diseases of children* 1959, *97* (5, Part 1), 517-23.
102. Curstedt, T.; Johansson, J. Different effects of surfactant proteins B and C - implications for development of synthetic surfactants. *Neonatology* 2010, *97* (4), 367-72.
103. Enhorning, G.; Robertson, B. Lung expansion in the premature rabbit fetus after tracheal deposition of surfactant. *Pediatrics* 1972, *50* (1), 58-66.
104. Enhorning, G.; Grossmann, G.; Robertson, B. Pharyngeal deposition of surfactant in the premature rabbit fetus. *Biology of the neonate* 1973, *22* (1), 126-32.
105. Adams, F. H.; Towers, B.; Osher, A. B.; Ikegami, M.; Fujiwara, T.; Nozaki, M. Effects of tracheal instillation of natural surfactant in premature lambs. I. Clinical and autopsy findings. *Pediatric research* 1978, *12* (8), 841-848.
106. Fujiwara, T.; Maeta, H.; Chida, S.; Morita, T.; Watabe, Y.; Abe, T. Artificial surfactant therapy in hyaline-membrane disease. *Lancet* 1980, *1* (8159), 55-9.
107. Halliday, H. L. Overview of clinical trials comparing natural and synthetic surfactants. *Biology of the neonate* 1995, *67 Suppl 1*, 32-47.
108. Echaide, M.; Autilio, C.; Arroyo, R.; Perez-Gil, J. Restoring pulmonary surfactant membranes and films at the respiratory surface. *Biochimica et biophysica acta* 2017, *1859* (9 Pt B), 1725-1739.
109. Curstedt, T.; Johansson, J. New synthetic surfactant–how and when? *Neonatology* 2006, *89* (4), 336-339.
110. Cochrane, C. G.; Revak, S. D.; Merritt, T. A.; Heldt, G. P.; Hallman, M.; Cunningham, M. D.; Easa, D.; Pramanik, A.; Edwards, D. K.; Alberts, M. S. The efficacy and safety of KL4-surfactant in preterm infants with respiratory distress syndrome. *Am J Respir Crit Care Med* 1996, *153* (1), 404-10.
111. Spragg, R. G.; Lewis, J. F.; Wurst, W.; Hafner, D.; Baughman, R. P.; Wewers, M. D.; Marsh, J. J. Treatment of acute respiratory distress syndrome with recombinant surfactant protein C surfactant. *American journal of respiratory and critical care medicine* 2003, *167* (11), 1562-1566.
112. Seehase, M.; Collins, J. J.; Kuypers, E.; Jellema, R. K.; Ophelders, D. R.; Ospina, O. L.; Perez-Gil, J.; Bianco, F.; Garzia, R.; Razzetti, R.; Kramer, B. W. New surfactant with SP-B and C analogs gives survival benefit after inactivation in preterm lambs. *PLoS One* 2012, *7* (10), e47631.
113. Herting, E.; Gan, X.; Rauprich, P.; Jarstrand, C.; Robertson, B. Combined Treatment with Surfactant and Specific Immunoglobulin Reduces Bacterial Proliferation in Experimental Neonatal Group B Streptococcal Pneumonia. *American Journal of Respiratory and Critical Care Medicine* 1999, *159* (6), 1862-1867.
114. Chimote, G.; Banerjee, R. In vitro evaluation of inhalable isoniazid-loaded surfactant liposomes as an adjunct therapy in pulmonary tuberculosis. *Journal of Biomedical Materials Research Part B: Applied Biomaterials* 2010, *94B* (1), 1-10.
115. Veen, A. v. t.; Mouton, J. W.; Gommers, D.; Lachmann, B. Pulmonary surfactant as vehicle for intratracheally instilled tobramycin in mice infected with Klebsiella pneumoniae. *British journal of pharmacology* 1996, *119* (6), 1145-1148.
116. Van 't Veen, A.; Gommers, D.; Verbrugge, S. J. C.; Wollmer, P.; Mouton, J. W.; Kooij, P. P. M.; Lachmann, B. Lung clearance of intratracheally instilled 99mTc-tobramycin using pulmonary surfactant as vehicle. *British Journal of Pharmacology* 1999, *126* (5), 1091-1096.
117. Banaschewski, B. J.; Veldhuizen, E. J.; Keating, E.; Haagsman, H. P.; Zuo, Y. Y.; Yamashita, C. M.; Veldhuizen, R. A. Antimicrobial and biophysical properties of

surfactant supplemented with an antimicrobial peptide for treatment of bacterial pneumonia. *Antimicrobial agents and chemotherapy* 2015, *59* (6), 3075-83.
118. Katkin, J. P.; Husser, R. C.; Langston, C.; Welty, S. E. Exogenous surfactant enhances the delivery of recombinant adenoviral vectors to the lung. *Hum Gene Ther* 1997, *8* (2), 171-6.
119. Walther, F. J.; David-Cu, R.; Lopez, S. L. Antioxidant-surfactant liposomes mitigate hyperoxic lung injury in premature rabbits. *Am J Physiol* 1995, *269* (5 Pt 1), L613-7.
120. Mikolka, P.; Mokra, D.; Kopincova, J.; Tomcikova-Mikusiakova, L.; Calkovska, A. Budesonide added to modified porcine surfactant Curosurf may additionally improve the lung functions in meconium aspiration syndrome. *Physiological research / Academia Scientiarum Bohemoslovaca* 2013, *62 Suppl 1*, S191-200.
121. Dani, C.; Corsini, I.; Burchielli, S.; Cangiamila, V.; Longini, M.; Paternostro, F.; Buonocore, G.; Rubaltelli, F. F. Natural surfactant combined with beclomethasone decreases oxidative lung injury in the preterm lamb. *Pediatric pulmonology* 2009, *44* (12), 1159-67.
122. Dani, C.; Corsini, I.; Burchielli, S.; Cangiamila, V.; Romagnoli, R.; Jayonta, B.; Longini, M.; Paternostro, F.; Buonocore, G. Natural surfactant combined with beclomethasone decreases lung inflammation in the preterm lamb. *Respiration; international review of thoracic diseases* 2011, *82* (4), 369-76.
123. Bai, X.; Xu, M.; Liu, S.; Hu, G. Computational Investigations of the Interaction between the Cell Membrane and Nanoparticles Coated with Pulmonary Surfactant. *ACS applied materials & interfaces* 2018.
124. Fan, Q.; Wang, Y. E.; Zhao, X.; Loo, J. S.; Zuo, Y. Y. Adverse biophysical effects of hydroxyapatite nanoparticles on natural pulmonary surfactant. *ACS nano* 2011, *5* (8), 6410-6.
125. Hu, G.; Jiao, B.; Shi, X.; Valle, R. P.; Fan, Q.; Zuo, Y. Y. Physicochemical properties of nanoparticles regulate translocation across pulmonary surfactant monolayer and formation of lipoprotein corona. *ACS nano* 2013, *7* (12), 10525-33.
126. Lin, X.; Bai, T.; Zuo, Y. Y.; Gu, N. Promote potential applications of nanoparticles as respiratory drug carrier: insights from molecular dynamics simulations. *Nanoscale* 2014, *6* (5), 2759-67.
127. Xu, Y.; Deng, L.; Ren, H.; Zhang, X.; Huang, F.; Yue, T. Transport of nanoparticles across pulmonary surfactant monolayer: a molecular dynamics study. *Physical Chemistry Chemical Physics* 2017, *19* (27), 17568-17576.
128. Hu, Q.; Bai, X.; Hu, G.; Zuo, Y. Y. Unveiling the molecular structure of pulmonary surfactant corona on nanoparticles. *ACS nano* 2017, *11* (7), 6832-6842.
129. Tarawneh, A.; Kaczmarek, J.; Bottino, M.; Sant'Anna, G. Severe airway obstruction during surfactant administration using a standardized protocol: a prospective, observational study. *Journal of Perinatology* 2012, *32* (4), 270.
130. Morley, C.; Miller, N.; Bangham, A.; Davis, J. Dry artificial lung surfactant and its effect on very premature babies. *The Lancet* 1981, *317* (8211), 64-68.
131. Wilkinson, A.; Jenkins, P.; Jeffrey, J. Two controlled trials of dry artificial surfactant: early effects and later outcome in babies with surfactant deficiency. *The Lancet* 1985, *326* (8450), 287-291.
132. Zhou, Q. T.; Tang, P.; Leung, S. S. Y.; Chan, J. G. Y.; Chan, H.-K. Emerging inhalation aerosol devices and strategies: Where are we headed? *Advanced drug delivery reviews* 2014.

133. Berggren, E.; Liljedahl, M.; Winbladh, B.; Andreasson, B.; Curstedt, T.; Robertson, B.; Schollin, J. Pilot study of nebulized surfactant therapy for neonatal respiratory distress syndrome. *Acta paediatrica (Oslo, Norway : 1992)* 2000, *89* (4), 460-4.
134. Walther, F. J.; Hernández-Juviel, J. M.; Waring, A. J. Aerosol delivery of synthetic lung surfactant. *PeerJ* 2014, *2*, e403.
135. Wolfson, M.; Wu, J.; Hubert, T.; Mazela, J.; Gregory, T.; Clayton, R.; Shaffer, T. Dose-Response to Aerosolized KL 4 Surfactant in the Spontaneously Breathing CPAP-Supported Preterm Lamb. *Pediatric research* 2011, *70* (S5), 751.
136. Hütten, M. C.; Kuypers, E.; Ophelders, D. R.; Nikiforou, M.; Jellema, R. K.; Niemarkt, H. J.; Fuchs, C.; Tservistas, M.; Razetti, R.; Bianco, F. Nebulization of Poractant alfa via a vibrating membrane nebulizer in spontaneously breathing preterm lambs with binasal continuous positive pressure ventilation. *Pediatric research* 2015, *78* (6), 664.
137. Sankar, M.; Gupta, N.; Jain, K.; Agarwal, R.; Paul, V. Efficacy and safety of surfactant replacement therapy for preterm neonates with respiratory distress syndrome in low- and middle-income countries: a systematic review. *Journal of Perinatology* 2016, *36* (S1), S36.
138. Mazela, J.; Merritt, T. A.; Gadzinowski, J.; Sinha, S. Evolution of pulmonary surfactants for the treatment of neonatal respiratory distress syndrome and paediatric lung diseases. *Acta paediatrica (Oslo, Norway : 1992)* 2006, *95* (9), 1036-48.
139. Liu, M.; Wang, L.; Li, E.; Enhorning, G. Pulmonary surfactant given prophylactically alleviates an asthma attack in guinea-pigs. *Clinical & Experimental Allergy* 1996, *26* (3), 270-275.
140. Mokra, D.; Mokry, J.; Drgova, A.; Petraskova, M.; Bulikova, J.; Calkovska, A. Intratracheally administered corticosteroids improve lung function in meconium-instilled rabbits. *Journal of physiology and pharmacology : an official journal of the Polish Physiological Society* 2007, *58 Suppl 5* (Pt 1), 389-98.
141. Wang, L.; Scabilloni, J. F.; Antonini, J. M.; Castranova, V.; Rojanasakul, Y.; Roberts, J. R.; Zhang, Z.; Mercer, R. R. Role of lung surfactant in phagocytic clearance of apoptotic cells by macrophages in rats. *Laboratory investigation* 2006, *86* (5), 458.
142. Chimote, G.; Banerjee, R. Effect of antitubercular drugs on dipalmitoylphosphatidylcholine monolayers: implications for drug loaded surfactants. *Respiratory physiology & neurobiology* 2005, *145* (1), 65-77.
143. Kolomaznik, M.; Calkovska, A.; Herting, E.; Stichtenoth, G. Biophysical Activity of Animal-Derived Exogenous Surfactants Mixed with Rifampicin. *Advances in experimental medicine and biology* 2014.
144. Birkun, A. Exogenous pulmonary surfactant as a vehicle for antimicrobials: assessment of surfactant-antibacterial interactions in vitro. *Scientifica* 2014, *2014*, 930318.
145. Niwa, Y.; Hiura, Y.; Sawamura, H.; Iwai, N. Inhalation exposure to carbon black induces inflammatory response in rats. *Circulation journal : official journal of the Japanese Circulation Society* 2008, *72* (1), 144-9.
146. Sung, J. H.; Ji, J. H.; Yoon, J. U.; Kim, D. S.; Song, M. Y.; Jeong, J.; Han, B. S.; Han, J. H.; Chung, Y. H.; Kim, J.; Kim, T. S.; Chang, H. K.; Lee, E. J.; Lee, J. H.; Yu, I. J. Lung function changes in Sprague-Dawley rats after prolonged inhalation exposure to silver nanoparticles. *Inhalation toxicology* 2008, *20* (6), 567-74.
147. Lundborg, M.; Bouhafs, R.; Gerde, P.; Ewing, P.; Camner, P.; Dahlen, S. E.; Jarstrand, C. Aggregates of ultrafine particles modulate lipid peroxidation and bacterial killing by alveolar macrophages. *Environmental research* 2007, *104* (2), 250-7.
148. Arora, S.; Jain, J.; Rajwade, J. M.; Paknikar, K. M. Cellular responses induced by silver nanoparticles: In vitro studies. *Toxicology letters* 2008, *179* (2), 93-100.

149. Taeusch, H. W.; Bernardino de la Serna, J.; Perez-Gil, J.; Alonso, C.; Zasadzinski, J. A. Inactivation of pulmonary surfactant due to serum-inhibited adsorption and reversal by hydrophilic polymers: experimental. *Biophysical journal* 2005, *89* (3), 1769-79.
150. Shelley, S. A. Oxidant-induced alterations of lung surfactant system. *The Journal of the Florida Medical Association* 1994, *81* (1), 49-51.
151. Schleh, C.; Rothen-Rutishauser, B.; Kreyling, W. G. The influence of pulmonary surfactant on nanoparticulate drug delivery systems. *Eur J Pharm Biopharm* 2011, *77* (3), 350-2.
152. Beck-Broichsitter, M.; Ruppert, C.; Schmehl, T.; Guenther, A.; Betz, T.; Bakowsky, U.; Seeger, W.; Kissel, T.; Gessler, T. Biophysical investigation of pulmonary surfactant surface properties upon contact with polymeric nanoparticles in vitro. *Nanomedicine* 2011, *7* (3), 341-50.
153. Beck-Broichsitter, M.; Ruppert, C.; Schmehl, T.; Gunther, A.; Seeger, W. Biophysical inhibition of synthetic vs. naturally-derived pulmonary surfactant preparations by polymeric nanoparticles. *Biochimica et biophysica acta* 2014, *1838* (1 Pt B), 474-81.
154. Hu, G.; Jiao, B.; Shi, X.; Valle, R. P.; Fan, Q.; Zuo, Y. Y. Physicochemical properties of nanoparticles regulate translocation across pulmonary surfactant monolayer and formation of lipoprotein corona. *ACS nano* 2013, *7* (12), 10525-10533.
155. Arick, D. Q.; Choi, Y. H.; Kim, H. C.; Won, Y. Y. Effects of nanoparticles on the mechanical functioning of the lung. *Adv Colloid Interface Sci* 2015, *225*, 218-28.
156. Curstedt, T.; Jornvall, H.; Robertson, B.; Bergman, T.; Berggren, P. Two hydrophobic low-molecular-mass protein fractions of pulmonary surfactant. Characterization and biophysical activity. *European journal of biochemistry / FEBS* 1987, *168* (2), 255-62.
157. Casals, C.; Herrera, L.; Miguel, E.; Garcia-Barreno, P.; Municio, A. M. Comparison between intra- and extracellular surfactant in respiratory distress induced by oleic acid. *Biochimica et biophysica acta* 1989, *1003* (2), 201-3.
158. Bligh, E. G.; Dyer, W. J. A rapid method of total lipid extraction and purification. *Canadian journal of biochemistry and physiology* 1959, *37* (8), 911-7.
159. Hidalgo, A., F.; Fresno, N.; Orellana, G.; Cruz, A.; Perez-Gil, Jesús. Efficient interfacially-driven vehiculization of corticosteroids by pulmonary surfactant. *Langmuir* 2017, *33* (32), 7929-7939.
160. Glahn-Martínez, B.; Benito-Peña, E.; Salis, F.; Descalzo, A. B.; Orellana, G.; Moreno-Bondi, M. C. Sensitive Rapid Fluorescence Polarization Immunoassay for Free Mycophenolic Acid Determination in Human Serum and Plasma. *Analytical chemistry* 2018, *90* (8), 5459-5465.
161. Rouser, G.; Siakotos, A. N.; Fleischer, S. Quantitative analysis of phospholipids by thin-layer chromatography and phosphorus analysis of spots. *Lipids* 1966, *1* (1), 85-6.
162. Bassler, D.; Plavka, R.; Shinwell, E. S.; Hallman, M.; Jarreau, P. H.; Carnielli, V.; Van den Anker, J. N.; Meisner, C.; Engel, C.; Schwab, M.; Halliday, H. L.; Poets, C. F.; Group, N. T. Early Inhaled Budesonide for the Prevention of Bronchopulmonary Dysplasia. *The New England journal of medicine* 2015, *373* (16), 1497-506.
163. Baud, O.; Alberti, C.; Mohamed, D.; Watterberg, K. Low-dose hydrocortisone in extremely preterm infants - Authors' reply. *Lancet* 2016, *388* (10050), 1158-9.
164. Nakamura, T.; Yonemoto, N.; Nakayama, M.; Hirano, S.; Aotani, H.; Kusuda, S.; Fujimura, M.; Tamura, M.; and The Neonatal Research Network, J. Early inhaled steroid use in extremely low birthweight infants: a randomised controlled trial. *Archives of disease in childhood. Fetal and neonatal edition* 2016.

165. Yeh, T. F.; Chen, C. M.; Wu, S. Y.; Husan, Z.; Li, T. C.; Hsieh, W. S.; Tsai, C. H.; Lin, H. C. Intratracheal Administration of Budesonide/Surfactant to Prevent Bronchopulmonary Dysplasia. *Am J Respir Crit Care Med* 2016, *193* (1), 86-95.
166. Ricci, F.; Murgia, X.; Razzetti, R.; Pelizzi, N.; Salomone, F. In vitro and in vivo comparison between poractant alfa and the new generation synthetic surfactant CHF5633. *Pediatr Res* 2016, *(in press)*.
167. Schurch, S.; Bachofen, H.; Goerke, J.; Possmayer, F. A captive bubble method reproduces the in situ behavior of lung surfactant monolayers. *Journal of applied physiology (Bethesda, Md. : 1985)* 1989, *67* (6), 2389-96.
168. Schoel, W. M.; Schurch, S.; Goerke, J. The captive bubble method for the evaluation of pulmonary surfactant: surface tension, area, and volume calculations. *Biochimica et biophysica acta* 1994, *1200* (3), 281-90.
169. Schurch, D.; Ospina, O. L.; Cruz, A.; Perez-Gil, J. Combined and independent action of proteins SP-B and SP-C in the surface behavior and mechanical stability of pulmonary surfactant films. *Biophysical journal* 2010, *99* (10), 3290-9.
170. Yu, S. H.; Possmayer, F. Lipid compositional analysis of pulmonary surfactant monolayers and monolayer-associated reservoirs. *Journal of lipid research* 2003, *44* (3), 621-9.
171. Yang, C. F.; Lin, C. H.; Chiou, S. Y.; Yang, Y. C.; Tsao, P. C.; Lee, Y. S.; Soong, W. J.; Jeng, M. J. Intratracheal budesonide supplementation in addition to surfactant improves pulmonary outcome in surfactant-depleted newborn piglets. *Pediatric pulmonology* 2013, *48* (2), 151-9.
172. Bernardino de la Serna, J.; Oradd, G.; Bagatolli, L. A.; Simonsen, A. C.; Marsh, D.; Lindblom, G.; Perez-Gil, J. Segregated phases in pulmonary surfactant membranes do not show coexistence of lipid populations with differentiated dynamic properties. *Biophysical journal* 2009, *97* (5), 1381-9.
173. Bernardino de la Serna, J.; Perez-Gil, J.; Simonsen, A. C.; Bagatolli, L. A. Cholesterol rules: direct observation of the coexistence of two fluid phases in native pulmonary surfactant membranes at physiological temperatures. *The Journal of biological chemistry* 2004, *279* (39), 40715-22.
174. Gunasekara, L.; Schurch, S.; Schoel, W. M.; Nag, K.; Leonenko, Z.; Haufs, M.; Amrein, M. Pulmonary surfactant function is abolished by an elevated proportion of cholesterol. *Biochimica et biophysica acta* 2005, *1737* (1), 27-35.
175. Leonenko, Z.; Gill, S.; Baoukina, S.; Monticelli, L.; Doehner, J.; Gunasekara, L.; Felderer, F.; Rodenstein, M.; Eng, L. M.; Amrein, M. An elevated level of cholesterol impairs self-assembly of pulmonary surfactant into a functional film. *Biophysical journal* 2007, *93* (2), 674-83.
176. Todorov, R.; Exerowa, D.; Alexandrova, L.; Platikanov, D.; Terziyski, I.; Nedyalkov, M.; Pelizzi, N.; Salomone, F. Behavior of thin liquid films from aqueous solutions of a pulmonary surfactant in presence of corticosteroids. *Colloids and Surfaces A: Physicochemical and Engineering Aspects* 2016, *(in press)*.
177. Lopez-Rodriguez, E.; Echaide, M.; Cruz, A.; Taeusch, H. W.; Perez-Gil, J. Meconium Impairs Pulmonary Surfactant by a Combined Action of Cholesterol and Bile Acids. *Biophysical journal* 2011, *100* (3), 646-655.
178. Lopez-Rodriguez, E.; Cruz, A.; Richter, R. P.; Taeusch, H. W.; Perez-Gil, J. Transient exposure of pulmonary surfactant to hyaluronan promotes structural and compositional transformations into a highly active state. *The Journal of biological chemistry* 2013, *288* (41), 29872-81.
179. Lopez-Rodriguez, E.; Ospina, O. L.; Echaide, M.; Taeusch, H. W.; Perez-Gil, J. Exposure to polymers reverses inhibition of pulmonary surfactant by serum, meconium, or

cholesterol in the captive bubble surfactometer. *Biophysical journal* 2012, *103* (7), 1451-9.
180. Lugones, Y.; Blanco, O.; Lopez-Rodriguez, E.; Echaide, M.; Cruz, A.; Perez-Gil, J. Inhibition and counterinhibition of Surfacen, a clinical lung surfactant of natural origin. *PLoS One* 2018, *13* (9), e0204050.
181. Kohler, E.; Jilg, G.; Avenarius, S.; Jorch, G. Lung deposition after inhalation with various nebulisers in preterm infants. *Archives of disease in childhood. Fetal and neonatal edition* 2008, *93* (4), F275-9.
182. Langmuir, I. The constitution and fundamental properties of solids and liquids. Part I. Solids. *Journal of the American chemical society* 1916, *38* (11), 2221-2295.
183. Langmuir, I. The constitution and fundamental properties of solids and liquids. II. Liquids. *Journal of the American Chemical Society* 1917, *39* (9), 1848-1906.
184. Cruz, A.; Pérez-Gil, J. Langmuir films to determine lateral surface pressure on lipid segregation. In *Methods in Membrane Lipids*; Springer, 2007, pp 439-457.
185. Wang, L.; Cruz, A.; Flach, C. R.; Perez-Gil, J.; Mendelsohn, R. Langmuir-Blodgett films formed by continuously varying surface pressure. Characterization by IR spectroscopy and epifluorescence microscopy. *Langmuir* 2007, *23* (9), 4950-8.
186. Keating, E.; Rahman, L.; Francis, J.; Petersen, A.; Possmayer, F.; Veldhuizen, R.; Petersen, N. O. Effect of cholesterol on the biophysical and physiological properties of a clinical pulmonary surfactant. *Biophysical journal* 2007, *93* (4), 1391-1401.
187. Yuan, C.; Johnston, L. Phase evolution in cholesterol/DPPC monolayers: atomic force microscopy and near field scanning optical microscopy studies. *Journal of microscopy* 2002, *205* (2), 136-146.
188. Lopez-Rodriguez, E.; Echaide, M.; Cruz, A.; Taeusch, H. W.; Perez-Gil, J. Meconium impairs pulmonary surfactant by a combined action of cholesterol and bile acids. *Biophysical journal* 2011, *100* (3), 646-55.
189. Stetten, A. Z.; Iasella, S. V.; Corcoran, T. E.; Garoff, S.; Przybycien, T. M.; Tilton, R. D. Surfactant-induced Marangoni transport of lipids and therapeutics within the lung. *Current Opinion in Colloid & Interface Science* 2018, *36*, 58-69.
190. Yan, W.; Piknova, B.; Hall, S. B. The collapse of monolayers containing pulmonary surfactant phospholipids is kinetically determined. *Biophysical journal* 2005, *89* (1), 306-314.
191. Pérez-Gil, J.; Keough, K. M. Interfacial properties of surfactant proteins. *Biochimica et Biophysica Acta (BBA)-Molecular Basis of Disease* 1998, *1408* (2-3), 203-217.
192. Amrein, M.; Von Nahmen, A.; Sieber, M. A scanning force-and fluorescence light microscopy study of the structure and function of a model pulmonary surfactant. *European biophysics journal* 1997, *26* (5), 349-357.
193. Zhang, H.; Wang, Y. E.; Fan, Q.; Zuo, Y. Y. On the low surface tension of lung surfactant. *Langmuir* 2011, *27* (13), 8351-8358.
194. Schurch, S.; Possmayer, F.; Cheng, S.; Cockshutt, A. M. Pulmonary SP-A enhances adsorption and appears to induce surface sorting of lipid extract surfactant. *American Journal of Physiology-Lung Cellular and Molecular Physiology* 1992, *263* (2), L210-L218.
195. Veldhuizen, E. J.; Batenburg, J. J.; van Golde, L. M.; Haagsman, H. P. The role of surfactant proteins in DPPC enrichment of surface films. *Biophysical journal* 2000, *79* (6), 3164-3171.
196. Rugonyi, S.; Biswas, S. C.; Hall, S. B. The biophysical function of pulmonary surfactant. *Respiratory physiology & neurobiology* 2008, *163* (1-3), 244-255.
197. Merckx, P.; De Backer, L.; Van Hoecke, L.; Guagliardo, R.; Echaide, M.; Baatsen, P.; Olmeda, B.; Saelens, X.; Pérez-Gil, J.; De Smedt, S. C.; Raemdonck, K. Surfactant

protein b (sp-b) enhances the cellular sirna delivery of proteolipid coated nanogels for inhalation therapy. *Acta Biomaterialia* 2018.
198. Kolomaznik, M.; Nova, Z.; Calkovska, A. Pulmonary surfactant and bacterial lipopolysaccharide: the interaction and its functional consequences. *Physiological research* 2017, *66*.
199. Sender, V.; Stamme, C. Lung cell-specific modulation of LPS-induced TLR4 receptor and adaptor localization. *Communicative & integrative biology* 2014, *7* (4), e29053.
200. Togbe, D.; Schnyder-Candrian, S.; Schnyder, B.; Doz, E.; Noulin, N.; Janot, L.; Secher, T.; Gasse, P.; Lima, C.; Coelho, F. R. Toll-like receptor and tumour necrosis factor dependent endotoxin-induced acute lung injury. *International journal of experimental pathology* 2007, *88* (6), 387-391.
201. Matute-Bello, G.; Frevert, C. W.; Martin, T. R. Animal models of acute lung injury. *American Journal of Physiology-Lung Cellular and Molecular Physiology* 2008, *295* (3), L379-L399.
202. Kino, T.; Hatanaka, H.; Miyata, S.; Inamura, N.; NISHIYAMA, M.; YAJIMA, T.; GOTO, T.; OKUHARA, M.; KOHSAKA, M.; AOKI, H. FK-506, a novel immunosuppressant isolated from a Streptomyces. *The Journal of antibiotics* 1987, *40* (9), 1256-1265.
203. Fan, Y.; Xiao, Y.-B.; Weng, Y.-G. In *Tacrolimus versus cyclosporine for adult lung transplant recipients: a meta-analysis*, Transplantation proceedings, 2009; Elsevier, pp 1821-1824.
204. Hachem, R. R.; Yusen, R. D.; Chakinala, M. M.; Meyers, B. F.; Lynch, J. P.; Aloush, A. A.; Patterson, G. A.; Trulock, E. P. A randomized controlled trial of tacrolimus versus cyclosporine after lung transplantation. *The Journal of Heart and Lung Transplantation* 2007, *26* (10), 1012-1018.
205. Webster, A. C.; Woodroffe, R. C.; Taylor, R. S.; Chapman, J. R.; Craig, J. C. Tacrolimus versus ciclosporin as primary immunosuppression for kidney transplant recipients: meta-analysis and meta-regression of randomised trial data. *Bmj* 2005, *331* (7520), 810.
206. Margreiter, R.; Group, E. T. v. C. M. R. T. S. Efficacy and safety of tacrolimus compared with ciclosporin microemulsion in renal transplantation: a randomised multicentre study. *The lancet* 2002, *359* (9308), 741-746.
207. Yu, Y.; Zhong, J.; Peng, L.; Wang, B.; Li, S.; Huang, H.; Deng, Y.; Zhang, H.; Yang, R.; Wang, C.; Yuan, J. Tacrolimus downregulates inflammation by regulating pro-/anti-inflammatory responses in LPS-induced keratitis. *Molecular Medicine Reports* 2017, *16* (5), 5855-5862.
208. Howell, J.; Sawhney, R.; Testro, A.; Skinner, N.; Gow, P.; Angus, P.; Ratnam, D.; Visvanathan, K. Cyclosporine and tacrolimus have inhibitory effects on toll-like receptor signaling after liver transplantation. *Liver Transplantation* 2013, *19* (10), 1099-1107.
209. Pereira, R.; Santos Medeiros, Y.; Fröde, T. S. Antiinflammatory effects of Tacrolimus in a mouse model of pleurisy. *Transplant immunology* 2006, *16* (2), 105-111.
210. Yoshino, T.; Nakase, H.; Honzawa, Y.; Matsumura, K.; Yamamoto, S.; Takeda, Y.; Ueno, S.; Uza, N.; Masuda, S.; Inui, K.; Chiba, T. Immunosuppressive effects of tacrolimus on macrophages ameliorate experimental colitis. *Inflammatory bowel diseases* 2010, *16* (12), 2022-33.
211. Jennings, C.; Kusler, B.; Jones, P. P. Calcineurin Inactivation Leads to Decreased Responsiveness to LPS in Macrophages and Dendritic Cells and Protects Against LPS-Induced Toxicity In Vivo. *Innate immunity* 2009, *15* (2), 109-120.

212. Kang, Y. J.; Kusler, B.; Otsuka, M.; Hughes, M.; Suzuki, N.; Suzuki, S.; Yeh, W.-C.; Akira, S.; Han, J.; Jones, P. P. Calcineurin negatively regulates TLR-mediated activation pathways. *The Journal of Immunology* 2007, *179* (7), 4598-4607.
213. Proctor, R.; Will, J.; Burhop, K.; Raetz, C. Protection of mice against lethal endotoxemia by a lipid A precursor. *Infection and immunity* 1986, *52* (3), 905-907.
214. West, M. A.; Heagy, W. Endotoxin tolerance: a review. *Critical care medicine* 2002, *30* (1), S64-S73.
215. van den Bosch, T. P. P.; Kannegieter, N. M.; Hesselink, D. A.; Baan, C. C.; Rowshani, A. T. Targeting the Monocyte–Macrophage Lineage in Solid Organ Transplantation. *Frontiers in Immunology* 2017, *8* (153).
216. Chang, K.-T.; Lin, H. Y.-H.; Kuo, C.-H.; Hung, C.-H. Tacrolimus suppresses atopic dermatitis-associated cytokines and chemokines in monocytes. *Journal of Microbiology, Immunology and Infection* 2016, *49* (3), 409-416.
217. Barbarino, J. M.; Staatz, C. E.; Venkataramanan, R.; Klein, T. E.; Altman, R. B. PharmGKB summary: cyclosporine and tacrolimus pathways. *Pharmacogenetics and genomics* 2013, *23* (10), 563.
218. Kannegieter, N. M.; Hesselink, D. A.; Dieterich, M.; Kraaijeveld, R.; Rowshani, A. T.; Leenen, P. J.; Baan, C. C. The effect of tacrolimus and mycophenolic acid on CD14+ monocyte activation and function. *PLoS One* 2017, *12* (1), e0170806.
219. Nagano, J.; Iyonaga, K.; Kawamura, K.; Yamashita, A.; Ichiyasu, H.; Okamoto, T.; Suga, M.; Sasaki, Y.; Kohrogi, H. Use of tacrolimus, a potent antifibrotic agent, in bleomycin-induced lung fibrosis. *European Respiratory Journal* 2006, *27* (3), 460-469.
220. Horita, N.; Akahane, M.; Okada, Y.; Kobayashi, Y.; Arai, T.; Amano, I.; Takezawa, T.; To, M.; To, Y. Tacrolimus and steroid treatment for acute exacerbation of idiopathic pulmonary fibrosis. *Internal Medicine* 2011, *50* (3), 189-195.
221. Robinson-Smith, T. M.; Saad, A.; Baughman, R. P. Interpretation of the Wright-Giemsa stained bronchoalveolar lavage specimen. *Laboratory Medicine* 2004, *35* (9), 553-557.
222. Nakamura, T.; Abu-Dahab, R.; Menger, M. D.; Schafer, U.; Vollmar, B.; Wada, H.; Lehr, C. M.; Schafers, H. J. Depletion of alveolar macrophages by clodronate-liposomes aggravates ischemia-reperfusion injury of the lung. *The Journal of heart and lung transplantation : the official publication of the International Society for Heart Transplantation* 2005, *24* (1), 38-45.
223. Bem, R. A.; Farnand, A. W.; Wong, V.; Koski, A.; Rosenfeld, M. E.; van Rooijen, N.; Frevert, C. W.; Martin, T. R.; Matute-Bello, G. Depletion of resident alveolar macrophages does not prevent Fas-mediated lung injury in mice. *American Journal of Physiology-Lung Cellular and Molecular Physiology* 2008, *295* (2), L314-L325.
224. Lachmann, B. The role of pulmonary surfactant in the pathogenesis and therapy of ARDS. In *Update 1987*; Springer, 1987, pp 123-134.
225. Raghavendran, K.; Willson, D.; Notter, R. Surfactant therapy for acute lung injury and acute respiratory distress syndrome. *Critical care clinics* 2011, *27* (3), 525-559.
226. Gregory, T. J.; Steinberg, K. P.; Spragg, R.; Gadek, J. E.; Hyers, T. M.; Longmore, W. J.; Moxley, M. A.; Cai, G.-Z.; Hite, R. D.; Smith, R. M. Bovine surfactant therapy for patients with acute respiratory distress syndrome. *American journal of respiratory and critical care medicine* 1997, *155* (4), 1309-1315.
227. Schenck, D. M.; Fiegel, J. Tensiometric and Phase Domain Behavior of Lung Surfactant on Mucus-like Viscoelastic Hydrogels. *ACS applied materials & interfaces* 2016, *8* (9), 5917-28.
228. Ganesan, S.; Comstock, A. T.; Sajjan, U. S. Barrier function of airway tract epithelium. *Tissue Barriers* 2013, *1* (4), e24997.

229. Echaide, M.; Autilio, C.; Arroyo, R.; Perez-Gil, J. Restoring pulmonary surfactant membranes and films at the respiratory surface. *Biochimica et biophysica acta* 2017, *(in press)*.
230. Davis, J. M.; Russ, G. A.; Metlay, L.; Dickerson, B.; Greenspan, B. S. Short-term distribution kinetics of intratracheally administered exogenous lung surfactant. *Pediatric research* 1992, *31* (5), 445.
231. Espinosa, F.; Shapiro, A.; Fredberg, J.; Kamm, R. Spreading of exogenous surfactant in an airway. *Journal of Applied Physiology* 1993, *75* (5), 2028-2039.